DYNAMICALLY LOADED JOURNAL BEARINGS

A thesis presented for the degree of

Doctor of Philosophy

in

Mechanical Engineering

in the

University of Canterbury

Christchurch

New Zealand

by

D.R. WALES B.E.(Hons)

May, 1975

CONTENTS

ABSTRACT

The aim of the work reported in this thesis was to develop a method, suitable for general design work, to determine the stability of a simple rotor mounted in hydrodynamic bearings. The rotor model used was a simple spring mass system, but the bearing model allowed a comprehensive range of bearing cross-sectional shapes and grooves to be assessed. The oil film equations were solved by the successive over-relaxation finite difference technique.

The problem was approached by considering the energy balance of the bearing-rotor system. The hydrodynamic oil pressure film in the bearing performs work on the journal and this is largely responsible for the decay or growth of the rotor motion. The behaviour of a simple rotor was investigated to determine if its influence on the bearing could be represented by a simple force locus as this would allow the oil film work to be calculated without marching out the rotor locus. In general, the force exerted by the rotor on the journal is too complex to allow a direct assessment of the stability of a system by this technique.

The flexibility and ease of operation of the directly loaded bearing computer program make it useful for comparisons of bearing design features and load conditions. An investigation was carried out into the effect of the bearing parameters on the oil film work when the journal is loaded with a circular force locus.

An attempt was made to reduce the computation necessary to march out the journal and rotor loci. The approach taken was to improve the utilisation of the information obtained from the oil film equations.

Although significant reductions in the computation were achieved, they were insufficient to justify the additional program complexity.

NOMENCLATURE

Unless otherwise specified, the following symbols are used in the text. A dot above a symbol, e.g. $\dot{e}$, indicates the derivative with respect to time.

ACC	Relaxation convergence tolerance
Br	Rotor damping coefficient
bxx	$\partial FX/\partial \dot{X}j$
bxy	$\partial FX/\partial \dot{Y}j$
byx	$\partial FY/\partial \dot{X}j$
byy	$\partial FY/\partial \dot{Y}j$
Cm	Minimum radial bearing clearance with the journal centre at the bearing centre.
D	Journal diameter.
DEL	Resultant non-dimensional oil film force
DT	Non-dimensional time step
e	Journal eccentricity
FX,FY	Non-dimensional oil film force, x and y components
FXJ,FYJ	Non-dimensional force applied to journal, x and y components
fx,fy	Dimensional force, x and y components
H	Non-dimensional oil film thickness
h	Dimensional oil film thickness
Ks	Rotor shaft stiffness
kxx	$\partial FX/\partial Xj$
kxy	$\partial FX/\partial Yj$
kyx	$\partial FY/\partial Xj$
kyy	$\partial FY/\partial Yj$
L	Bearing width

LOADAC	Load accuracy tolerance
m	Number of circumferential grid divisions
Mr	Rotor mass
n	Number of axial grid divisions
ORF	Over-relaxation factor
P	Non-dimensional pressure
$P_{X,Z}$	Non-dimensional pressure at point X, Z
$\bar{P}$	Non-dimensional pressure-height parameter (PH^2)
$\bar{P}_{X,Z}$	Non-dimensional pressure-height parameter at point X, Z
p	Dimensional pressure
R	Journal radius
r	Radial bearing clearance
r_0	Radial co-ordinate of segment centre with respect to bearing centre
RLV	Relative load velocity, $\dot{\phi}/\omega$
U,V	Journal surface velocity, X and Y components
u,v,w	Velocity in the x,y and z directions respectively
WORK	Non-dimensional work performed by the oil pressure film on the journal
X,Y,Z	Non-dimensional cartesian co-ordinates of the bearing surface
x,y,z	General dimensional cartesian co-ordinates
Xj,Yj	Non-dimensional journal centre co-ordinates
xj,yj	Dimensional journal centre co-ordinates
Xr,Yr	Non-dimensional rotor mass co-ordinates
γ	Angular co-ordinate of journal centre
ΔS	Non-dimensional applied static load
ΔT	Non-dimensional applied dynamic load
ΔX	Non-dimensional circumferential spacing of grid points

ΔZ	Non-dimensional axial spacing of grid points
ε	Journal eccentricity ratio
ε_0	Journal eccentricity ratio under static load alone
Θ	Angular position on bearing surface
λ	Angular co-ordinate of segment centre with respect to bearing centre
μ	Viscosity coefficient
ρ	Density
τ	Shear stress
ϕ	Angular position of applied dynamic load
ϕS	Angular position of applied static load
ψ	Attitude angle
ω	Journal angular velocity.

CHAPTER ONE

INTRODUCTION

The aim of the work described in this thesis was to produce a commercially acceptable method to assess the dynamic behaviour of a rotor mounted in hydrodynamic bearings. Although an enormous quantity of research has been done on the stability of bearings, a satisfactory method of analysis for industrial applications has not been developed. Those existing are either derived with approximations limiting their application or require considerable computer time to analyse a more comprehensive model, rendering them suitable only for problem cases or final design checks.

Thus, a programme of research was started to analyse journal bearing dynamic behaviour using a comprehensive bearing model, but keeping the method of analysis suitable for general design work.

I.1 BACKGROUND

A journal bearing can be simply described as a circular shaft (the journal) inside a bush of slightly larger diameter (the bearing) with a lubricant between the two allowing low friction relative angular motion. Bearings of this type have been used for centuries but Beauchamp Tower[1] in 1883 was the first to determine the importance of the lubricant. In an experiment with statically loaded journal bearings he observed that their frictional behaviour followed the laws of fluid mechanics rather than solids and that the peak lubricant pressure considerably exceeded the load over projected bearing area. He suggested that the journal and bearing were completely separated by the lubricant but was unable to offer an explanation for the pressure observation.

In 1886 Osborne Reynolds[2] derived a partial differential equation describing the generation of the lubricant pressure film. He found the film was produced by the journal running eccentrically in the bearing, thus forming a converging wedge. The viscous shear forces imposed on the lubricant by the rotation of the journal force the fluid into the wedge thereby increasing the pressure. A second mechanism of pressure generation occurs when the radial position of the journal in the bearing is not constant. The journal, approaching the bearing surface, forces out the lubricant creating a pressure film independent of the shaft rotation. These two mechanisms for generating load bearing oil films give rise to what are known as wedge and squeeze films respectively.

The equation derived by Reynolds forms the basis of present hydrodynamic bearing theory and bears his name. He presented a solution for a pure wedge (e.g. an inclined plate) of infinite width. Sommerfeld[3] in 1904 applied the theory to a full journal bearing of infinite length, but he failed to allow for film disruption in regions of negative pressure. The validity of this assumption was commented on by a number of researchers, including Reynolds, but it was Swift[4] in 1931 who established the boundary condition that the film ended with both the pressure and pressure derivative zero. Another closed solution was put forward by Ocvirk[5] in 1952. He assumed the bearing to be short and hence the axial pressure derivatives to be much greater than those in the circumferential direction. In this way he justified omitting the circumferential derivatives from his analysis.

Solution for a bearing of finite length was made by representing the pressure with an infinite series until Christopherson[6], 1941, introduced the finite difference technique. This employed an

iterative technique, known as the relaxation method, developed by Southwell[7] a year earlier. Christopherson used the same film boundary conditions as Swift and included in his solution the variations of the lubricant viscosity with pressure and temperature. Iterative methods of solution have been used by many investigators since and form the basis of the technique described in this thesis. They are well suited for high speed digital computers. The programming is relatively simple because the solution involves the repeated use of one set of equations. These methods also allow a variety of film boundary conditions to be satisfied, permitting bearing design features such as grooves to be included in the solution. Series solutions are still used, but they lack the flexibility of the finite difference technique.

The advent of digital computers and the increasing demand for better bearing performance stimulated an acceleration of work in the late 1950s and 1960s. Researchers considered the effects of assumptions made in deriving and solving Reynolds equation, for example turbulence, lubricant inertia, viscosity changes and bearing distortion, and conducted investigations into such topics as the influence of lubricant supply conditions, heat transfer and lubricant flow. Most of this work has been done for statically loaded bearings as computation time is still long and thus research expensive.

Interest in bearing dynamic behaviour developed with the film theory. The first report on bearing instability was made by Newkirk and Taylor[8] in 1925 following an experimental investigation. About the same time Stodola[9] conducted a theoretical analysis, but lacking a satisfactory solution to the film equation, his results were of little practical use. However, the linearised analysis used remains one of the principal tools

available to bearing designers.

This approach assumes that for small movement of the journal about its static equilibrium position, the film forces can be described by constant stiffness and damping coefficients. Thus repeated solutions of Reynolds equation are avoided and the bearing-rotor behaviour is simpler to analyse. A direct assessment of a system's stability is possible using, for example, the Routh-Hurwitz criterion[10].

Recent non-linear theoretical investigations have generally employed approximate film solutions to shorten computation time. As well as the long and short bearing solutions mentioned, new methods have been developed. For example, Warner[11], 1963, solved the film equation by multiplying the long bearing solution by a factor representing side leakage. Shelly and Ettles[12], 1970, assumed an axial pressure distribution to reduce their finite difference scheme to one dimension.

More comprehensive solutions have been produced. Someya[13], 1964, investigating the stability of a flexible rotor, used a series solution and Lloyd[14], 1966, a finite difference scheme in determining the dynamic behaviour of bearings in reciprocating machinery. Both of these capitalised on the circumferential symmetry of circular bearings to reduce computation. Ware[15], 1975, considered the general problem of a multi-mass rotor, including gyroscopic effects, supported in a number of bearings. He used a finite difference scheme which could handle non-circular bearing cross-sections.

I.2 SCOPE OF WORK

The work undertaken is divided into three parts :

(i) An improved technique for marching out the journal and

rotor loci. Primarily this involved better utilisation of the information obtained from solving the film equations.

(ii) Calculation of the work performed on the journal by the oil pressure film and with a knowledge of the rotor energy balance, an assessment of the system stability.

(iii) The third section, arising from (ii) is an investigation into the effects of various operating parameters on the work performed on the journal by the oil film.

A successive over-relaxation finite difference scheme is used to solve Reynolds equation and to calculate the displacement and velocity coefficients. The film boundary conditons adopted are those used by Swift :

$$P = \frac{\partial P}{\partial X} = \frac{\partial P}{\partial Z} = 0$$

at film formation and disruption. In defining the bearing model, the main assumptions are incompressible, isoviscous and inertialess lubricant and the journal and bearing are aligned and rigid. These assumptions are discussed more fully in Chapter 2. The model allows a variety of bearing geometries to be analysed, including non-circular cross-sections and axial and circumferential grooving.

The rotor model used is a single mass mounted symmetrically between two similar bearings on a light elastic shaft. This allows the system to be represented by a mass and a light journal joined by a spring. Provision has been made for viscous damping on the mass. Some work was conducted on a twin spring-mass-damper system.

The research undertaken failed to produce an economic technique

for assessing the stability of a bearing-rotor system. However, approaching the problem by analysing the oil pressure film work on the journal was found useful for comparative investigations and has potential for further development.

CHAPTER TWO

FILM EQUATIONS

In this chapter a brief description of the derivation of Reynolds equation is presented, together with the assumptions made for the present investigation. A fuller mathematical treatment of the derivation can be found in Pinkus and Sternlicht[16]. The numerical solution of this equation by the finite difference technique is described and the method used to determine the dynamic bearing coefficients outlined. The final section considers the energy transfer between the oil film and the journal and the influence this has on bearing and rotor stability.

II.1 REYNOLDS EQUATION

The equation of motion for a Newtonian fluid is the Navier Stokes equation. This is derived by considering the forces on an element of fluid and applying Newton's Second Law. The stress-strain relationship for a Newtonian fluid :

$$\tau = \mu \frac{\partial u}{\partial x}$$

is introduced, giving the x component of the general Navier Stokes equation as :

$$\rho fx - \frac{\partial p}{\partial x} + \frac{\partial}{\partial x}\left(2\mu\frac{\partial u}{\partial x} - \frac{2}{3}\mu\left(\frac{\partial u}{\partial x} + \frac{\partial v}{\partial y} + \frac{\partial w}{\partial z}\right)\right)$$

$$+ \frac{\partial}{\partial y}\left(\mu\left(\frac{\partial v}{\partial x} + \frac{\partial u}{\partial y}\right)\right) + \frac{\partial}{\partial z}\left(\mu\left(\frac{\partial u}{\partial z} + \frac{\partial w}{\partial x}\right)\right) = \rho \frac{du}{dt}$$

That is:

body force + pressure force + viscous force = inertia force.

Similarly for the y and z components.

To reduce this to Reynolds equation, the following assumptions are made :

(i) The film thickness, y, is small compared to its expanse in the x and z direction. It is usual design practice to have the clearance ratio, r/R, between .001 and .002. Thus :

(a) the curvature of the bearing is negligible allowing the film to be considered in cartesian co-ordinates;

(b) the pressure and viscosity are constant across the film, thus

$$\frac{\partial p}{\partial y} = \frac{\partial \mu}{\partial y} = 0.$$

The variation of viscosity can be significant, but treating it as a variable makes the problem too complex;

(c) the velocity derivatives with respect to y are greater than those with respect to x and z and the y velocity (v) is less than the other two components (u,w).

(ii) The lubricant inertia forces are small.

(iii) There are no body forces, e.g. gravitational or magneto-hydrodynamic forces.

(iv) The flow is laminar. This is not true for large bearings. The film is turbulent when the Reynolds number $\left(\frac{Ur\rho}{\mu}\right)$ is greater than 2000.

(v) There is no slip at the bearing surfaces. This is satisfactory for liquid lubricants, but considerable slip can occur with thin gas films.

Reynolds, in his analysis, also assumed the lubricant to be incompressible, but it is unnecessary to assume this at this stage.

The three components of the Navier Stokes equations reduce to :

$$\frac{1}{\mu}\frac{\partial p}{\partial x} = \frac{\partial^2 u}{\partial y^2}$$

$$\frac{1}{\mu}\frac{\partial p}{\partial z} = \frac{\partial^2 w}{\partial y^2}$$

Integrating these twice with the boundary conditions :

$$u = U_0 , \quad w = W_0 \text{ at } y = 0$$

$$u = U_h , \quad w = W_h \text{ at } y = h$$

yields :

$$u = \frac{1}{2\mu}\frac{\partial p}{\partial x} y\,(y-h) + (1-\frac{y}{h})\,U_0 + \frac{y}{h}\,U_h$$

$$w = \frac{1}{2\mu}\frac{\partial p}{\partial z} y\,(y-h) + (1-\frac{y}{h})\,W_0 + \frac{y}{h}\,W_h$$

The continuity equation for steady flow is :

$$\frac{\partial \rho u}{\partial x} + \frac{\partial \rho v}{\partial y} + \frac{\partial \rho w}{\partial z} = 0$$

Substitute for u and w, integrate with respect to y between the limits of h and 0 and differentiate to obtain :

$$\frac{\partial}{\partial x}\left(\frac{\rho h^3}{\mu}\frac{\partial p}{\partial x}\right) + \frac{\partial}{\partial z}\left(\frac{\rho h^3}{\mu}\frac{\partial p}{\partial z}\right) = 6\,(U_0-U_h)\frac{\partial \rho h}{\partial x}$$

$$+ 6\rho h \frac{\partial}{\partial x}(U_0+U_h) + 6(W_0-W_h)\frac{\partial \rho h}{\partial z}$$

$$+ 6\rho h \frac{\partial}{\partial z}(W_0+W_h) + 12\rho(V_h-V_0)$$

A number of the terms on the right hand side can be removed when applying this equation to a journal bearing. By taking the z axis as parallel to the bearing centre (Fig.2-1), the velocities W_0 and W_h can be made zero. Any axial movement of the journal would in most cases be small, of a size comparable to the bearing clearance, and occur at a frequency similar to the shaft speed. Thus as $r/R \doteq .001$, $w/u \doteq .001$.

The second term, $6\rho h \frac{\partial}{\partial x}(U_0+U_h)$, is also small. Referring to Fig.2-2, the boundary velocities U_0 and U_h are :

$$U_0 = 0$$

$$U_h = \omega R\cos(\eta+\beta) + \dot{e}\sin(\gamma-\theta-\eta) + e\dot{\gamma}\cos(\gamma-\theta-\eta)$$

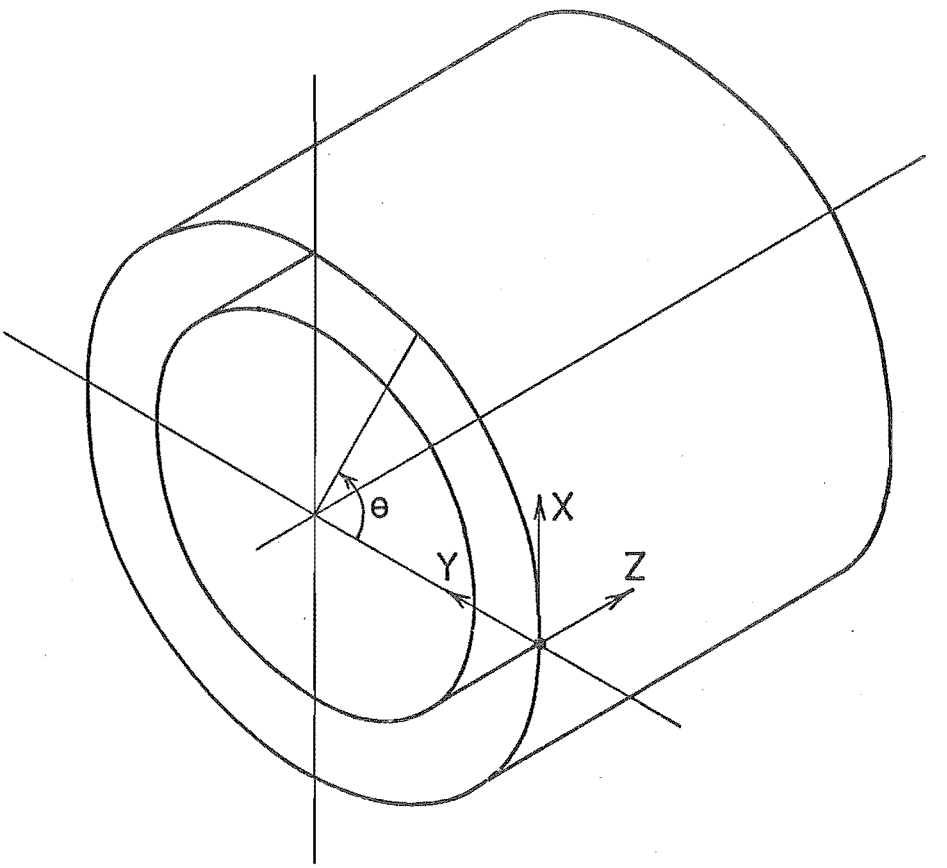

FIG. 2-1 BEARING SURFACE CO-ORDINATE SYSTEM.

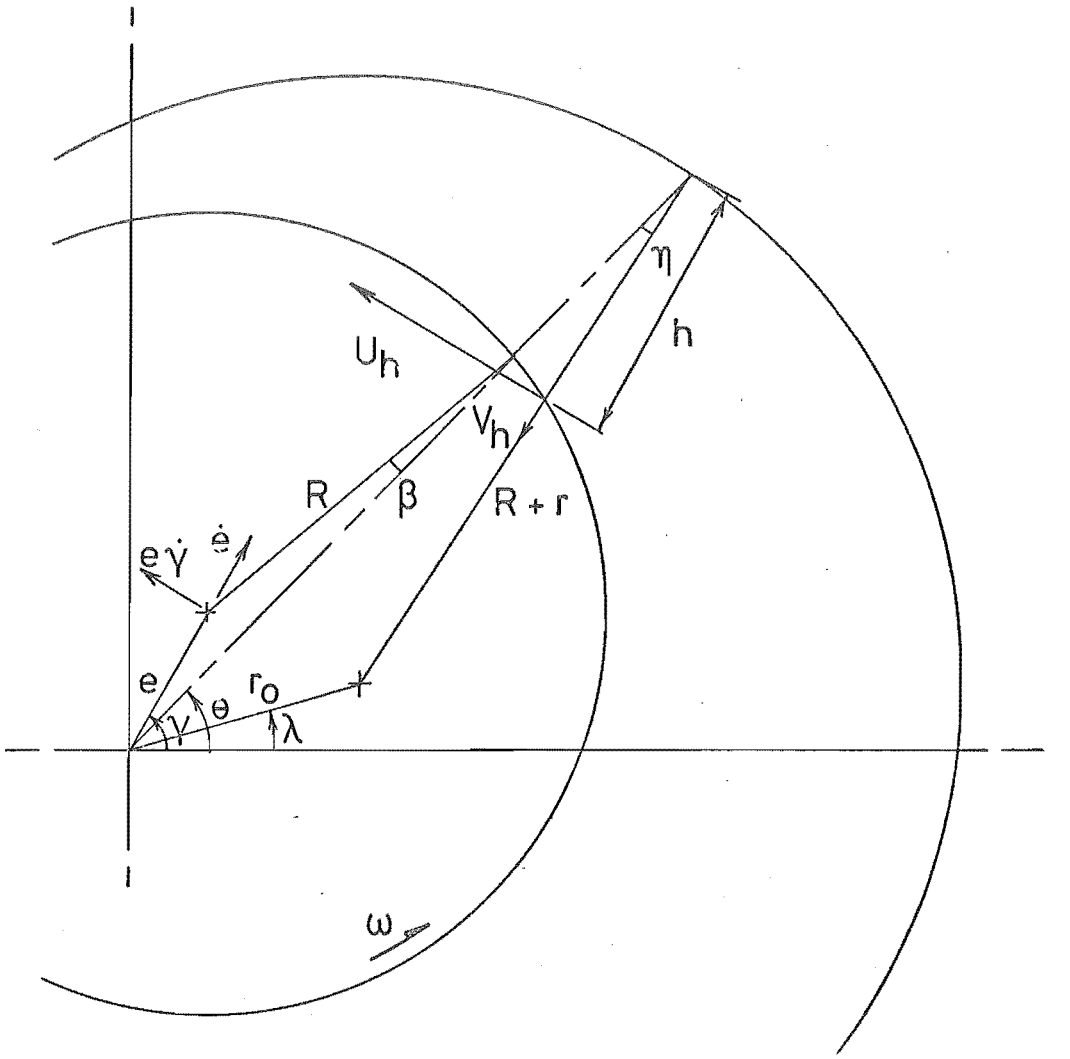

$$h = R + r + r_o \cos(\theta - \lambda + \eta) - e \cos(\gamma - \theta - \eta) - R \cos(\eta + \beta)$$
$$\doteq r + r_o \cos(\theta - \lambda) - e \cos(\theta - \gamma)$$

$$U_h = \omega R \cos(\eta + \beta) + \dot{e} \sin(\gamma - \theta - \eta) + e\dot{\gamma}\cos(\gamma - \theta - \eta)$$
$$\doteq \omega R$$

$$V_h = -\omega R \sin(\eta + \beta) - \dot{e} \cos(\gamma - \theta - \eta) + e\dot{\gamma}\sin(\gamma - \theta - \eta)$$
$$\doteq -\omega e \sin(\gamma - \theta) - \omega r_o \sin(\theta - \lambda) - \dot{e}\cos(\gamma - \theta) + e\dot{\gamma}\sin(\gamma - \theta)$$

FIG. 2-2. BEARING GEOMETRY – DEFINITION OF OIL FILM THICKNESS AND JOURNAL PERIPHERAL VELOCITY.

Differentiate with respect to x and disregard the terms of order $(r/R)^2$ or smaller,

$$h\frac{\partial}{\partial x}(U_0+U_h) \doteq -\frac{h\dot{e}}{R}\cos(\gamma-\theta) + \frac{he}{R}\dot{\gamma}\sin(\gamma-\theta)$$

Again referring to Fig.2-2, the film thickness can be expressed as :

$$h = R+r + r_0\cos(\theta-\lambda-\eta) - e\cos(\gamma-\theta-\eta) - R\cos(\eta+\beta)$$

Differentiate and neglect terms of order $(r/R)^2$ or smaller,

$$\frac{\partial h}{\partial x} \doteq -\frac{r_0}{R}\sin(\theta-\lambda) - \frac{e}{R}\sin(\gamma-\theta)$$

Thus

$$U_h\frac{\partial h}{\partial x} \doteq e\omega\sin(\theta-\gamma) - r_0\omega\sin(\theta-\lambda)$$

Also

$$V_h \doteq -e\dot{\gamma}\sin(\theta-\gamma) - \dot{e}\cos(\theta-\gamma) + \omega e\sin(\theta-\gamma) - \omega r_0\sin(\theta-\lambda)$$

Thus the term containing $h\frac{\partial}{\partial x}(U_0 + U_h)$ is smaller than V_h and $U_h\frac{\partial h}{\partial x}$ by a factor r/R.

Reynolds equation is now reduced to :

$$\frac{\partial}{\partial x}\left(\frac{\rho h^3}{\mu}\frac{\partial p}{\partial x}\right) + \frac{\partial}{\partial z}\left(\frac{\rho h^3}{\mu}\frac{\partial p}{\partial z}\right) = -6U_h\frac{\partial \rho h}{\partial x} + 12\rho V_h$$

For the purpose of the present investigation, four further simplifying assumptions were made, as follows :

(i) The lubricant viscosity is constant throughout the film;

(ii) The lubricant is incompressible;

(iii) The journal and bearing are perfectly aligned, i.e. $\frac{\partial h}{\partial z} = 0$;

(iv) There is no distortion of the journal or bearing surfaces.

All of these can have considerable effect on the bearing performance, particularly when operating at high eccentricities, and other workers have devised theoretical models to consider them. The work reported here was directed towards a rapid solution suitable for design work,

thus the improved accuracy obtained by considering these variables was not required.

It is more convenient to express Reynolds equation in terms of the journal centre displacement and velocity, either in polar or cartesian co-ordinates, and the journal angular velocity. Thus in polar co-ordinates :

$$\frac{\partial}{\partial x}\left(h^3\frac{\partial p}{\partial x}\right) + h^3\frac{\partial^2 p}{\partial z^2} = 6\mu\left[e(\omega-2\dot{\gamma})\sin(\theta-\gamma) - 2\dot{e}\cos(\theta-\gamma) - \omega r_0 \sin(\theta-\lambda)\right] \qquad \ldots 2.1a$$

and in cartesian co-ordinates :

$$\frac{\partial}{\partial x}\left(h^3\frac{\partial p}{\partial x}\right) + h^3\frac{\partial^2 p}{\partial z^2} = 6\mu\left[\omega(xj\sin\theta - yj\cos\theta) - 2(\dot{x}j\cos\theta + \dot{y}j\sin\theta) - \omega r_0 \sin(\theta-\lambda)\right] \qquad \ldots 2.1b$$

II.2 NON-DIMENSIONAL VARIABLES

The variables may be non-dimensionalised with the following substitutions :

Position on the bearing surface :

$$X = \frac{\theta}{2\pi} \qquad Z = \frac{z}{L}$$

Pressure and force :

$$P = \frac{p}{\mu\omega\left(\frac{R}{r}\right)^2} \qquad FX = \frac{fx}{\mu\omega LR\left(\frac{R}{r}\right)^2}$$

Displacements of magnitude comparable to the film thickness are non-dimensionalised by dividing by the radial bearing clearance r :

$$\varepsilon = \frac{e}{r}$$

$$H = \frac{h}{r}$$

$$= 1 + \frac{r_0}{r} \text{Cos } (2\pi X - \lambda) - \epsilon \text{Cos } (2\pi X - \gamma)$$

$$Xj = \frac{x_j}{r}$$

When dealing with dynamic loads and locus stepping it is convenient to non-dimensionalise time. The unit of time is taken as that required for the rotating bearing or rotor load (see Chapter 3) to sweep through one radian. Thus a non-dimensional time step is :

$$DT = \delta\text{time} \cdot \dot{\phi}$$

and velocities are transformed to :

$$\dot{X}j = \frac{\dot{x}j}{r\dot{\phi}}$$

For multi-lobe non-circular bearing designs the value of the radial clearance, r, used in the non-dimensional variables is the minimum radial clearance of the final bearing segment, that is, the segment which ends at θ = 360 degrees (see Fig.2-2).

II.3 FILM BOUNDARY CONDITIONS

Before Reynolds equation can be solved a choice of boundary conditions must be made. Firstly, consider the case when the oil film is not bounded by the bearing geometry, that is, grooves or the bearing edge. There are at least five possible mathematical models.

(i) The oil film is continuous throughout the bearing clearance. This implies a region of negative pressure where the wedge is divergent. It has long been realised that this does not occur and that the film is disrupted if the pressure drops below a certain value.

(ii) The oil film is continuous but negative pressures are disregarded after the solution of Reynolds equation. This

gives moderate agreement with experimental observations and has been used in cases where it simplifies the method of solution[14].

(iii) Film formation occurs at the point of maximum film thickness and breakdown occurs when

$$P = \frac{\partial P}{\partial X} = \frac{\partial P}{\partial Z} = 0$$

commonly used in the literature, this gives satisfactory results for steadily loaded aligned bearings.

(iv) The most sophisticated mathematical model assumes that film breakdown occurs when

$$\frac{\partial P}{\partial X} = \frac{\partial P}{\partial Z} = 0 \; ; \quad P = P_{dis}$$

and the film reforms when

$$\frac{\partial P}{\partial X} = \frac{12\pi}{H^3} \frac{H - H^*}{1 - \left(\frac{\pi D}{L}\right)^2 \left(\frac{\partial P}{\partial X} \Big/ \frac{\partial P}{\partial Z}\right)^2}$$

where

P_{dis} = oil film disruption pressure

H^* = film thickness at breakdown.

This was derived by Floberg and Jakobsson[17] considering the flow balance in the disrupted region. The film will withstand subatmospheric pressures, the disruption pressure being determined by the oil vapour pressure and the pressure at which dissolved gases come out of solution.

This boundary condition is difficult to satisfy computationally. McCallion, Lloyd and Yousif[18] used an iterative loop, involving a number of intermediate solutions to Reynolds equation, to obtain a complete solution. Such a procedure is very expensive and is thus unsuitable for this work.

(v) Film formation and breakdown occurs when

$$\frac{\partial P}{\partial X} = \frac{\partial P}{\partial Z} = P = 0.$$

These are the conditions employed in this thesis. They are ideally suited to the finite difference method of solution as they are invoked simply by setting negative pressures to zero as they occur in the calculation. This model differs from Model (iv) primarily in the point of film formation and the magnitude of the disruption pressure. As these are both low pressure regions the oil film forces will not be greatly affected. These conditions were used by Smalley[19] and found to give good agreement with experimental results.

When the oil pressure film extends the full width of the bearing the axial film boundary condition is :

$$P = 0 \quad \text{when} \quad Z = 0, 1.$$

This implies the film pressure is atmospheric at the edge of the bearing. The pressure derivative, $\frac{\partial P}{\partial Z}$, is not zero as this would deny side leakage.

In a similar manner the junction of the pressure film and a groove can be described. At the edge of the groove the film pressure is set to a predetermined value :

$$P = P_{groove}$$

The value of the pressure derivative was not defined in this investigation as each groove was assumed to supply or absorb sufficient oil to satisfy flow continuity.

II.4 FINITE DIFFERENCE SOLUTION

The method used to solve Reynolds equation is a successive over-

relaxation finite difference scheme on a five point star grid. The program developed (see Chapter 3) is capable of handling grooved bearings of non-circular cross-section thus a flexible method of solution was a prime requirement. As far as the author is aware, this is only offered by finite difference techniques. Many other solutions exist but although quicker to compute, they invariably place greater restrictions on the bearing geometry.

Reynolds Equation

When marching out the journal centre locus it is more convenient to use cartesian than polar co-ordinates. The non-dimensional form of Equation 2.1b is :

$$\frac{\partial}{\partial X} H^3 \frac{\partial P}{\partial X} + \left(\frac{\pi D}{L}\right)^2 H^3 \frac{\partial^2 P}{\partial Z^2} = 24\pi^2 \left(Xj \text{ Sin } 2\pi X - Yj \text{ Cos } 2\pi X - \frac{2\dot{\phi}}{\omega} (\dot{X}j \text{ Cos } 2\pi X - \dot{Y}j \text{ Sin } 2\pi X) - \frac{r_0}{r} \text{Sin}(2\pi X - \lambda) \right) \quad \ldots 2.2$$

To improve numerical accuracy the pressure was replaced by a non-dimensional pressure-height parameter $\bar{P} = PH^2$. This quantity is less dependent on X avoiding the sharp peaks that occur in both the wedge and squeeze pressure films as the journal approaches the bearing surface. Substituting :

$$\frac{\partial^2 \bar{P}}{\partial X^2} - \frac{1}{H} \frac{\partial \bar{P}}{\partial X} \cdot \frac{\partial H}{\partial X} - \frac{2\bar{P}}{H} \frac{\partial^2 H}{\partial X^2} + \left(\frac{\pi D}{L}\right)^2 \frac{\partial^2 \bar{P}}{\partial Z^2} = \frac{24\pi^2}{H} \left(Xj \text{ Sin } 2\pi X - Yj \text{ Cos } 2\pi X - \frac{2\dot{\phi}}{\omega} (\dot{X}j \text{ Cos } 2\pi X - \dot{Y}j \text{ Sin } 2\pi X) - \frac{r_0}{r} \text{ Sin } (2\pi X - \lambda) \right) \quad \ldots 2.3$$

The finite difference technique involves solving this equation at discrete points on the bearing surface. Using Taylor's expansion, the derivatives of the pressure-height parameter are expressed in terms of neighbouring points :

$$\frac{\partial \bar{P}}{\partial X} \doteq \frac{\bar{P}_{X+\Delta X,Z} - \bar{P}_{X-\Delta X,Z}}{2\Delta X} - \left(\frac{\Delta X^2}{6} \frac{\partial^3 \bar{P}}{\partial X^3}\right)$$

$$\frac{\partial^2 \bar{P}}{\partial X^2} \doteq \frac{\bar{P}_{X+\Delta X,Z} - 2\bar{P}_{X,Z} + \bar{P}_{X-\Delta X,Z}}{\Delta X^2} - \left(\frac{\Delta X^2}{12} \cdot \frac{\partial^4 \bar{P}}{\partial X^4}\right)$$

Also the axial derivative

$$\frac{\partial^2 \bar{P}}{\partial Z^2} \doteq \frac{\bar{P}_{X,Z+\Delta Z} - 2\bar{P}_{X,Z} + \bar{P}_{X,Z-\Delta Z}}{\Delta Z^2} - \left(\frac{\Delta Z^2}{12} \frac{\partial^4 \bar{P}}{\partial Z^4}\right)$$

In brackets are the most significant terms not considered. All other terms in Reynolds equation can be calculated directly for any point on the bearing surface.

Substituting into 2.3 gives :

$$\bar{P}_{X,Z} = \left(A_X \cdot \bar{P}_{X+\Delta X,Z} + B_X \cdot \bar{P}_{X-\Delta X,Z} + (\bar{P}_{X,Z+\Delta Z} + \bar{P}_{X,Z-\Delta Z}).C - RHS_X\right) / D_X \qquad \ldots 2.4$$

where

$$A_X = \frac{1}{\Delta X}\left(\frac{1}{\Delta X} - \frac{1}{2}\frac{\partial H}{\partial X}\right)$$

$$B_X = \frac{1}{\Delta X}\left(\frac{1}{\Delta X} + \frac{1}{2}\frac{\partial H}{\partial X}\right)$$

$$C = \left(\frac{\pi D}{L\Delta Z}\right)^2$$

$$RHS_X = \frac{24\pi^2}{H}\left(Xj \text{ Sin } 2\pi X - Yj \text{ Cos } 2\pi X - \frac{2\dot{\phi}}{\omega}(\dot{X}j \text{ Cos } 2\pi X - \dot{Y}j \text{ Sin } 2\pi X) - \frac{r_0}{r} \text{ Sin } (2\pi X - \lambda)\right)$$

$$D_X = \frac{2}{\Delta X^2} + 2\left(\frac{\pi D}{L\Delta Z}\right)^2 + \frac{2}{H}\frac{\partial^2 H}{\partial X^2}$$

The bearing surface is divided into a rectangular grid of m circumferential divisions and n axial divisions. The value of $\bar{P}_{X,Z}$ is calculated at each grid point in turn, sweeping from one end of the bearing surface to the other. This process is repeated (the relaxation part of the scheme) until successive values at each grid point differ

by less than a predetermined convergence accuracy criterion.

To increase the speed of convergence an over-relaxation factor, ORF, is used. The new estimate of the pressure-height parameter is made equal to the old estimate plus the over-relaxation factor times the change in the parameter.

$$\bar{P}^{n+1}_{X,Z} = \bar{P}^{n}_{X,Z} + ORF\left(\bar{P}^{n+1}_{X,Z} - P^{n}_{X,Z}\right)$$

Relaxation Grid

The bearing surface is divided into a rectangular grid of m by n divisions in the circumferential and axial directions respectively. The divisions in each are of constant length, thus :

$$X = \frac{1}{m}$$

$$Z = \frac{1}{n}$$

the non-dimensional bearing surface dimensions being 1 by 1. Variable grid divisions have been used by other workers[14] to give better accuracy in regions of high pressure, but for dynamically loaded non-circular bearing geometries these are difficult to program.

Bearing geometries are restricted to those having symmetry about the circumferential centre line of the bearing surface. This is not a severe constraint, as most designs exhibit this property and it allowed the relaxation process to be limited to half the bearing surface. The existence of the second half of the bearing is accounted for in the numerical procedure by the boundary condition :

$$\bar{P}_{X,\,\frac{1}{2}-\Delta Z} = \bar{P}_{X,\,\frac{1}{2}+\Delta Z}$$

Values of m and n of 48 and 8 were chosen for the work in this

thesis. This was based on a publication by Smalley, Lloyd, Horsnell and McCallion[20] giving the following results for a plain circular bearing of length to diameter ratio .75 using these grid dimensions.

E	.5	.8	.95
% Load Error	.2	.9	6.0
Basis of Error (Grid Size)	96 x 8	96 x 8	192 x 8

They also found that doubling the number of axial divisions made less than 1% improvement in the accuracy of the load parameter.

Boundary Conditions

The finite difference equation, 2.4, requires knowledge of the pressure-height parameter one grid point on each side of the point of calculation. Thus the grid must be one row in each direction greater than the region swept by the relaxation procedure.

In the axial direction the pressure at the edge of the bearing is zero and at the centre, where the surface is free from grooves, the pressure-height parameter is reflected across the centre line as it is calculated :

$$\bar{P}_{X,0} = 0 \quad , \quad \bar{P}_{X,\frac{1}{2}+\Delta Z} = \bar{P}_{X,\frac{1}{2}-\Delta Z}$$

These two points are outside the swept region and form the axial boundaries

Many bearing designs have, in the circumferential direction, a discontinuity in the bearing surface. This is usually a step or an abrupt alteration in the change of the film thickness, i.e. a discontinuity in

the first derivative. To allow the program to handle such designs it was decided to place a groove at each discontinuity (see III-2). In this way oil flow and pressure balances can be easily achieved.

When such features are absent, the bearing surface is continuous and the ends of the finite difference grid must be linked. This is achieved by setting

$$\bar{P}_{1+\Delta X,Z} = \bar{P}_{\Delta X,Z} \qquad \bar{P}_{-\Delta X,Z} = \bar{P}_{1-\Delta X,Z} .$$

Again the points on the left of these equalities are outside the swept region.

The extent of the oil pressure film on the unbroken bearing surface is fixed for both build-up and breakdown by setting negative values of the pressure-height parameter to zero as they occur in the relaxation procedure. This automatically imposes the boundary conditions :

$$P = \frac{\partial P}{\partial X} = \frac{\partial P}{\partial Z} = 0$$

discussed earlier.

Grooves are allowed for by setting the pressure at each grid point within the grooved area to a predetermined value and not modifying this with the relaxation procedure.

Over-Relaxation Factor

The over-relaxation factor is approximately optimised using the equations given by Lloyd and McCallion[21], namely :

$$ORF = \frac{2(1 - (1 - a^2)^{\frac{1}{2}})}{a^2}$$

where $$a = 1 - \frac{\pi^2 (4 + \left(\frac{\pi D}{L}\right)^2)}{2(m^2 + \left(\frac{\pi D n}{L}\right)^2)}$$

Thus this factor is dependent only on the bearing length to diameter ratio and the number of grid points.

An alternative scheme, developed by Carre[22] was considered. It involves calculating the over-relaxation factor as the relaxation proceeds and iterates to an optimum value. This would have meant a loss in efficiency as the first cycles of relaxation are computed without over-relaxation. Also, although not so important, it would have complicated the relaxation routine.

Lloyd and McCallion compared the values of the over-relaxation factor calculated by those two methods and found good agreement.

Relaxation Convergence Criterion

The relaxation process is continued until the maximum fractional change in the pressure-height parameter between successive iterations is less than the convergence tolerance ACC. This is achieved by checking the inequality :

$$\bar{P}^{n+1} - \bar{P}^{n} < ACC. \bar{P}^{n+1}$$

at each grid point and if this is found to be true over the entire grid the relaxation is terminated.

The value of ACC used in the work described in this thesis is 10^{-3}. This was chosen after a series of tests on a statically loaded plain circular bearing. Four eccentricity ratios were considered, .2, .5, .8 and .95 and for each the oil film forces were computed for convergence tolerances of 10^{-6}, 10^{-4}. 10^{-3} and 10^{-2}. The number of relaxation

cycles required was also recorded.

The results are tabulated in Figure 2-3. The change in the oil film forces as the tolerance is raised was small compared to the errors introduced by the pressure summation and grid dimensions. However, the saving in time, or number of relaxation cycles, was also small. Increasing the tolerance from 10^{-3} to 10^{-2} saved, on an average, 4½ cycles, but to ensure a minimal convergence error this was sacrificed. Lowering it to 10^{-4} incurred a greater time penalty whilst producing considerably less improvement in the accuracy.

II.5 OIL FILM FORCES

The oil film forces are calculated by integrating the pressure over the bearing surface :

$$FX = 2\pi \int_0^1 \int_0^1 P_{X,Z} \cos 2\pi X . dZ . dX$$

$$FY = 2\pi \int_0^1 \int_0^1 P_{X,Z} \sin 2\pi X . dZ . dX$$

where FX and FY are the components of the non-dimensional load that can be applied to the journal (see Fig.2-4). From these the load parameter and attitude angle are given by

$$DEL = (FX^2 + FY^2)^{\frac{1}{2}}$$

$$\psi = \gamma - \tan^{-1}\left(\frac{FY}{FX}\right)$$

The integration is performed numerically by Simpson's rule in the axial direction and the trapezoidal rule in the circumferential direction.

ECCENTRICITY RATIO	CONVERGENCE TOLERANCE	OIL FILM FORCE	X COMPONENT	Y COMPONENT	NO. OF ITERATION CYCLES
.2	10^{-6}	.319571	−.311245	−.0724731	58
	10^{-4}	.319571	−.311245	−.0724733	45
	10^{-3}	.319571	−.311245	−.0724745	39
	10^{-2}	.319566	−.311237	−.0724845	33
.5	10^{-6}	1.18742	−.647158	−.995570	54
	10^{-4}	1.18742	−.647159	−.995569	42
	10^{-3}	1.18742	−.647167	−.995563	35
	10^{-2}	1.18742	−.647196	−.995542	31
.8	10^{-6}	5.49151	−4.50276	−3.14354	57
	10^{-4}	5.49151	−4.50276	−3.14354	41
	10^{-3}	5.49152	−4.50277	−3.14353	34
	10^{-2}	5.49152	−4.50279	−3.14352	32
.95	10^{-6}	33.5149	−31.7853	−10.6274	54
	10^{-4}	33.5149	−31.7853	−10.6274	44
	10^{-3}	33.5149	−31.7853	−10.6274	39
	10^{-2}	33.5149	−31.7853	−10.6274	33

FIG. 2-3 EFFECT OF RELAXATION CONVERGENCE TOLERANCE (ACC) ON THE NUMBER OF CYCLES OF CALCULATION AND ON THE CHANGE IN THE OIL FILM FORCE VALUES CALCULATED.

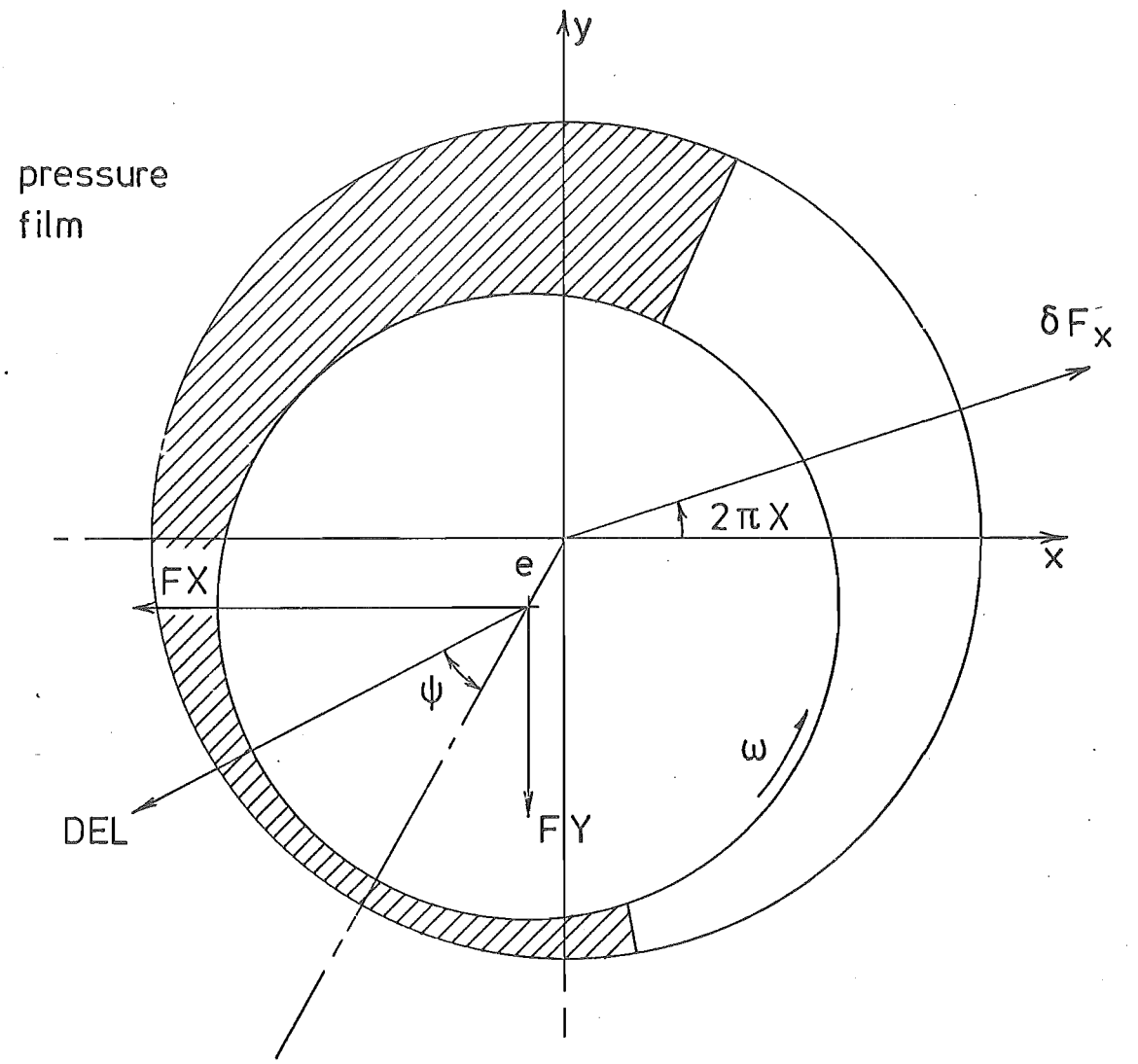

FIG. 2-4 OIL FILM FORCE SIGN CONVENTION.
FORCES REPRESENT THE LOAD THAT CAN BE APPLIED TO THE JOURNAL. COMPONENTS SHOWN HAVE NEGATIVE VALUES.

Axial Summation

The integration performed is :

$$\delta F_X = \int_0^1 P_{X,Z}\, dZ$$

along each axial grid line in the pressure film.

Applying Simpson's rule we have :

$$\delta F_X = \frac{\Delta Z}{3}\left[P_{X,0} + 4P_{X,\Delta Z} + 2P_{X,2\Delta Z} \cdots\cdots\cdots + 4P_{X,\frac{1}{2}-\Delta Z} + 2P_{X,\frac{1}{2}} \cdots\cdots\cdots + 4P_{X,1-\Delta Z} + P_{X,1}\right]$$

However, the pressure at the edge of the bearing is zero :

$$P_{X,0} = P_{X,1} = 0$$

and the pressure distribution is symmetrical about the bearing centre line, that is :

$$P_{X,\frac{1}{2}-i\Delta Z} = P_{X,\frac{1}{2}+i\Delta Z} \qquad i = 1,2,\ldots\ldots \frac{n}{2}$$

Thus the integral contracts to :

$$\delta F_X = \frac{2.\ \Delta Z}{3}\left[4P_{X,\Delta Z} + 2P_{X,2\Delta Z} \cdots\cdots + P_{X,\frac{1}{2}}\right]$$

Circumferential Summation

The two integrals are :

$$FX = 2\pi \int_a^b \delta F_X \,\mathrm{Cos}\, 2\pi X.dX$$

$$FY = 2\pi \int_a^b \delta F_X \,\mathrm{Sin}\, 2\pi X.dX$$

where a and b are the positions of film formation and breakdown respectively for each pressure film. With non-circular bearing geometries there is usually more than one pressure film due to the fact that a number of converging clearances exist. The numerical form of these integrals, using the trapezoidal rule, is :

$$FX = 2\pi.\Delta X \left[\frac{1}{2}\delta F_a \text{ Cos } 2\pi a + \delta F_{a+\Delta X} \text{ Cos } 2\pi(a + \Delta X) \ldots\ldots + \frac{1}{2}\delta F_b \text{ Cos } 2\pi b\right]$$

$$FY = 2\pi.\Delta X \left[\frac{1}{2}\delta F_a \text{ Sin } 2\pi a + \ldots\ldots \delta F_{b-\Delta X} \text{ Sin } 2\pi(b-\Delta X) + \frac{1}{2}\delta F_b \text{ Sin } 2\pi b\right]$$

Accuracy

The choice of the numerical integration techniques was made with reference to the work carried out by Lloyd[14]. He found that in the circumferential direction, Simpson's rule was not significantly better than the trapezoidal rule. For an infinitely short bearing (Ocvirk solution) with 32 circumferential mesh points, the summation error was found to be less than 1% for ε less than 0.9 rising to 5% at ε = .97.

The axial summation was found by Lloyd to require Simpson's rule. This gave an error of less than 1% for a unit squeeze film ($\frac{\dot{\varepsilon}}{\omega} = 1$) when ε = .975 and $\frac{L}{D}$ = .75.

II.6 DYNAMIC BEARING COEFFICIENTS

The dynamic bearing coefficients are required for marching out the journal centre locus (see Chapter 3). The coefficients are the partial derivatives of the oil film force components with respect to the journal displacement and velocity. Thus small changes in the film force can be

calculated from the relationships.

$$FX \doteq FX_0 + \frac{\partial FX}{\partial Xj} . \delta Xj + \frac{\partial FX}{\partial Yj} . \delta Yj + \frac{\partial FX}{\partial \dot{X}j} . \delta \dot{X}j + \frac{\partial FX}{\partial \dot{Y}j} . \delta \dot{Y}j$$

$$FY \doteq FY_0 + \frac{\partial FY}{\partial Xj} . \delta Xj + \frac{\partial FY}{\partial Yj} . \delta Yj + \frac{\partial FY}{\partial \dot{X}j} . \delta \dot{X}j + \frac{\partial FY}{\partial \dot{Y}j} . \delta \dot{Y}j$$

The derivatives, or dynamic bearing coefficients, are themselves functions of Xj, Yj, $\dot{X}j$ and $\dot{Y}j$, thus the relationship is true only for small changes in these parameters.

The oil film thickness at a small journal displacement δXj, δYj from a known position Xj_0, Yj_0, is given by

$$H \doteq H_0 + \frac{\partial H}{\partial Xj} . \delta Xj + \frac{\partial H}{\partial Yj} . \delta Yj$$

The pressure-height parameter can be expressed in a similar form :

$$\bar{P} = \bar{P}_0 + \frac{\partial \bar{P}}{\partial Xj} . \delta Xj + \frac{\partial \bar{P}}{\partial Yj} . \delta Yj + \frac{\partial \bar{P}}{\partial \dot{X}j} . \delta \dot{X}j + \frac{\partial \bar{P}}{\partial \dot{Y}j} . \delta \dot{Y}j \quad \ldots 2.5$$

Substituting these into Reynolds equation, 2.3, and varying each of the journal parameters Xj, Yj, $\dot{X}j$ and $\dot{Y}j$ in turn, four partial differential equations can be obtained :

$$H_0 Re\left(\frac{\partial \bar{P}}{\partial Xj}\right) = 24\pi^2 \operatorname{Sin} 2\pi X + RHS.\operatorname{Cos} 2\pi X + 2\bar{P}_0 \left(4\pi^2 \operatorname{Cos} 2\pi X + \frac{\operatorname{Cos} 2\pi X}{H_0} . \frac{\partial^2 H_0}{\partial X^2}\right) + \frac{\partial \bar{P}_0}{\partial X} \left(2\pi \operatorname{Sin} 2\pi X + \frac{\operatorname{Cos} 2\pi X}{H_0} . \frac{\partial H_0}{\partial X}\right)$$

$$H_0 Re\left(\frac{\partial \bar{P}}{\partial Yj}\right) = -24\pi^2 \operatorname{Cos} 2\pi X + RHS.\operatorname{Sin} 2\pi X + 2\bar{P}_0 \left(4\pi^2 \operatorname{Sin} 2\pi X + \frac{\operatorname{Sin} 2\pi X}{H_0} . \frac{\partial^2 H_0}{\partial X^2}\right) + \frac{\partial \bar{P}_0}{\partial X} \left(-2\pi \operatorname{Cos} 2\pi X + \frac{\operatorname{Sin} 2\pi X}{H_0} . \frac{\partial H_0}{\partial X}\right)$$

$$H_0 Re\left(\frac{\partial \bar{P}}{\partial \dot{X}j}\right) = -48\pi^2 \frac{\dot{\phi}}{\omega} \text{Cos } 2\pi X$$

$$H_0 Re\left(\frac{\partial \bar{P}}{\partial \dot{Y}j}\right) = -48\pi^2 \frac{\dot{\phi}}{\omega} \text{Sin } 2\pi X$$

where

$$Re\left(\frac{\partial \bar{P}}{\partial Xj}\right) = \frac{\partial^2}{\partial X^2}\left(\frac{\partial \bar{P}}{\partial Xj}\right) - \frac{1}{H_0}\frac{\partial H_0}{\partial X}\frac{\partial}{\partial X}\left(\frac{\partial \bar{P}}{\partial Xj}\right) - \frac{2}{H_0}\frac{\partial^2 H_0}{\partial X^2}\left(\frac{\partial \bar{P}}{\partial Xj}\right) + \left(\frac{\pi D}{L}\right)^2 \frac{\partial^2}{\partial Z^2}\left(\frac{\partial \bar{P}}{\partial Xj}\right)$$

$$RHS = \frac{24\pi^2}{H_0}\left(Xj \text{ Sin } 2\pi X - Yj \text{ Cos } 2\pi X - \frac{2\dot{\phi}}{\omega}\left(\dot{X}j \text{ Cos } 2\pi X - \dot{Y}j \text{ Sin } 2\pi X\right) - \frac{r_0}{r} \text{Sin } (2\pi x - \lambda)\right) \qquad ...2.6$$

These four partial differential equations are solved by a finite difference scheme similar to that used for determining the film pressure. The pressure-height parameter is then replaced with the pressure by the relationship :

$$\frac{\partial P}{\partial a} = \frac{1}{H^2}\left(\frac{\partial \bar{P}}{\partial a} - \frac{2\bar{P}}{H}\frac{\partial H}{\partial a}\right) \qquad a = Xj,\ Yj,\ \dot{X}j,\ \dot{Y}j$$

and the derivative summed over the bearing surface to give the two force derivatives :

$$\frac{\partial FX}{\partial a},\ \frac{\partial FY}{\partial a}$$

The boundary condition used for the finite difference scheme is that the pressure derivatives $\frac{\partial P}{\partial a}$ are zero outside the pressure film and at all points inside a groove. The program maintains the groove pressure at a constant value thus the derivatives are automatically zero. On the axial boundary of the pressure film

$$P_{X,0} = P_{X,1} = 0$$

which again are independent of the journal position and velocity.

In the circumferential direction this boundary condition implies that the extent of the pressure film remains constant. This is satisfactory as the dynamic bearing coefficients are correct only for the particular oil pressure film that existed when calculating P_0. It was assumed that the infinitesimal changes in the journal displacement and velocity implied in the definition of the pressure derivative :

$$\frac{\partial P}{\partial a} = \lim_{\Delta a \to 0} \frac{\Delta P}{\Delta a} \qquad a = Xj,\ Yj,\ \dot{X}j,\ \dot{Y}j$$

have little effect on the position of the oil pressure film boundaries.

As for the pressure distribution, symmetry about the bearing surface centre line is maintained thus the relaxation is performed only on half the bearing surface.

The over-relaxation factor employed is the same as that used for the pressure calculation (Section II.4). The equations to be solved, 2.6, are the same type, second order elliptical, and the variables that determine the over-relaxation factor, that is, the mesh size and bearing length to diameter ratio, have the same value.

Relaxation Convergence Criterion

The accuracy requirement for the dynamic bearing coefficients is not as severe as for the oil film force. The coefficients are used to estimate the film force in each locus step and are assumed to apply over a range of journal displacements and velocities. The coefficients actually vary in a non-linear manner and this is the major limiting factor on the step length. Small errors in calculating them will, therefore, have minor influences on the program behaviour. The forces calculated from the pressure distribution are used to check the accuracy of each locus step and are thus required to be of a higher accuracy than that of

the dynamic bearing coefficients.

A further consideration was computation time. Four relaxation procedures are required to calculate the eight coefficients but only one for the oil film force. Time-saving in the calculation of the coefficients is thus of much more importance to program efficiency.

Relaxation is terminated when the change in the relaxed parameter between successive iteration cycles at every grid point is less than the tolerance set.

$$\frac{\partial \bar{P}}{\partial a}^{n+1} - \frac{\partial \bar{P}}{\partial a}^{n} < 10.\mathrm{ACC}.\left(\frac{\partial \bar{P}}{\partial a}^{n}\right)_{max}$$

$$a = Xj,\ Yj,\ \dot{X}j,\ \dot{Y}j$$

Basing the tolerance on the maximum parameter value, $\left(\frac{\partial \bar{P}}{\partial a}^{n}\right)_{max}$, ensures that convergence is not held up by minor changes in regions of small parameter values. The choice of ten times the tolerance used in the pressure relaxation was made after conducting trial computations on a plain circular bearing for unit wedge (effective rotational speed of the journal, $1 - \frac{2\dot{Y}}{\omega}$, of 1.0) and unit squeeze films (radial journal velocity of 1.0). These results are shown in Figures 2-5 and 2-6.

Two calculations were made at each journal velocity and displacement. The first with ACC set at 10^{-3} and the second at 10^{-7} to form a basis for the error calculations. The relaxation cycles required for each calculation and the percentage error in the coefficients are shown. The velocity coefficients, bxy and byx, for the squeeze film are not shown as these are theoretically zero and thus error calculations would be meaningless.

ECCENTRICITY RATIO	% ERROR *		CYCLES FOR † ACC OF		% ERROR		CYCLES FOR ACC OF		% ERROR		CYCLES FOR ACC OF		% ERROR		CYCLES FOR ACC OF	
	kxx	kyx	10^{-7}	10^{-3}	kxy	kyy	10^{-7}	10^{-3}	bxx	byx	10^{-7}	10^{-3}	bxy	byy	10^{-7}	10^{-3}
·2	5·0	·5	44	16	1·1	2·6	43	16	1·2	5·4	43	16	5·6	·6	45	16
·5	1·2	·32	44	16	·36	·37	43	17	·5	1·0	43	17	1·6	·33	44	16
·8	·11	·12	42	17	—	—	42	18	·13	·15	42	18	·2	—	43	17
·95	—	—	44	20	—	—	43	19	—	—	42	18	—	—	44	20

* Percentage error based on value of coeffient calculated with convergence tolerance (ACC) of 10^{-7}. Errors less than 0·1% shown as —.

† No. of iteration cycles required to calculate the coefficients for convergence tolerances (ACC) of 10^{-7} and 10^{-3}.

FIG. 2-5 EFFECT OF RELAXATION CONVERGENCE TOLERANCE ON THE ACCURACY AND NUMBER OF CYCLES OF CALCULATION OF THE DYNAMIC BEARING COEFFICIENTS. UNIT WEDGE OIL PRESSURE FILM.

ECCENTRICITY RATIO	% ERROR *		CYCLES FOR† ACC OF		% ERROR		CYCLES FOR ACC OF		% ERROR		CYCLES FOR ACC OF		% ERROR		CYCLES FOR ACC OF	
	kxx	kyx	10^{-7}	10^{-3}	kxy	kyy	10^{-7}	10^{-3}	bxx	byx	10^{-7}	10^{-3}	bxy	byy	10^{-7}	10^{-3}
·2	·7	1·6	42	15	2·4	·12	38	14	·54		44	15		1·3	41	15
.5	·45	·9	39	14	1·4	—	38	15	·42		40	13		·38	37	15
·8	—	—	40	14	·12	—	38	16	·13		41	14		—	39	15
·95	—	—	42	17	·14	—	39	15	—		42	15		—	42	17

* Percentage error based on value of coefficient calculated with convergence tolerance (ACC) of 10^{-7}. Errors less than 0·1% shown as —.

† No. of iteration cycles required to calculate the coefficients for convergence tolerances (ACC) of 10^{-7} and 10^{-3}.

FIG. 2-6. EFFECT OF RELAXATION CONVERGENCE TOLERANCE ON THE ACCURACY AND NUMBER OF CYCLES OF CALCULATION OF THE DYNAMIC BEARING COEFFICIENTS. UNIT SQUEEZE OIL PRESSURE FILM.

The choice of the tolerance was a compromise between accuracy and speed. The value, 10^{-3}, gave good accuracies for eccentricities above 0.5 with computation times of half those for the pressure calculation. The errors increased as the eccentricity ratio was reduced, but they remained of the same order as the errors introduced by using the bearing coefficients in the locus marching procedure.

II.7 OIL FILM WORK

The stability of a rotating system is very much dependent on the behaviour of its bearings. The bearings provide a mechanism to excite or dampen the vibratory motion of the rotor, drawing energy from the rotation of the shaft. This is particularly important with hydrodynamic bearings because the asymmetry of the oil pressure film enables considerable quantities of energy to be transferred.

There are three mechanisms of oil pressure film generation :

(i) Hydrostatic: The pressure in the bearing grooves is created by external pumping.

(ii) Wedge: This is the dragging of the oil into the converging film by the rotation of the journal. The film is modified by the angular velocity of the journal about the bearing centre.

(iii) Squeeze: A radial journal velocity produces a pressure film by forcing the oil out from between the closing journal and bearing surfaces. This film is symmetrical about the eccentricity vector.

The wedge and squeeze terms can be seen in the polar co-ordinate form of Reynolds equation (2.1a). The right hand side of this is :

$$RHS = 6\mu(e(\omega - 2\dot{\gamma}) \text{ Sin } (\theta - \gamma) - 2\dot{e} \text{ Cos } (\theta - \gamma) - \omega r_0 \text{Sin } (\theta - \lambda)$$

Wedge Squeeze

The third term applies to non-circular geometries where the bearing segment centre and the co-ordinate system centre do not coincide.

The effect of the journal centre angular velocity on the wedge film is clearly shown. For $\dot{\gamma}$ less than half the shaft speed, a trailing film exists as depicted in Fig. 2-7. The oil film force has a component in the direction of the journal motion, provided the journal centre rotation is in the same direction as the shaft rotation, and energy is fed into the rotating system. Damping occurs if $\dot{\gamma} > \frac{\omega}{2}$ as a leading film is formed.

The condition $\dot{\gamma} = \frac{\omega}{2}$ is known as half speed whirl. The wedge film ceases to exist leaving the squeeze film to support the bearing load. Obviously a positive radial velocity cannot be maintained indefinitely and the journal collapses onto the bearing surface. Physically half speed whirl occurs when the velocity of the wedge is equal to the mean velocity of the carried flow. Continuity is satisfied at all points on the bearing surface, thus the mechanism of wedge film generation no longer exists.

The influence of the wedge film on the stability of a system is perhaps most clearly shown by the model in Figure 2-8. This model represents a light elastic shaft, stiffness 2Ks, with a central rotor mass 2Mr mounted in two identical light plain circular journal bearings. The system is depicted whirling about the bearing centre with angular velocity $\dot{\gamma}$, equal to the natural frequency of the system, and a trailing film. The work done by the oil pressure film on the journal per rotor revolution, assuming a constant eccentricity, is :

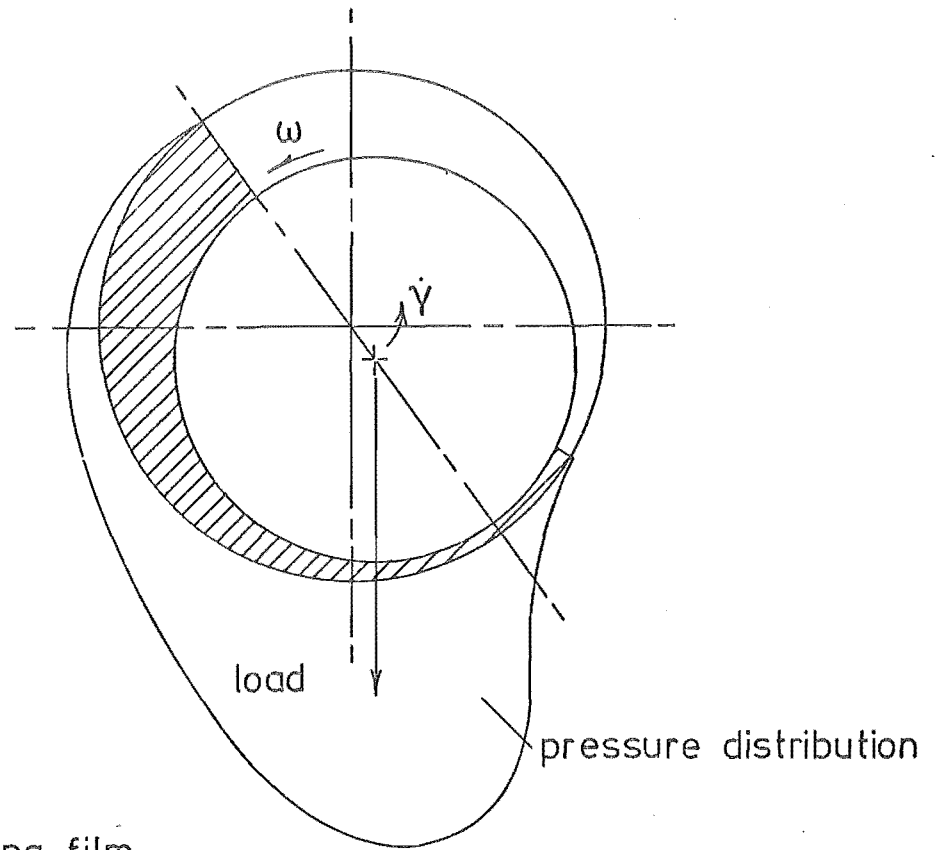

trailing film

$\dot{\gamma} < \omega/2$

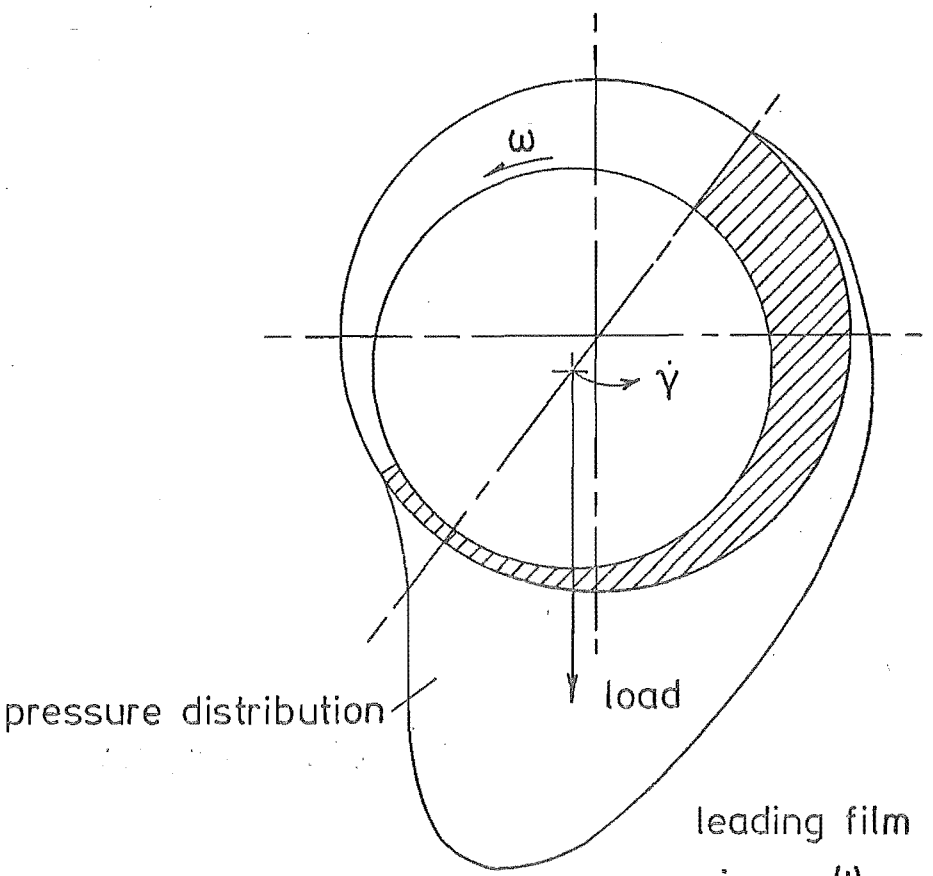

leading film

$\dot{\gamma} > \omega/2$

FIG. 2-7 WEDGE OIL PRESSURE CONFIGURATIONS

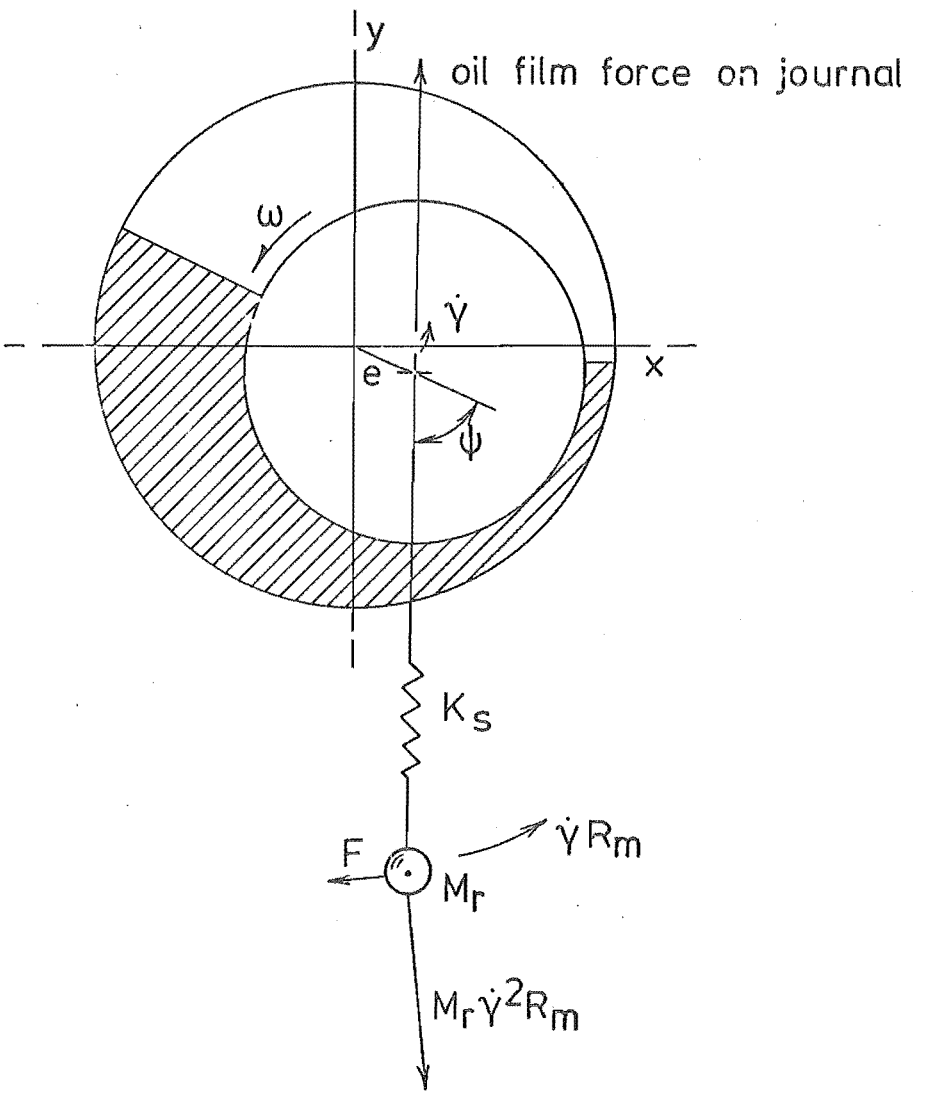

FIG. 2-8 SIMPLE ROTOR MODEL; SINGLE MASS AND LIGHT JOURNAL.

$$WORK = DEL.Sin\psi.2\pi\varepsilon.$$

A force balance on the rotor mass can be achieved only with the addition of the force F. This may be applied as damping or by acceleration of the rotor. An elementary analysis of the system geometry will show that the energy dissipated in the damper, or added to the rotor, equals the pressure film work. Thus, the trailing film excites the rotor.

In general, the oil film work is too complex to assess analytically so numerical methods are required. The journal centre locus is marched out in time and the work increment calculated at each step :

$$\delta WORK = -(FXJ_n + FXJ_{n-1}) \frac{\delta Xj}{2} - (FYJ_n + FYJ_{n-1}) \frac{\delta Yj}{2} \qquad ...2.7$$

where $FXJ_{n-1} FYJ_{n-1}$ = Journal load components at the beginning of the nth step.

FXJ_n, FYJ_n = Journal load components at the end of the nth step.

$\delta Xj, \delta Yj$ = Journal centre step.

The force applied to the journal is used in this equation. In marching out the journal locus the journal position and velocity at the end of a time step are estimated to achieve a force balance on the journal between the applied load and the oil film force (see III.3). For each locus step errors are introduced into the work calculation by the incorrect journal step and the incorrect forces resulting from calculating the film forces at a displacement and velocity containing the locus step error. By using the applied journal load the latter is avoided, but this does not necessarily improve the accuracy of the calculation. For example, with a linear elastic system (i.e. a simple spring), the work is determined by the end conditions and is thus independent of the intermediate steps. If the relationship between the displacement and force is modified, as would happen if the applied

load was used for the work calculation instead of the calculated force, the accuracy for a step would improve, but not the calculation as a whole. Numerical experiments were conducted (see VI.1) and these showed no significant difference between the two methods of calculation for a wedge oil pressure film.

When calculating the oil film work the bearing can be loaded by the rotor or the latter can be represented by a force locus. Initially a circular force locus, that is, a constant magnitude vector rotating at constant speed with the possible addition of a static component, was used for this purpose, but except for a few special cases, it was found to be inadequate. In general, even an undamped single mass rotor model was found to be too complex to represent as a simple force locus. However, this technique is of benefit to assess the stability characteristics of a rotor bearing combination. This is discussed fully in Chapter 6.

The oil film subjects the journal to a viscous shear drag. Again, because of the film asymmetry, this affects the journal's transverse motion. The frictional force has two parts, one due to the pressure flow and the second to the carried flow. By considering the velocity profile, the shear force at any point on the journal surface is :

$$\delta SF = \frac{r}{R}\left(\frac{H}{4\pi}\frac{\partial P}{\partial X} + \frac{1}{H}\right) 2\pi\delta X.\delta Z \qquad \ldots 2.8$$

If the x and y components of this are summed, the film asymmetry leaves a resultant force on the journal.

The effect of friction was not included in the analysis for two reasons :

(i) The effect of the friction is stabilizing on an unstable

system. Cameron, Akers and Michaelson[23] found that the friction was stabilizing although it was never found to transform an unstable system to a stable one. Omission of friction thus errs on the side of safety.

(ii) The effect is small. The first term in Equation 2.8, the shear force due to the oil film pressure, can be integrated over the bearing surface to give the drag force for a wedge film in a plain circular bearing.

$$\frac{\text{FORCE}}{\text{DEL}} = \frac{r}{R}\,\frac{\varepsilon}{2}\,\text{Sin}\,\psi\ .$$

Derivation of this equation can be found in Cameron[24]. Consider the magnitude of each term :

$$\text{Sin}\,\psi < 1$$

$$\varepsilon/2 \ < .5$$

$$r/R \ = 0(.001)$$

Thus:

$$\frac{r}{R}\cdot\frac{\varepsilon}{2}\cdot\text{Sin}\,\psi \ = \ 0(.05\%)$$

This is the total drag force arising from the pressure flow, thus any translational forces generated will be of equal or smaller magnitude.

The x and y components of the shear force due to the carried flow can also be determined by integration over the bearing surface. Consider a position X on the bearing surface as shown in Figure 2-9. The x and y components of the shear force are :

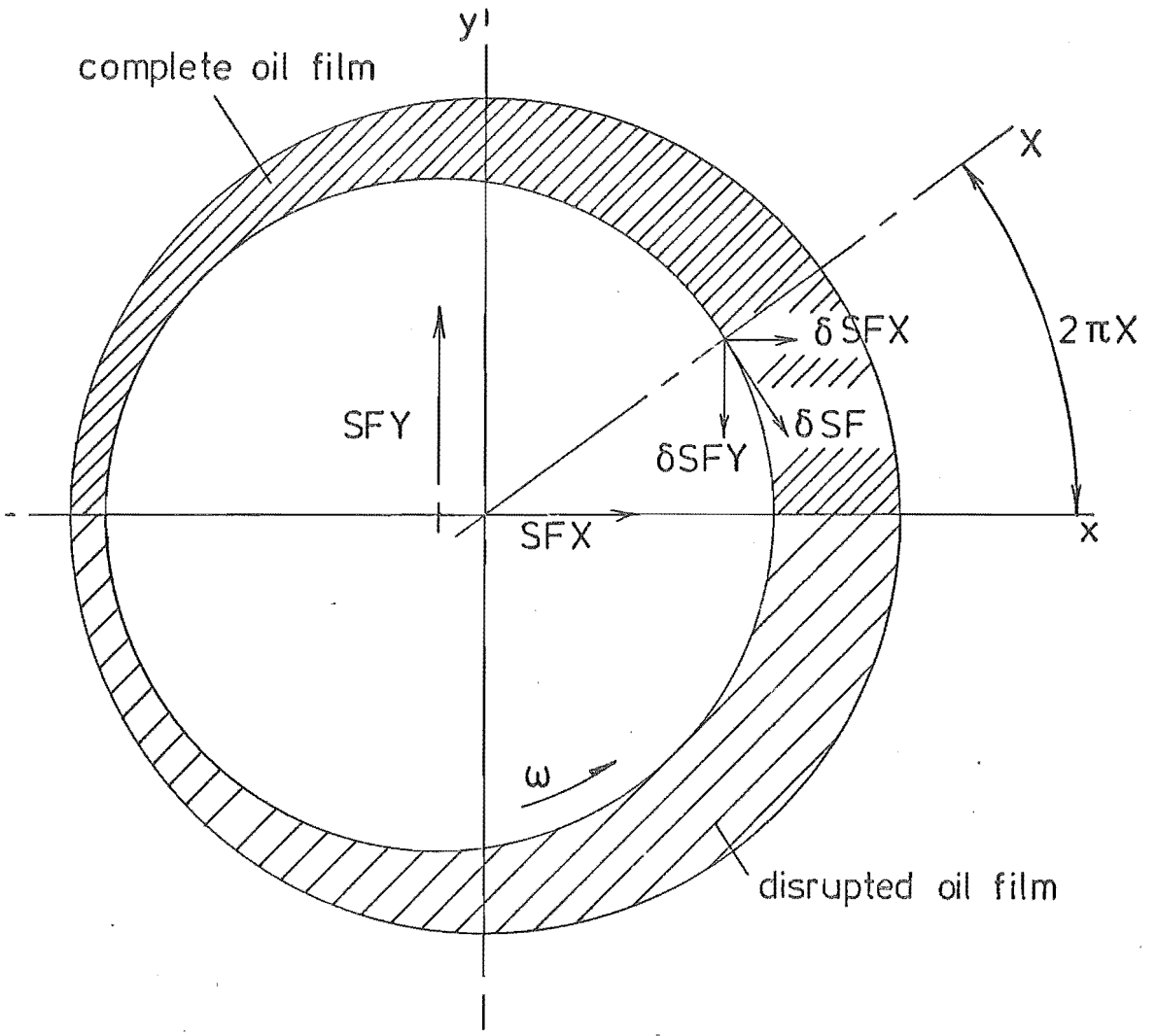

FIG 2-9 VISCOUS SHEAR FORCES ON THE JOURNAL SURFACE AND THEIR RESULTANT TRANSLATIONAL COMPONENTS SFX AND SFY.

$$SFX = \int_0^1\int_0^1 2\pi\frac{r}{R}\ \frac{\text{Sin } 2\pi X}{H}\ dX.dZ$$

$$SFY = \int_0^1\int_0^1 2\pi\frac{r}{R}\ \frac{(-\text{Cos } 2\pi X)}{H}\ dX.dZ \qquad ...2.9$$

As none of the variables are functions of the axial displacement, Z, integration in this direction is readily achieved. Before integration with respect to X can be performed, a number of assumptions are necessary :

(a) The bearing is circular and ungrooved. The film thickness is then :

$$H = 1 + \varepsilon \text{ Cos } 2\pi X.$$

(b) The film is complete in the convergent section of the bearing, $0 < X < .5$, but disrupts into streamers as the clearance increases. The aggregate width of the streamers, ℓ, is obtained by applying flow continuity between the point of minimum film thickness, $X = .5$, and a general point X.

$$\frac{\omega R}{2}\ \ell\ H = \frac{\omega R}{2}\ 1.(1 - \varepsilon)$$

$$\ell = \frac{1 - \varepsilon}{H}$$

The integrals 2.9 become :

$$SFX = \int_0^{\frac{1}{2}} \frac{2\pi r}{R}\ \frac{\text{Sin } 2\pi X}{1+\varepsilon\text{Cos}2\pi X}\ .\ dX + \int_{\frac{1}{2}}^1 \frac{2\pi r}{R}\ \frac{(1-\varepsilon)\text{Sin}2\pi X}{(1+\varepsilon\text{Cos}2\pi X)^2}\ .\ dX$$

$$SFY = \int_0^{\frac{1}{2}} \frac{2\pi r}{R}\ \frac{(-\text{Cos}2\pi X)}{1+\varepsilon\text{Cos}2\pi X}\ .\ dX + \int_{\frac{1}{2}}^1 \frac{2\pi r}{R}\ \frac{(1-\varepsilon)\,(-\text{Cos}2\pi X)}{(1+\varepsilon\text{Cos}2\pi X)^2}\ .\ dX$$

Evaluate the x component first. Substitute :

$$H = 1 + \varepsilon\text{Cos } 2\pi X.$$

$$SFX = \frac{r}{R}\left(\int_{1+\varepsilon}^{1-\varepsilon}\frac{-dH}{\varepsilon H} + \int_{1-\varepsilon}^{1+\varepsilon}\frac{1-\varepsilon}{\varepsilon}\frac{-dH}{H^2}\right)$$

$$= \frac{r}{R}\left(\frac{1}{\varepsilon}\log_e\left(\frac{1+\varepsilon}{1-\varepsilon}\right) - \frac{2}{1+\varepsilon}\right)$$

For the y component the Sommerfeld substitution is required :

$$\text{Cos } \beta = \frac{\varepsilon + \text{Cos } 2\pi X}{1 + \varepsilon \text{Cos } 2\pi X}$$

Thus:

$$SFY = -\frac{2\pi r}{R}\left(\int_0^{\frac{1}{2}}\frac{1}{\varepsilon} - \frac{1}{\varepsilon(1+\varepsilon\text{Cos}2\pi X)}\,dX + \int_{\frac{1}{2}}^{1}\frac{1-\varepsilon}{\varepsilon}\left(\frac{1}{1+\varepsilon\text{Cos}2\pi X} - \frac{1}{(1+\varepsilon\text{Cos}2\pi X)^2}\right)dX\right)$$

$$= -\frac{2\pi r}{\varepsilon R}\left(\frac{1}{2} - \int_0^{\pi}\frac{1}{2\pi}\frac{d\beta}{(1-\varepsilon^2)^{\frac{1}{2}}} + \int_{\pi}^{2\pi}\frac{1-\varepsilon}{2\pi}\left(\frac{1}{(1-\varepsilon^2)^{\frac{1}{2}}} - \frac{1-\varepsilon\text{Cos}\beta}{(1-\varepsilon^2)^{\frac{3}{2}}}\right)d\beta\right)$$

$$= \frac{\pi r}{\varepsilon R}\left(\frac{1}{(1-\varepsilon^2)^{\frac{1}{2}}} + \frac{\varepsilon^2}{(1+\varepsilon)(1-\varepsilon^2)^{\frac{1}{2}}} - 1\right)$$

From these two components the resultant translational force arising from the carried flow can be calculated :

$$SF = (SFX^2 + SFY^2)^{\frac{1}{2}}$$

These forces have been evaluated for a bearing of length to diameter ratio .75 and clearance ratio .001. The results, tabulated in Figure 2-10, show that the ratio of shear force to oil film force increases as the eccentricity ratio is lowered. The maximum value calculated was .32% at an eccentricity ratio of 0.1 thus the influence of the shear friction is small.

The values of the force components calculated were positive. Referring to Figure 2-9, it can be seen that the translational force will, therefore, oppose a forward whirl of the journal thus inducing stability.

FIG. 2-10 TRANSLATIONAL FORCES GENERATED BY THE VISCOUS DRAG ON THE JOURNAL SURFACE. L/D = .75, r/R = .001, WEDGE FILM, PLAIN CIRCULAR GEOMETRY.

ε	DEL	$\psi°$	SFX	SFY	SF	$\frac{SF}{DEL}$ %	$\frac{DEL \sin\psi}{SFY}$
0	0	90	0	0	0	—	—
.1	.151	80.7	.000171	.000445	.000477	.32	335
.3	.524	68.7	.00052	.00126	.00136	.26	387
.5	1.180	56.5	.00087	.00215	.00232	.20	458
.7	2.96	42.5	.00129	.00361	.00383	.13	554
.9	14.1	25.2	.00139	.00793	.00805	.06	757
.975	73.9	13.7	.00349	.0183	.0186	.03	956

If the journal operates with a leading film, simulated in Figure 2-9 by reversing the rotation of the shaft, the shear force assists the whirl, thus reducing the damping effect of the oil pressure film.

The result for a trailing film agrees with the findings of Cameron, Akers and Michaelson. However, it is not clear in their paper what effect friction had on a stable system and thus a comparison for a leading film cannot be made.

The work performed by the oil film on the journal for a constant speed, constant amplitude journal centre whirl is given by :

$$\text{WORK} = 2\pi\varepsilon\,(\text{DEL}.\text{Sin}\psi - \text{SFY}).$$

The choice of axes for the calculation of the shear force components was such that SFY is perpendicular to the journal eccentricity vector. For the shear force to render the system stable :

$$\text{SFY} > \text{DEL}.\text{Sin}\,\psi$$

or

$$\frac{\text{DEL}.\text{Sin}\,\psi}{\text{SFY}} < 1$$

The value of this ratio is also tabulated in Figure 2-10. It far from satisfies the inequality thus agreeing with the observation of Cameron, Akers and Michaelson that the effect of friction never transformed an unstable system to a stable one.

From this elementary investigation it is apparent that the translational force resulting from the viscous shear drag of the oil film on the journal is small compared to the oil pressure force. Although this force affects the stability of a bearing-rotor system, the work of Cameron, Akers and Michaelson[23] and the calculations presented here show its influence to be small and that it does not change the direction of the energy flow between the oil film and journal.

CHAPTER THREE

COMPUTER PROGRAM

In this chapter the program to analyse a dynamically loaded journal bearing is described. The first section considers the general layout of the program and describes briefly its function and capabilities. This is followed by three sections describing the system used to define the bearing surface geometry and the techniques employed to march out the journal and rotor loci.

III.1 GENERAL DESCRIPTION

The program has two major tasks. The first is to march out the journal centre locus when the bearing is subjected to a load that is time dependent. The second is to calculate the work done by the oil film force on the journal as the journal moves around this locus.

There are two basic variants of the program, the difference arising from the method of loading the bearing. In the first the journal is loaded directly by a predetermined force locus. This consists of a stationary force plus a constant magnitude force vector rotating at a constant angular velocity. These forces represent the static and dynamic loads transmitted to the bearing through the rotor shaft. The validity of assuming the dynamic load to take this form is discussed in Chapter 6.

The second variant incorporates either a single or twin mass rotor model (Figures 3-4 and 3-5). The bearing is now loaded by the forces transmitted through the rotor shaft. The rotor mass, or masses, can be loaded with a static and rotating force to simulate external loads; for example, rotor weight and out of balance.

The program was written to handle a wide variety of bearing designs. The cross-sectional shape of the bearing is defined by up to three circular arcs thus allowing designs such as elliptical, spiral and three lobe to be considered. Provision has also been made for a comprehensive pattern of grooves which may be pressurised.

Apart from the locus stepping section the flow diagrams for the programs are very similar. A simplified diagram is shown in Fig. 3-1 and a complete source listing for the directly loaded journal program is given in the Appendix together with a brief summary of the role of each subroutine.

At the beginning of the main loop, Fig. 3-1, the minimum oil film thickness is calculated and checked to ensure the journal is within the bearing clearance. Reynolds equation is then solved, as described in Chapter 2, and the pressure distributions summed to obtain the oil film forces. The accuracy of each locus step is assessed by checking the force balance on the journal. The time increment for the next step is adjusted according to this check or, if the accuracy is sufficiently poor, the step repeated with a reduced time increment.

The work performed by the oil film on the journal is calculated at this stage using Equation 2.7

Calculation of the dynamic bearing coefficients involves four relaxation procedures and summing the results over the bearing surface. The mean coefficients for the next locus step are estimated by linear extrapolation from these coefficients and the set calculated at the preceding locus position.

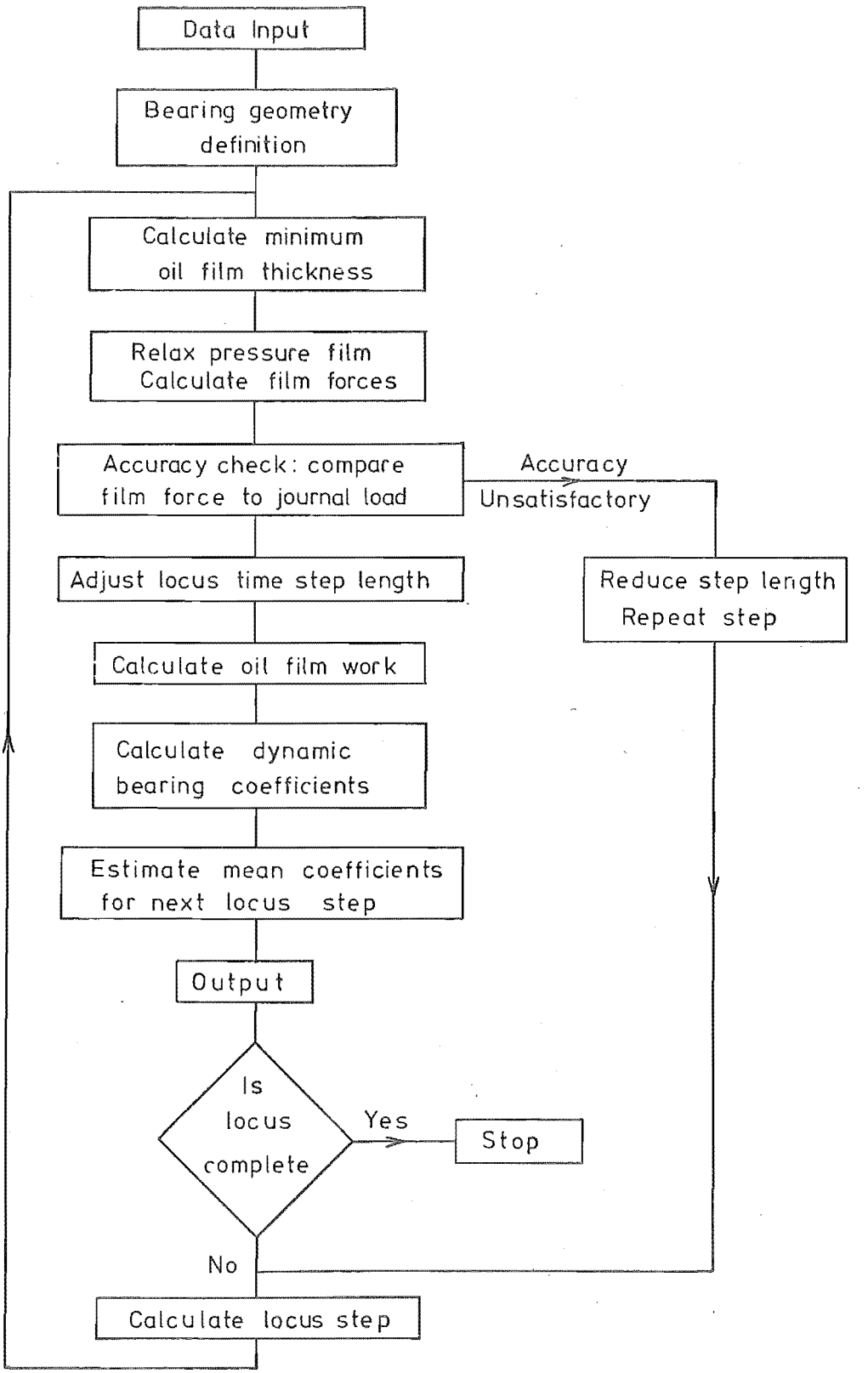

FIG. 3-1 PROGRAM FLOW DIAGRAM

The program for the directly loaded journal is halted after two cycles of the rotating load. The first of these is required to remove the transients introduced by the starting conditions. If the program incorporates a rotor model it can be terminated after any number of load cycles or when a specified computation time has elapsed.

III.2 BEARING GEOMETRY

The bearing cross-sectional geometry is defined as a series of circular arcs. Up to three of these segments can be used, but they must subtend equal angles at the bearing centre and together make up a complete 360° bearing. The first segment of a three land bearing is shown in Fig. 3-2 with the journal positioned at the centre of the segment. The radial clearance, r, is the difference between the segment and journal radii. The clearance space is the area remaining within the segment when the journal radius is reduced to zero. This is a convenient way to show the journal position and bearing surface together. If the bearing was drawn to scale the bearing clearance would be imperceptible because the clearance ratio r/R is of the order of .001. The clearance space is used in later chapters to bound the journal locus. It does not, however, necessarily form the limit of possible journal movement.

The minimum clearance of the segment, Cm, is the minimum film thickness when the journal is at the bearing centre. The value of this parameter for the final segment, that is, the third segment for a three land bearing, is used to non-dimensionalize the system's variables (see II.2) for multi-land bearings.

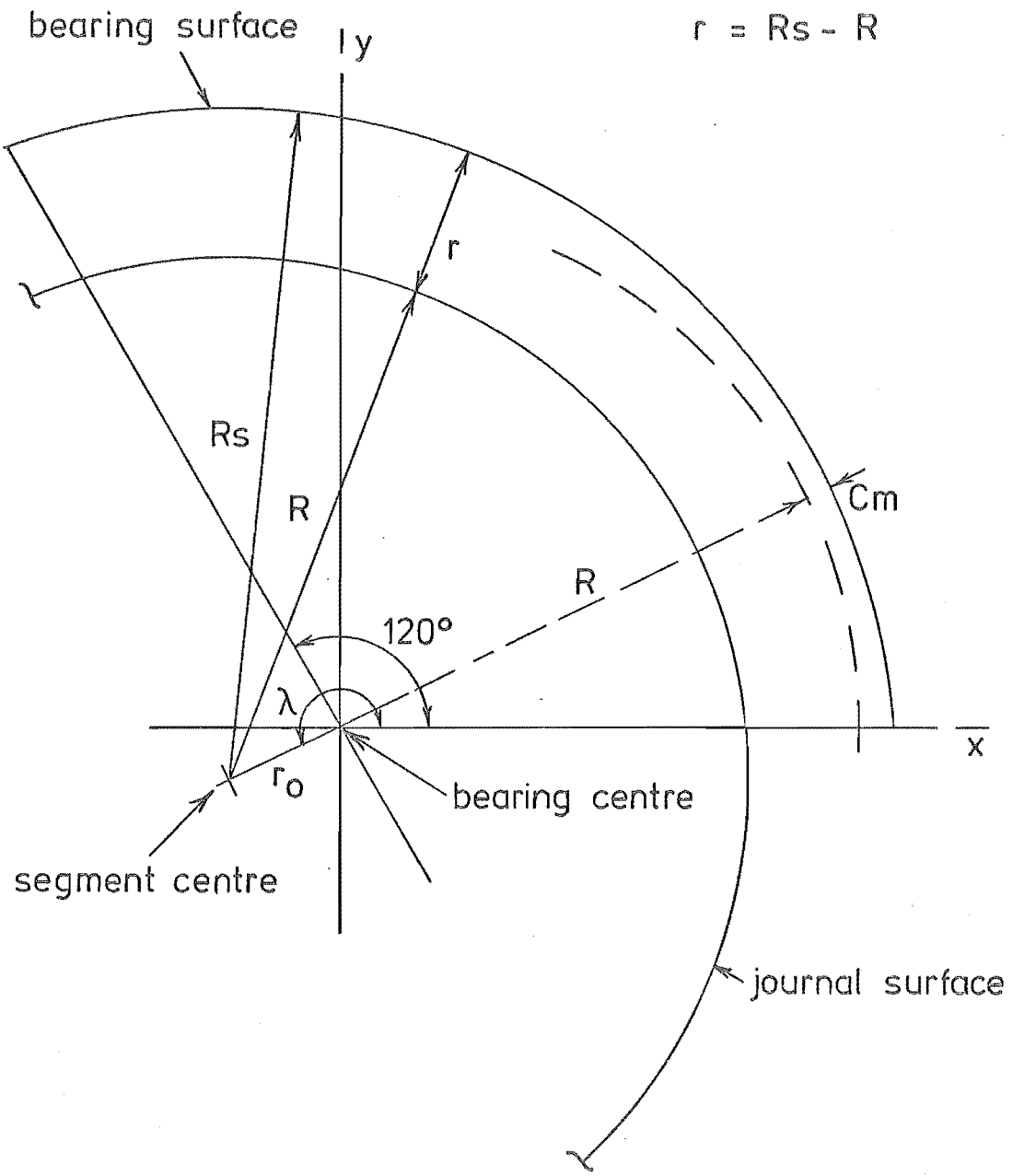

FIG. 3-2. DEFINITION OF BEARING CROSS-SECTION GEOMETRY. FIRST SEGMENT SHOWN OF A THREE SEGMENT BEARING.

The co-ordinate system, both cartesian and polar, used to describe the journal and the rotor positions are based on the bearing centre.

The permissible grooving for each segment is shown in Fig. 3-3. The inlet and outlet grooves are of the same width, but their length may vary. One slot of unrestricted size and position may be incorporated in each segment half. The program data to define the grooves relates to half the bearing surface only, leaving the program to impose symmetry about the centre of the bearing.

Discontinuities in the film thickness or its derivatives occur at the junction of segments with non-circular bearing geometries. Finite difference solution of Reynolds equation at these points will fail to give pressure and flow balance. This can be overcome by treating each segment as a separate partial arc bearing and adjusting the entry and exit boundary conditions to achieve the balance. However, this requires an additional iterative loop to be placed around the pressure film relaxation and is thus expensive to compute. The problem was avoided for this program by the restriction that a groove must be placed wherever a film discontinuity exists. This effectively separates the bearing segments and ensures a pressure balance. The flow balance is assumed to be satisfied by the oil supply system to the groove.

III.3 LOCUS STEPPING - DIRECTLY LOADED JOURNAL

The journal centre locus is marched out in a series of time steps. The load applied to the journal is defined as a function of time and thus its value at the end of a step is known. Using the dynamic bearing coefficients the journal displacement and velocity required to produce an equal oil film force are calculated. At the new position

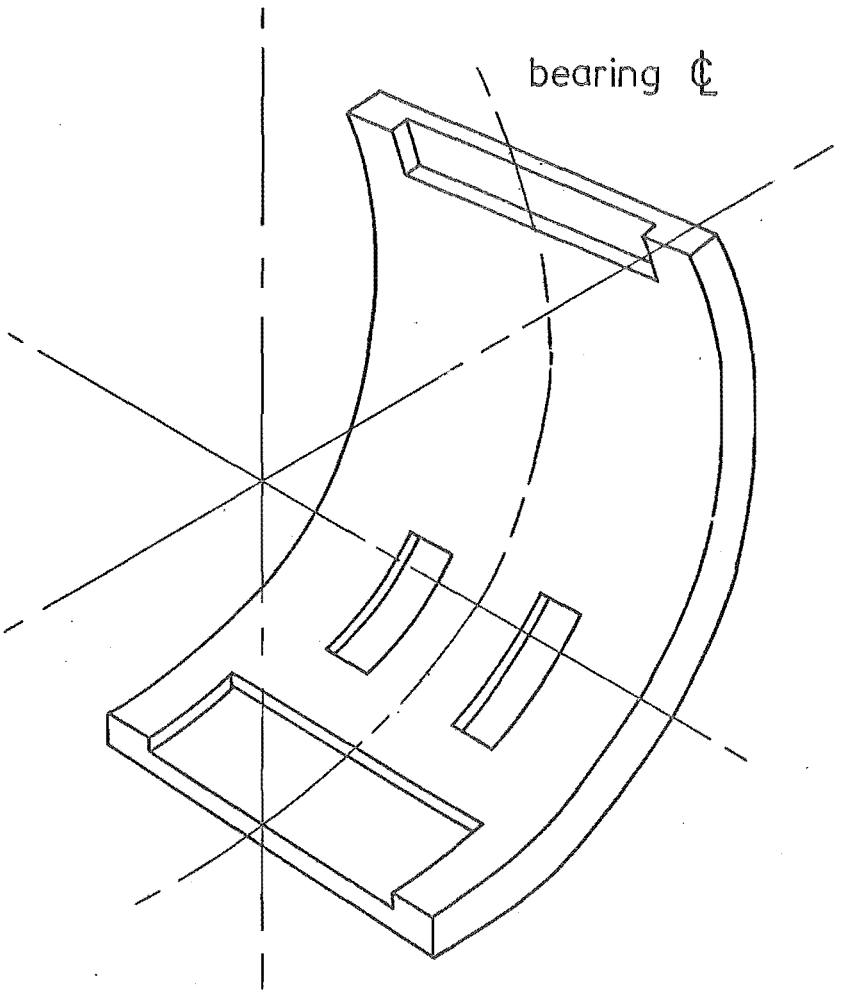

FIG 3-3 PERMISSIBLE BEARING SEGMENT GROOVING.

the film equations are solved to check the force balance on the journal, and hence the accuracy of the step, and to obtain the dynamic bearing coefficients in preparation for the next step.

At the beginning of a step the oil film force, dynamic bearing coefficients and journal displacement and velocity are known. After a small time δt the x component of the film force is approximately :

$$FX_{\delta t} = FX_0 + kxx_0\ \delta Xj + kxy_0\ \delta Yj + bxx_0\ \delta \dot{X}j + bxy_0\ \delta \dot{Y}j \qquad ...3.1$$

The discrepancy in this equation is produced by assuming the bearing coefficients to be constant. It was found that the marching technique was considerably improved by replacing the coefficients calculated at the beginning of the step with the mean values estimated for the proposed step by linear extrapolation.

$$kxx = kxx_0 + \frac{1}{2}(kxx_0 - kxx_{-Dt})\frac{\delta t}{Dt}$$

where Dt is the length of the previous step.

The load applied to the journal by the force locus is solely a function of time and thus defined at the end of the step. To achieve a force balance on the journal the oil film force and the journal load must be equal, thus :

$$FX_{\delta t} = FXJ_{\delta t}$$

By assuming a constant journal acceleration throughout the step the change in the x component of the journal displacement and velocity are given by :

$$\delta Xj = (\dot{X}j_0 + \dot{X}j_{\delta t})\frac{\delta t}{2} \qquad ...3.2$$

$$\delta \dot{X}j = \dot{X}j_{\delta t} - \dot{X}j_0 \qquad ...3.3$$

Substituting from these four equations into Equation 3.1 gives :

$$FXJ_{\delta t} = FX_0 + kxx \frac{\delta t}{2}\left(\dot{X}j_{\delta t} + \dot{X}j_0\right) + bxx\ (\dot{X}j_{\delta t} - \dot{X}j_0)$$
$$+ kxy \frac{\delta t}{2}\ (\dot{Y}j_{\delta t} + \dot{Y}j_0) + bxy\ (\dot{Y}j_{\delta t} - \dot{Y}j_0)$$
$$= FX_0 + \dot{X}j_0\ (kxx \frac{\delta t}{2} - bxx) + \dot{X}j_{\delta t}(kxx\frac{\delta t}{2} + bxx)$$
$$+ \dot{Y}j_0\ (kxy \frac{\delta t}{2} - bxy) + \dot{Y}j_{\delta t}\ (kxy \frac{\delta t}{2} + bxy) \qquad ...3.4$$

A similar expression can be derived for the y component, thus there are two simultaneous equations to solve for $\dot{X}j_{\delta t}$ and $\dot{Y}j_{\delta t}$.

Thus:

$$\dot{X}j_{\delta t} = \frac{ac.bb - bc.ab}{aa.bb - ba.ab}$$

$$\dot{Y}j_{\delta t} = \frac{bc.aa - ac.ba}{aa.bb - ba.ab}$$

where

$$aa = kxx \frac{\delta t}{2} + bxx$$

$$ab = kxy \frac{\delta t}{2} + bxy$$

$$ac = FXJ_{\delta t} - FX_0 - \dot{X}j_0\ (kxx \frac{\delta t}{2} - bxx) - \dot{Y}j_0\ (kxy \frac{\delta t}{2} - bxy)$$

$$ba = kyx \frac{\delta t}{2} + byx$$

$$bb = kyy \frac{\delta t}{2} + byy$$

$$bc = FYJ_{\delta t} - FY_0 - \dot{Y}j_0(kyy\ \delta t - byy) - \dot{X}j_0\ (kyx \frac{\delta t}{2} - byx)$$

The new journal position can now be calculated:

$$Xj_{\delta t} = Xj_0 + (\dot{X}j_0 + \dot{X}j_{\delta t}) \frac{\delta t}{2}$$

$$Yj_{\delta t} = Yj_0 + (\dot{Y}j_0 + \dot{Y}j_{\delta t}) \frac{\delta t}{2}$$

The accuracy of each step is checked by calculating the oil film force at the new journal position and velocity and comparing it to the applied load. The error is expressed as a fraction of the applied load.

$$WACC = \frac{((FX - FXJ)^2 + (FY - FYJ)^2)^{\frac{1}{2}}}{(FXJ^2 + FYJ^2)^{\frac{1}{2}}}$$

This is compared to the tolerance, LOADAC, and according to the result, one of four actions taken :

(i) WACC < .1 LOADAC - step length increased.

(ii) .1 LOADAC < WACC < .5 LOADAC - step length unchanged.

(iii) .5 LOADAC < WACC < LOADAC - step length reduced.

(iv) LOADAC < WACC - step length reduced and step repeated.

The marching process does not assume an accurate force balance at the beginning of the step. The required change in the oil film force is :

$$\delta F = FXJ_{\delta t} - FX_0$$

If the error at the close of the preceding step was E

$$\delta F = FXJ_{\delta t} - (FXJ_0 - E)$$

Thus each step seeks to remove the errors of previous steps. In this way the program avoids accumulating errors, a problem that often plagues systems solved by marching techniques.

III.4 LOCUS STEPPING WITH ROTOR MODEL

Single Step

The bearing-rotor system and model are shown in Figure 3-4. The rotor is a single mass mounted on a light elastic shaft midway between two identical hydrodynamic bearings. The rotor mass is also coupled to ground by viscous dampers. As the system is symmetrical about the mass only half the rotor is required for the computer model. The system is represented by a point mass Mr joined to a light journal by a spring. The external loading on the mass, in addition to the viscous damping, is comprised of a static load and a constant magnitude rotating force vector. The latter permits simulation of dynamic loads such as out of balance.

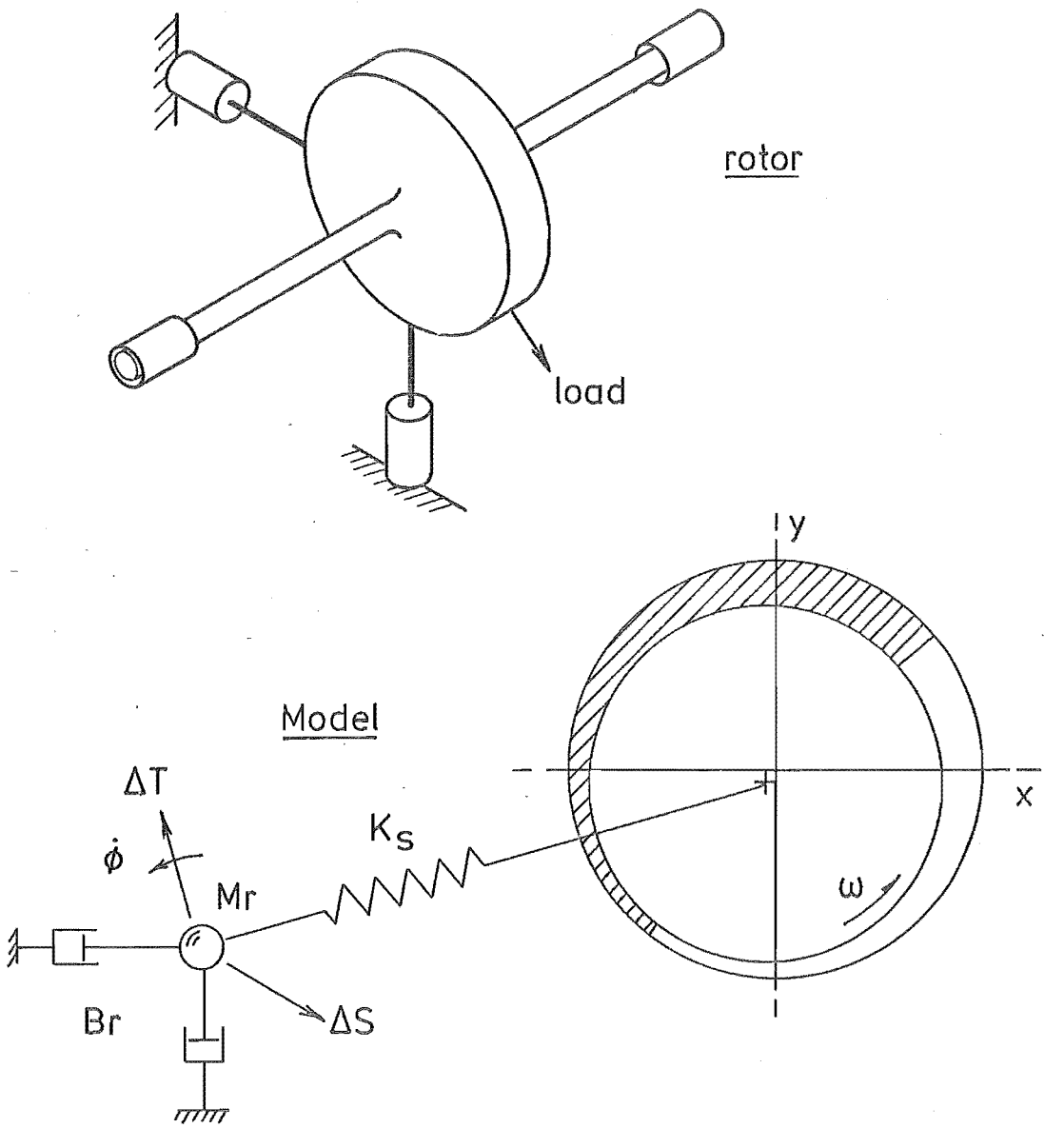

FIG. 3-4 SINGLE MASS ROTOR MODEL

The locus marching technique is an extension of the method used for the directly loaded journal. In this case the force applied to the journal is defined by the deflection of the shaft, that is, the extension of the spring Ks. The journal load is given by :

$$FXJ = Ks\,(Xr - Xj)$$

$$FYJ = Ks\,(Yr - Yj) \qquad \ldots 3.6$$

The equations of motion for the rotor mass are :

$$Mr\ddot{Xr} = FXT + Ks(Xj - Xr) - Br\dot{Xr}$$

$$Mr\ddot{Yr} = FYT + Ks\,(Yj - Yr) - Br\dot{Yr} \qquad \ldots 3.7$$

The rotor acceleration is assumed to be a linear function of time within each step. Taking the time t to be zero at the beginning of the step and δt at the end, the x component of the rotor acceleration is :

$$\ddot{Xr}_t = \ddot{Xr}_0 + (\ddot{Xr}_{\delta t} - \ddot{Xr}_0)\,\frac{t}{\delta t}$$

By integrating this twice, the velocity and displacement at the end of the step are obtained.

$$\dot{Xr}_{\delta t} = a + \ddot{Xr}_{\delta t}\,\frac{\delta t}{2} \qquad \ldots 3.8$$

$$Xr_{\delta t} = b + \ddot{Xr}_{\delta t}\,\frac{\delta t^2}{6} \qquad \ldots 3.9$$

where

$$a = \dot{Xr}_0 + \ddot{Xr}_0\,\frac{\delta t}{2}$$

$$b = Xr_0 + \dot{Xr}_0\,\delta t + \ddot{Xr}_0\,\frac{\delta t^2}{3}$$

Using equations 3.8 and 3.9 the x component of equation 3.7 can be written as :

$$Mr(Xr_{\delta t} - b)\,\frac{6}{\delta t^2} = FXT_{\delta t} + Ks(Xj_{\delta t} - Xr_{\delta t}) - \frac{3Br}{\delta t}\left(\left(\frac{\delta t}{3}a - b\right) + Xr_{\delta t}\right)$$

And thus, collecting terms :

$$Xr_{\delta t} = aa\,Xj_{\delta t} + bb$$

where

$$aa = Ks\Big/\left(\frac{Mr6}{\delta t^2} + Ks + \frac{3.Br}{\delta t}\right)$$

$$bb = \left(FXT + \frac{Mr6}{\delta t^2}\,.\,b - \frac{3Br}{\delta t}\left(\frac{\delta t}{3}a - b\right)\right)\Big/\left(\frac{Mr6}{\delta t^2} + Ks + \frac{3Br}{\delta t}\right)$$

Substituting into 3.6 :

$$FXJ_{\delta t} = Ks\ ((aa - 1)\ Xj_{\delta t} + bb)$$

The constants a, b, aa and bb can be evaluated at the start of each step thus the journal load has been reduced to a function of $Xj_{\delta t}$ only. The problem can now be treated in a manner similar to that used for the directly loaded journal.

Applying a force balance to the journal :

$$FX_{\delta t} = FX\dot{J}_{\delta t}$$
$$= Ks\ ((aa - 1)\ Xj_{\delta t} + bb)$$

Now from Equation 3.2 :

$$Xj_{\delta t} = Xj_0 + (\dot{X}j_0 + \dot{X}j_{\delta t})\ \frac{\delta t}{2}$$

Thus:

$$FX_{\delta t} = Ks\left((aa - 1)(Xj_0 + \left(\dot{X}j_0 + \dot{X}j_{\delta t}\right)\frac{\delta t}{2}) + bb\right)$$

And thus the equation equivalent to 3.4 is :

$$Ks\ [(aa - 1)(Xj_0 + \dot{X}j_0\ \frac{\delta t}{2}) + bb] + Ks\ (aa - 1)\ \dot{X}j_{\delta t}\ \frac{\delta t}{2}$$
$$= FX_0 + \dot{X}j_0\ (kxx\ \frac{\delta t}{2} - bxx) + \dot{X}j_{\delta t}\ (kxx\ \frac{\delta t}{2} + bxx)$$
$$+ \dot{Y}j_0\ (kxy\ \frac{\delta t}{2} - bxy) + \dot{Y}j_{\delta t}\ (kxy\ \frac{\delta t}{2} + bxy).$$

The y component can be derived in a similar manner. The resulting simultaneous equations in $\dot{X}j_{\delta t}$ and $\dot{Y}j_{\delta t}$ are solved and the rotor acceleration, velocity and displacement and the journal displacement calculated. Using these values the oil film force is calculated and the force balance on the journal checked to determine the accuracy of the locus step. As for the directly loaded journal, the step length is adjusted according to the results of this check.

Multiple Step

An alternative scheme devised was to use a predictor-corrector

routine to march out the locus within each time step. Thus the program has two marching schemes. The inner one, the predictor-corrector routine, is restarted at the beginning of each of the outer steps and uses the dynamic bearing coefficients calculated at this time. The outer scheme involves the solution of the film equations to calculate the dynamic bearing coefficients and to check the accuracy of the locus. As before, the adjustment of the step length is made at this point.

The predictor-corrector routine used is a scientific subroutine package published by I.B.M. It uses Hamming's modified predictor-corrector method to solve a system of first order ordinary differential equations for a given set of initial conditions.

The development of a multiple step program was undertaken for two reasons :

(i) To reduce the locus stepping errors, primarily for the rotor mass. The single step scheme assumes the rotor acceleration to be a linear function of time. The errors introduced by this become increasingly important as the step length is increased, thus limiting the maximum step length that can be used.

(ii) A more flexible solution was considered desirable to allow more complex rotor models to be investigated in future programs. For the investigation described in this thesis the rotor model was limited to two damped spring-mass systems each connected to the massless journal. The model is shown in Fig. 3.5

Two programs were written using the multiple step scheme both employing the twin mass rotor model. The second of these was developed

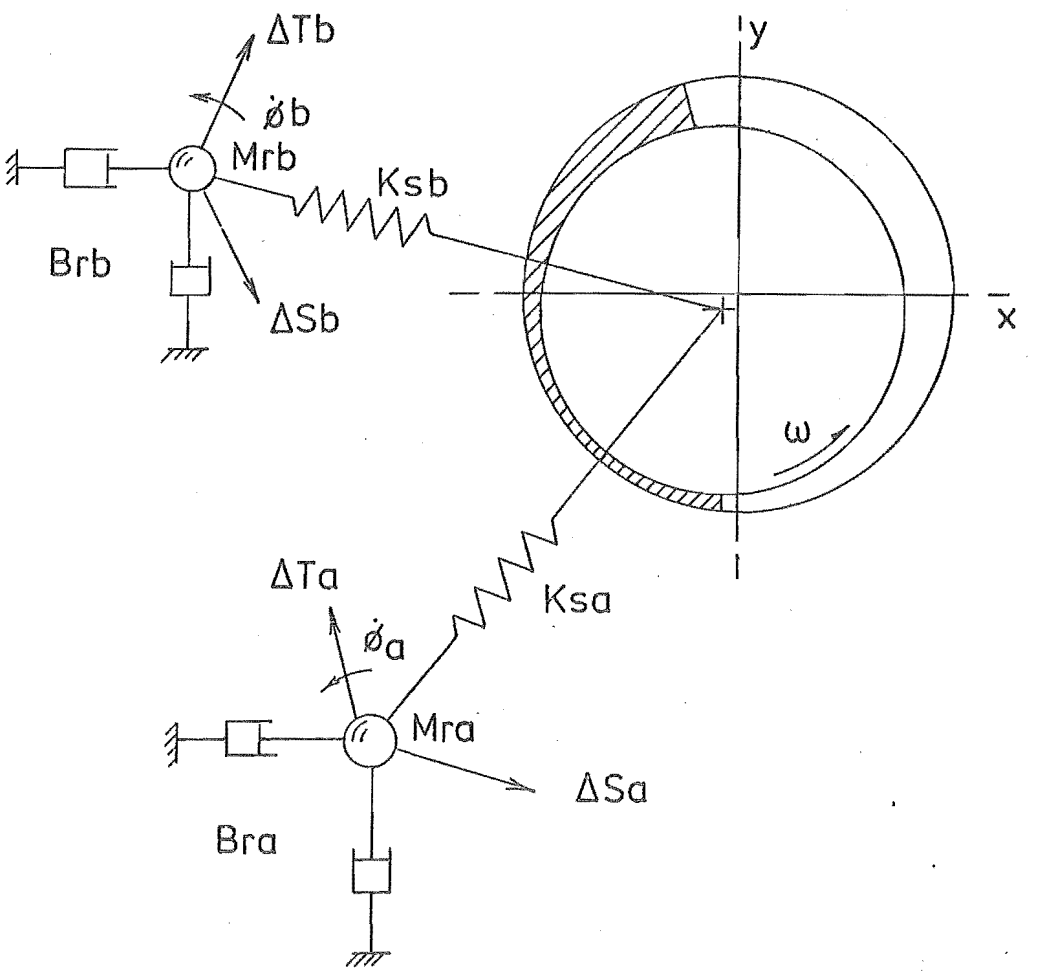

FIG. 3-5 TWIN MASS ROTOR MODEL

for the investigation described in Chapter 5. The aim of this was to greatly reduce the computation time required to solve a bearing-rotor system and thus make a full solution a more practical design tool. The approach taken was to record the dynamic bearing coefficients in the preceding locus cycle and to use these to predict the change in the coefficients over the present step. The dynamic bearing coefficients were then known as a function of the journal position and they could be varied within the predictor-corrector routine.

The first program assumed the dynamic bearing coefficients to be constant throughout the step. The x component of the equations of motion for the two masses are :

$$Mra.\ddot{X}ra = FXTa + Ksa\ (Xj - Xra) - Bra.\dot{X}ra$$

$$Mrb.\ddot{X}rb = FXTb + Ksb\ (Xj - Xrb) - Brb.\dot{X}rb$$

Thus at time t :

$$\frac{dXra}{dt} = \dot{X}ra_t$$

$$\frac{d\dot{X}ra}{dt} = (FXTa_t + Ksa\ (Xj_t - Xra_t) - Bra\ \dot{X}ra_t)/Mra$$

$$\frac{dXrb}{dt} = \dot{X}rb_t$$

$$\frac{d\dot{X}rb}{dt} = (FXTb_t + Ksb\ (Xj_t - Xrb_t) - Brb\ \dot{X}rb_t)/Mrb$$

A similar set of equations describes the y component.

The motion of the journal is defined by the force balance :

$$Ksa\ (Xra_t - Xj_t) + Ksb\ (Xrb_t - Xj_t) = FX_0 + kxx\ (Xj_t - Xj_0) + kxy\ (Yj_t - Yj_o) + bxx\ (\dot{X}j_t - \dot{X}j_0) + bxy\ (\dot{Y}j_t - \dot{Y}j_0)$$

$$Ksa\ (Yra_t - Yj_t) + Ksb\ (Yrb_t - Yj_t) = FY_0 + kyx\ (Xj_t - Xj_0) + kyy\ (Yj_t - Yj_0) + byx\ (\dot{X}j_t - \dot{X}j_0) + byy\ (\dot{Y}j_t - \dot{Y}j_0)$$

Rearranging :

$$\frac{dXj}{dt} = \frac{1}{DEN}\,(ac + aa.Xj_t + ab.Yj_t + Ksa\ (byy.Xra_t - bxy.Yra_t) + Ksb(byy.Xrb_t - bxy.Yrb_t))$$

$$\frac{dYj}{dt} = \frac{1}{DEN}\,(bc + ba.Xj_t + bb.Yj_t + Ksa\ (bxx.Yra_t - byx.Xra_t) + Ksb\ (bxx.Yrb_t - byx.Xrb_t))$$

where

$$aa = kyx.bxy - byy\ (kxx + Ksa + Ksb)$$

$$ab = bxy\ (kyy + Ksa + Ksb) - kxy.byy$$

$$ba = byx\ (kxx + Ksa + Ksb) - kyx.bxx$$

$$bb = kxy.byx - bxx\ (kyy + Ksa + Ksb)$$

$$ad = -FX_0 + kxx.Xj_0 + kxy.Yj_0 + bxx.\dot{X}j_0 + bxy.\dot{Y}j_0$$

$$bd = -FY_0 + kyx.Xj_0 + kyy.Yj_0 + byx.\dot{X}j_0 + byy.\dot{Y}j_0$$

$$ac = ad.byy - bd.bxy$$

$$bc = bd.bxx - ad.byx$$

$$DEN = bxx.byy - bxy.byx$$

The remainder of the program - oil film force calculation, locus step accuracy check, step length adjustment and dynamic bearing coefficient calculation - is similar to that used for the directly loaded journal.

CHAPTER FOUR

PROGRAM EVALUATION

In this chapter the validity of the programs developed is established by comparison with published experimental results. The correlation achieved was good, particularly for the bearing-rotor model. Although it was not intended as such, the results of this comparison illustrate well the behaviour of a simple rotor in hydrodynamic bearings and the fallibility of predicting instability by linearised analysis.

The first section of the chapter considers the major approximations made in deriving the oil film equations and their influence on the program results. An assessment of the errors introduced by the oil film boundary conditions, the numerical solution of the film equations and the locus marching scheme is also made.

IV.1 PROGRAM ACCURACY

The accuracy of the program is affected by a number of factors. The principal sources of error can be divided into four groups :-

(a) Errors introduced by the assumptions made in deriving the oil film equations.

(b) Approximation of the film behaviour by the oil film boundary model.

(c) Numerical errors in the solution of the film equations.

(d) Errors in the locus marching.

The magnitude of many of these errors is dependent on the conditions under which the bearing is running. The following sections assess each of these and indicates the conditions under which the errors are likely

to be large. References are included permitting a more detailed investigation if it is required.

Oil Film Equation Assumptions

(a) Laminar Flow - the oil film was assumed to be completely laminar. This is incorrect as the flow normally exhibits some degree of turbulence and can be expected to become fully turbulent when the Reynolds number exceeds 2000, that is :

$\frac{urρ}{μ} > 2000$ where $u = ωR$, journal surface speed.

Huggins[25] conducted an experimental investigation into the transition from laminar to turbulent flow for a 24 inch diameter elliptical bearing. He noted a definite transition at a Reynolds number of approximately 2000, but found that the flow was never truly laminar. He concluded that the non-laminar behaviour was produced by turbulence introduced at the grooves in the bearing surface and by the inertia of the oil film. (This was assumed to be negligible when deriving Reynolds equation). The influence of both of these decreased as the Reynolds number was reduced. Experimental work by Duffin and Johnson[26] showed that for a 19 inch diameter circular bearing, the bearing behaviour agreed with laminar flow theory up to a Reynolds number of 1000.

The parameter most sensitive to the change in flow regimes is the viscous shear friction. The investigation conducted for this thesis did not involve calculation of this, thus the primary error produced by assuming laminar flow did not occur. The film flow regime does, however, also affect the oil pressure film forces. From the experimental work mentioned above, satisfactory agreement with experimental results can be expected for Reynolds numbers less than 1000. If the bearing surface is heavily grooved this figure may have to be reduced.

(b) Lubricant Viscosity - The lubricant viscosity is a function of temperature and pressure. For a statically loaded bearing the oil film pressure and temperature both reach their maximum value in the region of minimum film thickness. Their effect on the film pressure generation, is, however, different. The viscosity is lowered by increased temperature and raised by higher pressure. Usually the thermal effect is more significant thus variation of the viscosity derates the bearing; that is, a higher eccentricity is required to maintain the same load.

The influence of temperature on the performance of a statically loaded journal bearing has been investigated by a number of authors both theoretically and experimentally[27,28]. In general, their results show that the isoviscous assumption introduces significant errors, in the order of tens of percent, which are dependent on the bearing and its operating condition. McCallion and Smalley found the error to increase with the journal eccentricity and authors of both references found the bearing outlet viscosity to be the best value to assume for an isoviscous model.

These results are for a statically loaded bearing. When the bearing is dynamically loaded the position of the oil film can change at a rate comparable to the journal surface velocity. Under these conditions mixing of the lubricant will be different and the point of maximum bearing surface temperature will change. It is quite conceivable that these two will reduce the variation of the film temperature around the bearing thereby improving the isoviscous assumption.

Experimental work by Middleton[29] supports this suggestion. He found that the journal eccentricity required for a load rotating at shaft speed was less than that for an equal static load. From

Reynolds equation, 2.1a, the eccentricities would be expected to be equal. Middleton attributed the change to a lower temperature in the lubricant at the point of minimum film thickness.

With the static load, a single part of the bearing surface is continually subjected to the high temperature oil. There is considerable circumferential flow of energy in the bush (see 28, 30); thus the oil entering the region of minimum film thickness is preheated. With the synchronous load a single region of the shaft is always at the point of minimum film thickness. However, the shaft is more effectively cooled by a central circumferential groove as was used in Middleton's test bearing, because the oil flow past its high temperature region is greater than the flow observed by the bearing surface in the static load case. Thus the peak shaft temperature is lower and the viscosity variation around the film reduced.

(c) Journal Alignment - Perfect alignment of the journal and bearing axes was assumed. Although this is generally incorrect and misalignment can be readily incorporated in a computer solution[19], it was considered unwise to complicate the investigation carried out for this thesis with any additional variables.

Design charts for the effect of journal misalignment have been published by McCallion and Smalley[31].

(d) Bearing Distortion - The bearing was assumed to be perfectly rigid. A theoretical examination of a thin bearing shell backed by a rigid housing was conducted by Hooke, Brighton and O'Donoghue[32]. Their results show that distortion of the bearing surface has little effect on the relationship between bearing load and minimum oil film thickness.

The authors concluded that for thin bearing shells constructed of materials with Poisson's ratio less than 0.4, surface deformation is proportional to the film pressure.

Oil Film Boundary Conditions

The oil film boundary conditions adopted for this investigation were used by McCallion and Smalley[31] and found to give results which compared favourably with experimental values. However, under conditions of very light bearing loads the assumption that the film breaks down at zero gauge pressure and cannot sustain subatmospheric values, can introduce errors. Under such conditions small changes in the disruption pressure can significantly influence the bearing behaviour as shown by Lloyd[14]. He found that changing the disruption pressure from atmospheric to zero was capable of completely changing the journal centre locus.

Turbo-machinery bearings, however, rarely operate under light loads as these film conditions have been found to promote instability. Situations in which the magnitude of the disruption pressure is important are thus unlikely to be encountered.

Numerical Accuracy of the Oil Film Equation Solution

The accuracy of the journal centre locus and oil film work calculation are not dependent on the accuracy of the dynamic bearing coefficients. The coefficients are used solely to march out the journal centre locus and the accuracy of this is controlled by adjusting the step length. Thus the errors involved in determining the coefficients affect the length of the step, but not its quality.

Numerical errors in the oil film force arise in three ways :

(a) Incomplete convergence of the pressure relaxation;

(b) finite difference approximation of the pressure derivatives;

(c) Summation of the pressure over the bearing surface.

The error arising from (a) was shown to be insignificant (Figure 2-3). Those resulting from the finite difference approximation and pressure summation increase rapidly with the journal eccentricity and are each of the order of 5% for an eccentricity ratio of 0.95 (see II.4 and II.5).

Step Accuracy

The accuracy of the journal centre locus is controlled by checking the force balance on the journal at the conclusion of each step and adjusting the step length according to the result (see III.3). For the majority of the work described in this thesis, the tolerance on the force balance, LOADAC, was 5%. If the error in the force balance exceeded this figure, the step was repeated; if it exceeded 2.5% the succeeding step length reduced and if the balance was better than 0.5% the step length increased. Experience with the program showed that this gave an average error in the force balance of between 1 and 2 percent.

IV.2 OIL FILM FORCES

The first step in checking the validity of the program was to compare the oil film force of a statically loaded bearing to experimental results. For this purpose the results of Glienicke[33] were used.

Glienicke conducted experimental work to determine the stiffness and damping coefficients of a number of turbine bearings. To check his experimental results he did a preliminary investigation of a statically loaded plain circular journal bearing. His results are shown in Figure

4-1 and are presented as a plot of non-dimensional journal load against journal eccentricity ratio and the journal centre locus as the applied load is slowly increased.

The choice of program data with which to perform the comparison was largely arbitrary. Glienicke's paper supplies no details of the test parameters apart from the bearing clearance ratio and length to diameter ratio. The limitations of the test rig, with regard to the bearing load, shaft speed and bearing dimensions, are described and the data was retained within these limits.

The test data was :

L/D = .5

D = 120 mm (4.72 in)

Shaft Speed = 1500 r.p.m.

Viscosity = 0.2 poise (2.9×10^{-6} reyns)

r/R = 0.0019

The results are shown in Figure 4-1 and it can be seen that they agree well with the experimental values. The greatest variation in both the journal centre locus and load parameter occur at an eccentricity of 0.6. The percentage difference in the journal load at this point is approximately 20%, but at eccentricities higher than 0.7, the correlation is very good.

The bearing model used in the computer program requires only the journal eccentricity ratio and bearing length to diameter ratio to define the non-dimensional oil film force. However, many of the factors likely to cause discrepancies between the experimental and theoretical results are dependent on other parameters, as discussed earlier, and as these are not known, it is not possible to suggest reasons for the variation in

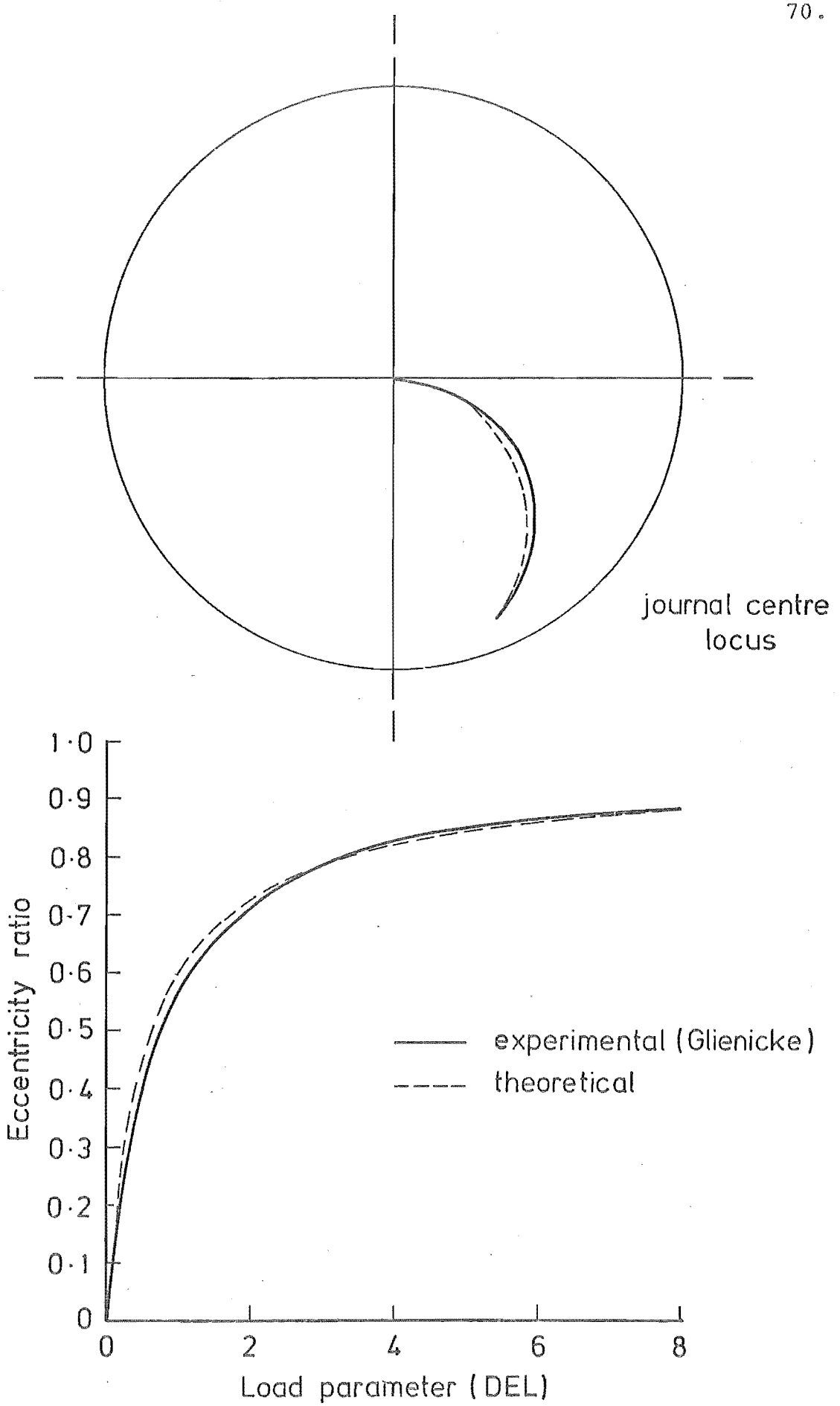

FIG 4-1 COMPARISON OF JOURNAL CENTRE LOCUS AND LOAD PARAMETER WITH EXPERIMENTAL RESULTS. PLAIN CIRCULAR BEARING, $L/D = 0 \cdot 5$

the results.

The discrepancies between Glienicke's results and the theoretical solutions published in his paper are similar to those discovered in this comparison. This suggests that the solution of the bearing model by the program is correct and that the discrepancies lie either in the bearing model or in the experimental results.

From this comparison it was concluded that the computer program was solving the oil film force equation satisfactorily and that a reasonable agreement with experimental results could, in general, be expected. The latter is, of course, dependent on the conditions under which the bearing operates.

IV.3 DYNAMIC BEARING COEFFICIENTS

The dynamic bearing coefficients are used in the computer program to estimate the oil film forces at the end of a proposed step. The accuracy criterion is, therefore, not necessarily agreement with experimentally determined values, but satisfaction of the equation :

$$\delta FX = kxx.\delta Xj \qquad Yj = \text{constant}$$

for each of the eight coefficients.

To check this, the coefficients kxx and bxx were plotted against Xj, for Yj = 0, and the values of these coefficients calculated from the change in the oil film force, superimposed on the curves. The stiffness term $\delta FX/\delta Xj$ was calculated over a displacement interval of 0.1 and the damping term for a velocity change of 0.01 to 0.

The results are shown in Figure 4-2 and excellent correlation was obtained between the two values.

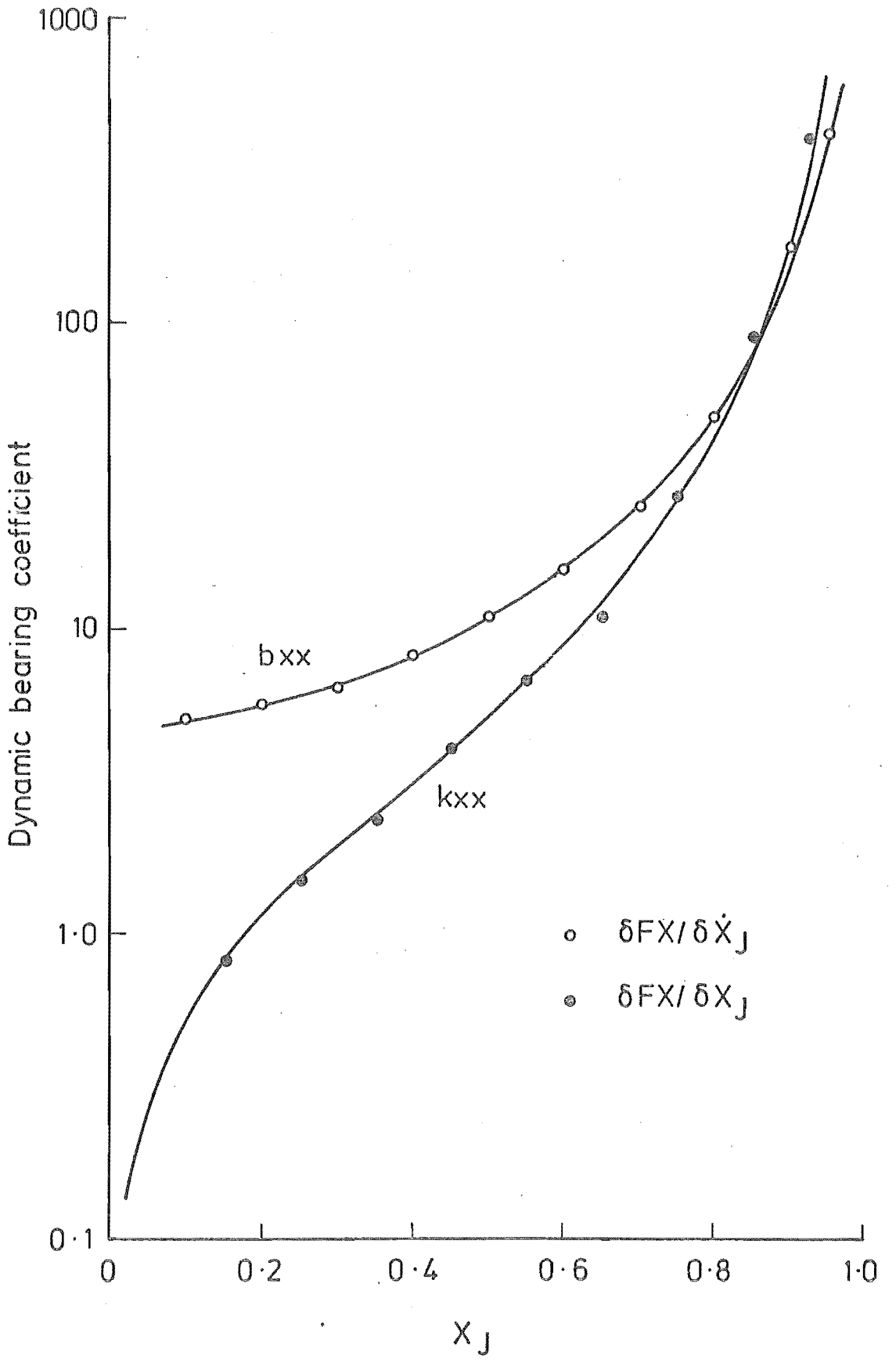

FIG 4-2 COMPARISON OF DYNAMIC BEARING COEFFICIENTS AND OIL FILM FORCE CHANGE.
PLAIN CIRCULAR BEARING, $L/D = 1{\cdot}0$, $Y_J = 0$.

IV.4 DIRECTLY LOADED BEARING

Comparison of the journal centre locus of a directly loaded bearing was made with the experimental results published by Shawki and Freeman[34]. The authors of this paper built a test rig to investigate the performance of a circular journal bearing loaded directly with a static and sinusoidal load. Both load components were in the same plane.

The test bearing had a length to diameter ratio of 1.5 and a clearance ratio of .0016. Two comparative runs were made, both with a sinusoidally alternating load, that is, no static load component. The non-dimensional load parameter was 5.1 and the relative load velocity, $\dot{\phi}/\omega$, .2 and .933. The bearing load was defined by :

$$FXJ = 5.1 \cos \phi$$

$$FYJ = 0.$$

The results of the comparison are shown in Figures 4-3 and 4-4. The solid line is the journal centre locus measured by Shawki and Freeman and the broken line the computed locus. Reasonable agreement was obtained for the lower relative load speed, but at 0.933, although the journal response is similar, the loci vary by a considerable amount.

The difference between the theoretical and experimental results is unlikely to be caused by variation of the lubricant viscosity within the oil film or distortion of the bearing surface as both of these have a small effect at low journal eccentricities. The Reynolds number, Urp/μ, based on the test rig maximum shaft speed and assuming typical lubricant viscosity and density (1500 r.p.m., 2.9×10^{-6} reyns, specific gravity = 1) is 33, hence the film will be predominantly laminar.

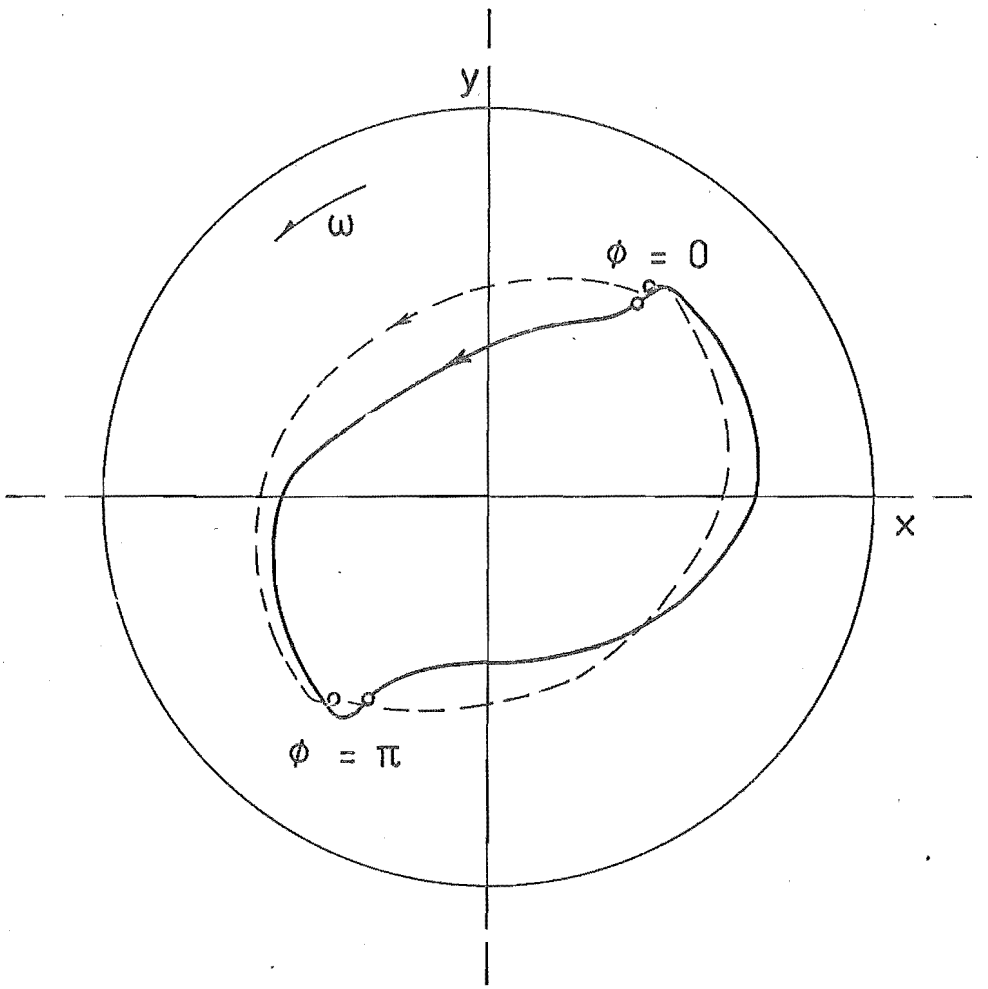

Journal load

FXJ = 5·1 Cos ϕ

FYJ = 0

$\dot{\phi}/\omega$ = 0·2

L/D = 1·5

--- theoretical

—— experimental (Shawki, Freeman)

FIG. 4-3 COMPARISON OF DIRECTLY LOADED BEARING JOURNAL CENTRE LOCUS WITH EXPERIMENTAL RESULTS.

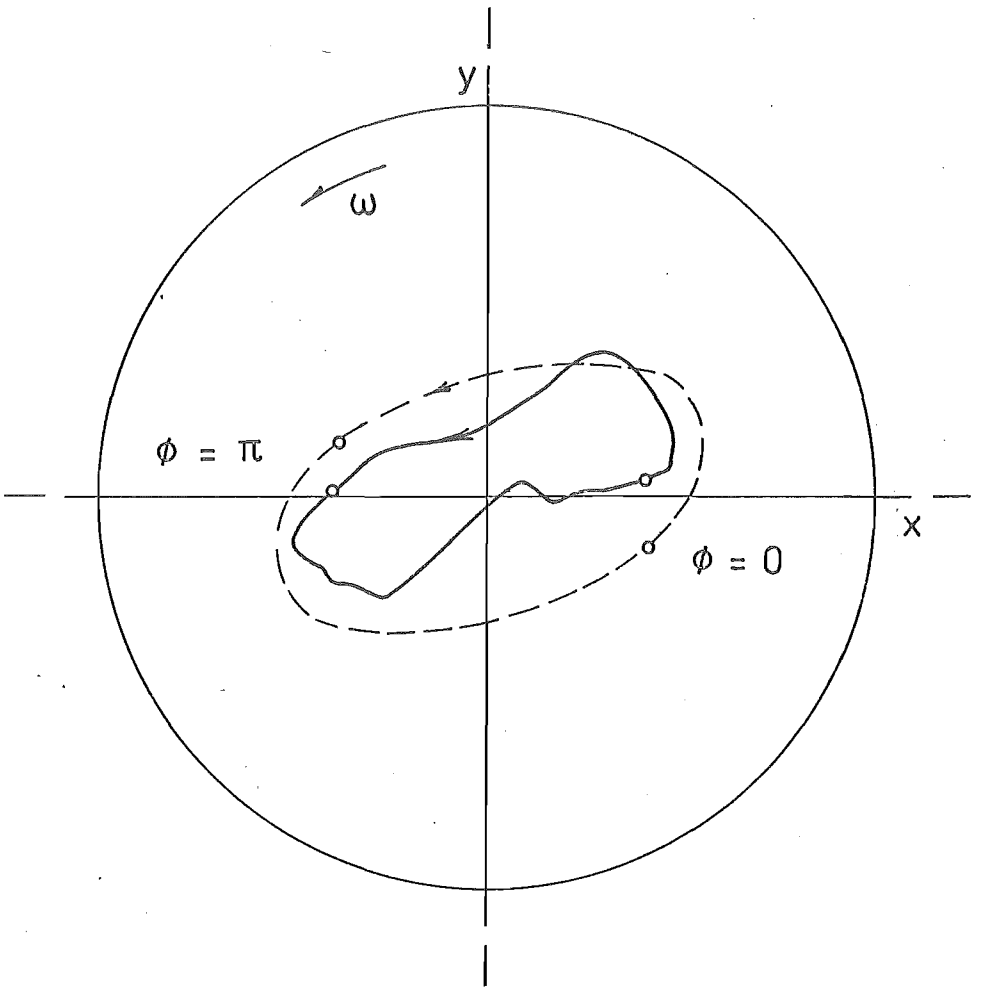

Journal load

FXJ = 5·1 Cos ϕ

FYJ = 0

$\dot{\phi}/\omega$ = 0·933

L/D = 1·5

--- theoretical

—— experimental (Shawki, Freeman)

FIG. 4-4 COMPARISON OF DIRECTLY LOADED BEARING JOURNAL CENTRE LOCUS WITH EXPERIMENTAL RESULTS.

The oil film boundary conditions adopted for the theoretical solution could, however, differ significantly from those existing in the test bearing. The film disruption pressure can be important if the dimensional bearing load is small, particularly as the sinusoidal applied force gives periods of zero bearing load. Also, at low journal eccentricities, there is a tendency for the film not to disrupt, this being possible by the generation of subatmospheric pressures.

A maximum value for the bearing load can be estimated by considering the limits of the test rig. The maximum load frequency for the rig was 3 cycles per second, thus to obtain a relative load velocity of 0.933 the shaft speed would have to be 20.2 radians per second or less. Assuming a typical lubricant viscosity of 2.9×10^{-6} reyns, the dimensional bearing load over project area is :

$$\frac{F}{L.D} = 116 \text{ lb/in}^2.$$

Because the bearing load is sinusoidal there will be two periods per load cycle of 15 degrees of load angle during which the bearing load over projected area falls below 15 lb/in^2. Thus subatmospheric disruption pressure would certainly modify the locus. At the lower relative load velocity this restriction on the bearing load is not as severe and hence the influence of the disrupted film region reduced. Closer agreement between the two loci was in fact found.

In general, subatmospheric disruption pressures will reduce the size of the journal centre locus as the positive oil film pressures are reinforced by the disrupted region on the opposite side of the journal. A more detailed assessment is difficult as the pressure of the film in this region is not known and would probably be a function of both time and the position on the journal surface.

Lubricant was supplied at 30 lb/in^2 to the experimental bearing through two pairs of holes at 90 and 270 degrees as measured from the positive x axis. This was simulated on the computer and found to have negligible effect on the journal locus. Experience with the program has shown that the hydrostatic lift from supply grooves is usually small, but disruption of the oil pressure film by the groove has a more marked effect.

Both the applied load and bearing geometry are symmetrical about the y axis; thus, taking into account the journal rotation, the journal locus should be skew-symmetrical about this axis. This was obtained with the theoretical solutions, but not the experimental results. This suggests that either the bearing load was not purely sinusoidal or difficulty was experienced in measuring the journal position.

Although only moderate agreement between the theoretical and experimental results was obtained, the differences are such that they are unlikely to have been caused by errors in the computer program. Taking into consideration the approximations made in deriving the oil film equations and the difficulties involved in determining the journal centre locus experimentally, the correlation between the two solutions shown here is acceptable.

IV.5 ROTOR MODEL

Finally a check of the programs incorporating single and twin mass rotor models was made. For this the experimental results of Brown and France[35] were used. The authors of this paper conducted a theoretical and experimental investigation into the amplitude of journal and

rotor motion of a flexible rotor mounted in plain circular hydrodynamic bearings. The theoretical solution was developed as an approximate method to determine the whirl amplitude of pump rotors operating under conditions predicted to be unstable by linearised analysis.

The experimental pump shaft consisted of a single rotor 6 in (152mm) in diameter and 4 in (102mm) long mounted on a 2¼ in (57mm) diameter shaft midway between two hydrodynamic bearings. The bearing centre lines were 30 in (762mm) apart. The bearings were plain circular, of 2¼ in (57mm) diameter and length and a radial clearance of .003 in (.075mm). The static bearing load was 37.4 lb (166N). The results used in this comparison were obtained with a rotor unbalance of .021 lb.in (2.4×10^{-4} kg.m) and a lubricant viscosity of 5.8×10^{-7} reyns (4 cP). The experimental rig was capable of shaft speeds up to 10,000 r.p.m. and the rotor was found to pass through a synchronous critical speed at 7,500 r.p.m.

The first program run was made at 10,000 r.p.m. with a single mass rotor model. The value of the mass was taken as that of the rotor plus half the shaft (.115 lb sec^2/in) and the stiffness evaluated assuming the shaft to be simply supported at the bearing centres and the rotor to be rigid (1.03×10^5 lb/in). Damping of 5% of the critical value was added to stablize the rotor mass as previous program experience had shown that the rotor model could be excited by the marching process. A small amount of damping had cured this without greatly affecting the journal or rotor locus. The system was started from rest and a half shaft speed whirl was observed, similar to the experimental results, but this was found to be a transient and the motion slowly decayed to a synchronous whirl.

The effect of the rotor damping and the initial conditions were

investigated next. Removing the damping increased the journal and rotor whirl amplitude slightly and the synchronous component of the motion was more pronounced. This was expected as viscous damping has more effect on high frequency motion. Changing the initial journal and rotor displacements also produced minor changes in the whirl amplitudes and ratio of synchronous to half speed whirl components. However, neither the damping or the initial conditions changed the basic response of the system: a transient half speed whirl with a smaller synchronous component.

Journal mass was added to the model by using the twin mass rotor program and assigning a high value to the second stiffness, namely one hundred times the shaft stiffness. This gave a critical speed for the journal spring mass system alone of 107,000 r.p.m. The total journal mass; that is, both bearings, was taken as the portion of the shaft not included in the rotor mass. This gave a value of .08 lb sec^2/in. Damping on the rotor mass was retained and the system again run at 10,000 r.p.m. This gave excellent correlation with the experimental results of Brown and France and the two results are shown in Fig. 4-5. Both synchronous and half speed whirls were observed.

A number of further runs were made with the same mass distribution. At 18000 r.p.m. both the journal and rotor whirled at .43ω with rapidly increasing amplitude. Under these conditions the system locked onto the critical speed of the rotor (approximately 7,500 r.p.m.) and as the whirl frequency was less than half the shaft speed, a trailing wedge oil film existed feeding energy into the motion.

The critical speed of the rotor in rigid bearings was 9,000 r.p.m. Running the model at this shaft speed failed to excite a resonant rotor whirl demonstrating the importance of the bearing stiffness to the system response.

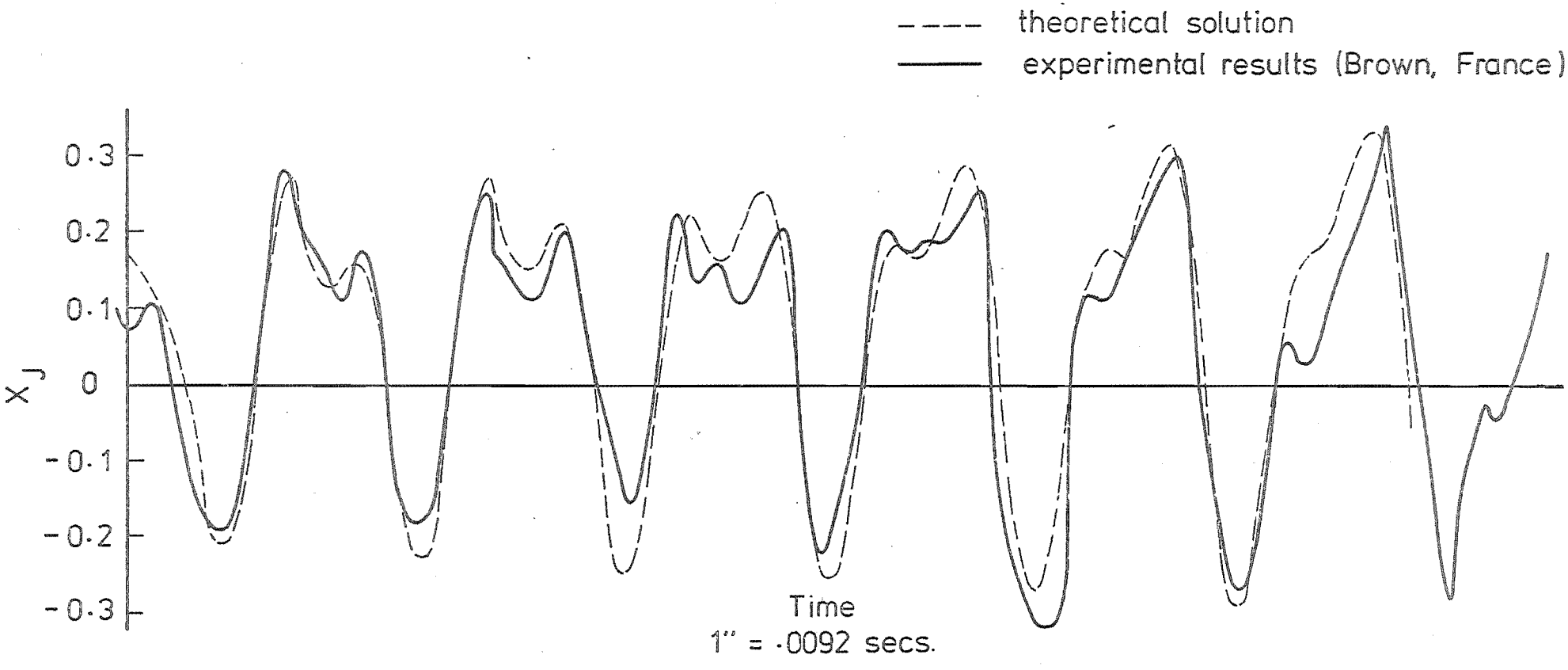

FIG 4-5 COMPARISON OF JOURNAL CENTRE MOTION WITH EXPERIMENTAL RESULTS. JOURNAL LOADED WITH TWO SPRING MASS SYSTEMS REPRESENTING A SIMPLE ROTOR AND JOURNAL MASS.

Brown and France observed a synchronous critical speed of 7,500 r.p.m. but this did not appear in the theoretical solution. A redistribution of the mass was made to include the effect at shaft over-hang. This increased the rotor mass; the values of the rotor and journal masses then being .129 and .066 lb sec^2/in respectively. Starting the system from rest a combination of synchronous and half speed whirls were obtained, but the latter appeared as a decaying transient. Restarting the program with initial conditions simulating a synchronous whirl resulted in a small half speed component which decayed rapidly leaving the synchronous motion reported by Brown and France.

Although the rotor shaft speed was high, the Reynolds number, calculated at 10,000 r.p.m. and assuming the lubricant to have a specific gravity of one, is 600, thus the flow would be predominantly laminar. The bearing ran at low eccentricities, thus distortion of the bearing surface and variation in the film viscosity would be minimal. The bearing load over projected area was small and thus the disrupted region of the oil film could be expected to influence the journal motion. However, the correlation between experimental and theoretical results was very good, suggesting that if the film did break down at other than atmospheric pressure, the influence on the bearing, under these conditions, must have been small.

This comparison with the experimental work of Brown and France shows the ability of the program to model simple bearing-rotor systems. It also illustrates the behaviour of such a system allowing the following conclusions to be drawn :

(a) Prediction of instability by linearised analysis does not necessarily mean an unbounded motion of the rotor or journal. The point of instability for this rotor was calculated by

Brown and France to be 7,000 r.p.m. but both the experimental and theoretical results showed a limited amplitude whirl at shaft speeds higher than this;

(b) the out of balance excites a synchronous motion and, for a system linearly unstable operating above its critical speed, the resultant motion is a combination of synchronous and half speed whirls;

(c) both the journal and rotor undergo synchronous whirls when the shaft speed equals the critical speed;

(d) at shaft speeds greater than twice the critical speed an unstable whirl occurs of frequency equal to that critical speed;

(e) the natural frequency of the rotor alone is not important, the effect of the bearing stiffness must also be considered;

(f) introduction of journal mass favours the establishment of half speed whirl.

CHAPTER FIVE

FULL SOLUTION

To march out the displacement loci for a bearing-rotor system requires considerable computer time and is, therefore, expensive. The solution obtained applies to one set of initial conditions or forcing functions and thus a number of computer runs are required to analyse a system. Increasing the complexity of the system model also increases the computation. Few systems can be represented by a single bearing model, as used for this investigation, and it is necessary to consider a multi-bearing, multi-mass system. Thus, a full solution analysis of a bearing-rotor system is expensive and only suitable for problem cases or final design checks.

The length of computation arises from the time required for the finite difference solutions of the oil film equations and the need for these solutions to be repeated at frequent intervals around the locus. The latter is necessary because the non-linearity of the dynamic bearing coefficients restricts their use to small changes in journal displacement and velocity from the conditions at which they were calculated.

The aim of the work reported in this chapter was to considerably reduce the computation time necessary for a full solution of a bearing-rotor system, by improved utilisation of the dynamic bearing coefficients. The alternative approach, to reduce the time required to solve the oil film equations, was not taken as the techniques of faster solution sacrifice both accuracy and generality of the solution to obtain their improvement. Many of the techniques reported require circumferential bearing symmetry[13,14] or, by assuming an axial pressure distribution, reduce the possible bearing surface grooving[12]. The finite difference

technique used in this investigation to solve the oil film equations, has been developed and used by many authors; thus significant savings in computation are unlikely to be obtained by any further development.

The program developed was based on the twin mass rotor program described in Chapter 3. The program incorporates the same rotor model and will accept the same bearing designs.

V.1 ALTERNATIVE SCHEMES

A number of modifications to the computer program were tried. The best of these achieved a small reduction in computation time, but because of additional program complexity they were considered to be unsatisfactory.

A simple form of predictor-corrector was tried. This involved stepping from point 1 to point 2 in the usual manner and evaluating the oil film force and the dynamic bearing coefficients at this point. The step was then retaken, finishing at point 3, using the coefficients just calculated at point 2 to estimate a mean value for the step. The oil film force only was evaluated at the final point and this was used to check the accuracy of the step. The dynamic coefficients used to start the next step were those calculated at point 2. This scheme increased the average step length by approximately 20%, but the additional computation time required for the evaluation of the extra oil film force absorbed this and the net gain was zero.

If the dynamic bearing coefficients were stored as a function of the journal displacement and velocity, repeat calculations for the same parameters could be avoided. However, the quantity of information is enormous. Allowing for twenty values of each of the four parameters

the storage requirement is 1.28 million words. Also, the number of repeated calculations would be small except in cases of very small change between cycles of the journal centre locus.

A plain circular bearing exhibits circumferential symmetry. The non-circular bearing designs are made up of a series of arcs, thus evaluating the dynamic bearing coefficients with respect to a co-ordinate system rotating with the eccentricity vector could reduce the variation of the coefficients around the journal locus. If this is so, longer locus steps could be taken. To investigate this, the dynamic coefficients for an elliptical bearing design were calculated and it was found, even for regular journal loci, that the variation in the coefficients was not significantly reduced.

The change in the length of the locus step is determined by the accuracy of the force balance at the end of the preceding step and is achieved by multiplying or dividing by a constant. An alternative scheme was devised expressing the new step as a function of the error in the load balance. It proved to be very dependent on the choice of function and on the data on which the program was run. An improvement was made by including the old step length in the function, but as the savings in time were small, and the scheme was unreliable, no further work was undertaken.

V.2 LINEAR EXTRAPOLATION OF DYNAMIC BEARING COEFFICIENTS

The first attempt to improve the utilisation of the dynamic bearing coefficients within the basic program structure was to estimate, by linear extrapolation, the average value of the coefficients for the proposed locus step. The extrapolation was based on the starting point and the previous

point at which the film equations were solved, and the coefficients estimated for the midpoint of the proposed step. The extrapolation was done with respect to time as a system based on change in the journal position and velocity would require prior knowledge of these parameters at the conclusion of the step and would thus be difficult to program.

This produced good results. For a circular journal centre locus, eccentricity ratio 0.6, in a plain circular bearing the number of locus steps required per cycle of the journal locus was reduced from 55 to 32, a reduction of 42%.

This scheme was adopted for use in all the programs as significant savings are obtained for small increases in complexity and computation. The programming itself is straightforward, which is important if the program is to be used on a commercial basis, and the additional storage requirements small. The reliability of the scheme has been proven by its extensive use in both the directly loaded journal program and the rotor model program.

V.3 UTILISATION OF PREVIOUS CYCLE DATA

Bearing-rotor systems which require the greatest computation time are those whose loci change slowly with time. The journal centre locus varies little from cycle to cycle, thus the possibility exists of using the information calculated in the preceding cycle to assist the marching process. The principal factor limiting the length of a locus step is the non-linearity of the dynamic bearing coefficients. If the change of the coefficients during a step could be predicted, the step length would increase, thus reducing the computation time per cycle of journal centre locus.

This was achieved by storing the dynamic bearing coefficients as they were calculated and in the following locus cycle using these values to estimate the change of the coefficients within a step. The twin mass rotor model program, on which this program was based, has two marching schemes. The outer one involves the solution of the oil film equations, checking the accuracy of the locus and organising the inner marching scheme - the predictor-corrector routine. The inner scheme marches the locus within each step. The predictor-corrector routine requires the dynamic bearing coefficients to be expressed as a function of the journal displacement, thus storing the coefficients with respect to time is not possible. A two-dimensional storage array incorporating the two cartesian co-ordinates of the journal displacement is complicated and not necessary if the assumption is made that the change in journal position between consecutive cycles is small. The technique used was to estimate the centre of the journal motion, normally the journal static equilibrium position could be used, and define a locus position by its angular displacement (alpha) with reference to this point. The eight bearing coefficients were stored with respect to this value.

From the stored information, the first derivative of each of the dynamic bearing coefficients with respect to alpha was calculated. The step length of the predictor-corrector call was defined in terms of alpha and the coefficient derivatives were calculated from the change in their values over this range of alpha during the preceding cycle. The predictor-corrector routine was supplied with the coefficients at the beginning of the step and their first derivative, and from these, the values of the coefficients were estimated for each point on the locus. The differences between this program and the twin mass rotor model program described in Chapter 3 were that the dynamic bearing coefficients were expressed as linear functions of the journal position, instead of constants,

and that the length of the predictor-corrector call step was controlled by the journal position rather than time.

Approximations made in calculating the dynamic bearing coefficients do not increase the program errors. The accuracy of the program was controlled by the force balance at the conclusion of each of the outer steps and the step length adjusted to meet the required tolerance.

The application of this method of coefficient evaluation is dependent on the existence of a suitable journal centre locus. The behaviour of the program with unsuitable loci was not investigated as an estimation of the saving in computation time was considered to be the first objective.

The program was tested on a circular journal locus in a plain circular bearing, as used in Section V.2. The number of steps required per locus cycle was reduced to 21 from the 32 required for the linear extrapolation scheme described in the same section.

In general, the variation of the dynamic bearing coefficients is not linear. Analysis of the program results showed that the step length was lower when the second derivative of the coefficients was high. Thus, the program was extended to consider both the first and second derivatives of the coefficients.

As before, the coefficients were stored with respect to alpha. For each step the data stored at alpha nearest the midpoint of the step and the values on either side of this were extracted. To these three values, for each of the eight bearing coefficients, a quadratic equation in alpha was fitted with alpha measured from the beginning of the proposed step. The constant term was thus the value estimated from the stored data, of

the bearing coefficient at the beginning of the step and this was replaced with the coefficient value just calculated with the oil film equations. Thus, in effect, the first and second derivatives were calculated from the previous cycle and the constant term from the present cycle. The quadratic equation's information was transferred to the predictor-corrector routine and the value of the bearing coefficients estimated at each point on the locus within the step.

The program was tested on the same data as the linear scheme and showed no improvement. Analysis of the results suggested that random variations in the dynamic bearing coefficients calculated from the oil film equations, due primarily to errors in the journal displacement and velocity, were reducing the accuracy with which the quadratic equations could be determined. To overcome this it was decided to smooth the stored data.

V.4 SECOND DEGREE, SMOOTHED-DATA SCHEME

Irregularities in the stored dynamic bearing coefficients were found to upset the second degree scheme of coefficient prediction described above. To solve this, it was decided to investigate smoothing the stored data.

A high degree of accuracy for the smoothing routine was not required and thus sophisticated techniques were not needed. The technique used was to take a five point average with a sample length of 0.1 radians using linear interpolation to obtain sample values between points at which solutions of the oil film equations had been performed. The choice of the number of samples and sample length was based on the change of the coefficients within the locus cycle and the maximum step length the program was

permitted to take. The test data was the full whirl in a plain circular bearing described previously and the variation of the coefficients with alpha was approximately sinusoidal of period π. If the total length of the sample is too long, the basic sinusoidal nature of the data is destroyed, but if too small, that is, less than a step length, the effectiveness of the smoothing is impaired. The value chosen, 0.5, equalled half the maximum permitted step length as the program was unlikely to run, at that stage in its development, with larger steps. The scheme worked satisfactorily and only reduced the peak to peak amplitude of the data by approximately 7%. The period was within 2% of π. Nine and fifteen point schemes were tried with a variety of weights on the samples, but no significant improvement was obtained.

The smoothed data was used as before to determine eight quadratic equations expressing the change of the coefficients within the locus step. Initially the second degree scheme was also used in the first locus cycle to determine the coefficients, but it was found that linear extrapolation, with respect to alpha, was more suited to this task. The smoothed data was not used for this as it necessitated removing the extrapolation at least 0.2 radians from the start of the step.

Testing the program, again on the circular data, showed that the steps required per locus cycle were reduced to 17. This corresponds to an average step length of 21 degrees.

V.5 EFFECT OF LOCUS ACCURACY CONSTANTS

A limited investigation was conducted into the effect on the computation time of the value of the load accuracy tolerance (LOADAC) and the size of the locus step length change. It was found that increasing

the tolerance reduced the computation time and that the relationship between the two was approximately linear.

Three values of load accuracy tolerance were tried - 5, 7 and 10%. The average program step length increased with the tolerances as did the mean error in the force balance between the applied journal load and oil film force. The latter relationship was nearly linear and in all cases tested the average error in the force balance was approximately one quarter of the load accuracy tolerance. A tolerance of 10% was used to obtain the results reported in this chapter.

The tolerance at which the program reduced the step length was changed from 0.5 LOADAC to 0.4 LOADAC. This also reduced the average program error and step length. As no benefit was derived from the modification it was not retained.

The factor by which the locus step length was modified according to the force balance error was tried at values of two and the square root of two. The latter generally proved to be the more successful, giving a slightly larger average step length for the same locus accuracy, but the improvement was dependent on the program data. This factor was subsequently used in all programs.

V.6 SUMMARY

The overall reduction in computation time was approximately 70%, but the cost of analysing a bearing-rotor system is still high. The greatly increased program complexity, the restrictions on the form of the journal locus which the program can handle and the still significant computation time make this method of full solution unsuitable for design work.

It is the opinion of the author that further work along the lines considered here will result in increasing program sophistication for small reductions in computation. To significantly reduce the computation time of a full solution, a radically new approach will be necessary.

Of the methods developed, the linear extrapolation technique is the best. It offers considerable time saving over schemes using the dynamic bearing coefficients calculated at the beginning of the step, but does not reduce the versatility of the program or significantly increase its complexity. This technique was adopted for all the locus marching programs.

CHAPTER SIX

WORK PERFORMED BY THE OIL FILM ON THE JOURNAL AND THE BEHAVIOUR OF THE ROTOR

The two existing techniques for assessing the stability of a bearing-rotor system are linearised analysis of the bearing coefficients calculated at the static equilibrium position and full solution involving marching out the journal and rotor loci for a given set of initial conditions. Both of these have limitations. The linearised solution can only be applied for small journal displacement from the static equilibrium position and the full locus solution is expensive to compute.

The stability of a bearing-rotor system is very much dependent on the work performed by the oil pressure film on the journal. In the absence of external rotor forces, such as damping forces, the oil film work is entirely responsible for the excitation or damping of the rotor motion. If the film work could be simply determined without marching out the full system solution, the system stability could be assessed without the limitations of the existing techniques. It was proposed to represent the rotor with a force locus, initially with a circular locus, and applying this directly to the journal, calculate the oil film work. From this, decay or growth of the rotor motion could be determined for a particular amplitude and frequency of rotor vibration. Thus, with a small number of computer runs, the behaviour of the bearing-rotor system could be predicted.

However, the work reported in this chapter showed that, except for a few special cases, even a simple flexible rotor could not be represented by a single force locus. A direct assessment of the bearing-rotor system is therefore not possible with this technique. However, usage

of the oil film work does have potential for further development and for qualitative investigations into the behaviour of the oil pressure film.

VI.1 ACCURACY OF THE OIL FILM WORK CALCULATION

If a plain circular bearing is loaded only with a constant magnitude force rotating at a constant angular velocity, the journal centre will follow a path of constant eccentricity at the same angular velocity. Thus, the work performed by the oil pressure film on the journal can be calculated from the static bearing performance data with the equation :

$$\text{WORK} = 2\pi\varepsilon_0 \text{ DELS } (1 - 2.\text{RLV}) \sin\psi$$

The wedge oil pressure film is modified by the angular velocity of the eccentricity vector (see Equation 2.1a), hence the term 1 - 2.RLV is required to convert the static load to the actual film force. The attitude angle is determined by the journal eccentricity and is not affected by the journal centre rotation. The relative load velocity (RLV) is used in place of $\dot{\gamma}/\omega$ as, for this bearing loading, the angular velocities of the load and journal centre are equal.

The accuracy of the computer program's numerical calculation of the oil film work was checked with this loading. A plain circular bearing of length to diameter ratio 0.75 was used and the relative load velocity was 0.3. In Section II.7 the method of calculation of the oil film work is described and the choice of the force vector on which to base this calculation was discussed. To compare the two calculations, the film work was evaluated using both the applied bearing load and the oil film force. The results, tabulated in Fig. 6-1, were obtained with a load accuracy tolerance of 5%.

ECCENTRICITY RATIO ε	OIL FILM FORCE DEL	ATTITUDE ANGLE ψ°	OIL FILM WORK $2\pi\varepsilon$ DEL Sin ψ	NUMERICAL CALCULATION USING APPLIED LOAD		NUMERICAL CALCULATION USING OIL FILM FORCE	
				WORK	ERROR%	WORK	ERROR%
·2	·1278	76·89	·1565	·1577	+ ·77	·1551	—·89
·5	·4750	56·97	1·251	1·259	+ ·64	1·243	-·64
·7	1·1800	42·98	3·539	3·556	+ ·48	3·525	-·40
·8	2·1966	34·92	6·321	6·371	+·79	6·353	+·51
·9	5·609	25·48	13·645	13·625	-·15	13·617	-·21
·95	13·406	18·49	25·375	25·559	+·73	25·487	+·44

FIG. 6-1 COMPARISON OF OIL FILM WORK CALCULATED NUMERICALLY AND FROM STATIC BEARING DATA.

The percentage errors in the numerical results are based on the values calculated from the static journal parameters. In all cases the error is less than one percent and has no apparent relationship to the journal eccentricity ratio. This suggests that the magnitude of the error is controlled by the load accuracy tolerance (LOADAC) and not the program data. The results show no significant difference in accuracy between the two numerical calculations.

Summary

The error involved in the calculation of the oil pressure film work is in the order of one percent. For the conditions under which this accuracy check was performed, no significant difference in accuracy was found between calculating the film work with the applied journal load and the oil film force. The applied load was used for the work described in this thesis.

VI.2 CORRELATION OF ROTOR LOCUS GROWTH AND OIL FILM WORK

The validity of the rotor model programs is established in Chapter 4, by comparing the program results to published experimental data, and the accuracy of the oil film work calculation is shown in the preceding section. By using the rotor model programs and comparing the calculated oil film work to the change in the rotor energy, the concept of the oil pressure film performing work on the journal, and thereby exciting or damping the rotor motion, can be established.

The data chosen for the comparison was a single mass rotor and a plain circular bearing of length to diameter ratio 0.75. The rotor static load was such as to require a journal static eccentricity ratio of 0.7. The system was started from its equilibrium position by an impuse sufficient to produce a maximum dynamic bearing load

equal to half the static load. Under this loading the journal centre does not immediately orbit the bearing centre. The choice of the rotor shaft stiffness and the system critical speed is important. The critical speed largely determines the direction of the energy flow between the oil pressure film and the journal (see Chapter 7) and the ratio of the bearing stiffness to rotor shaft stiffness determines the degree of influence the bearing has on the rotor and hence the rate of decay or growth of the rotor motion. A stiffness ratio of 2:1 was chosen and a critical speed for the rotor alone of 0.32ω. These gave a system critical speed of approximately 0.26ω.

The program was run for four cycles of the rotor locus and the oil film excited the rotor motion into a growing elliptical whirl. The net work performed by the oil film on the journal over this period was 2.124 (non-dimensional value) and the increase in rotor energy was 2.130. This gives an error in the energy balance of .006 (0.3%) which is within the one percent error found in the oil film work calculation in the previous section. The maximum discrepancy in the energy balance was .044, occurring in the third locus cycle, but in general the error was less than .01.

This accuracy of energy balance is satisfactory for the bearing-rotor system considered. When the oil film work per cycle is small, the energy transfer at various points on the locus is still significant. The error in the energy balance is related to the total energy transferred, not the net flow, thus under these conditions an error of one percent is significant and must be considered in an analysis.

This degree of accuracy in the energy balance would be unlikely to have been achieved if the accuracy of the oil film work was not of a

similar order or if the equations of motion of the rotor had been incorrectly formulated. Although these two were taken as being correct to establish the role of the oil film work, achieving an energy balance would be unlikely if this assumption was not justified. There is the possibility that an error would not manifest itself as an energy discrepancy or that a number of errors could be compensating, but considering the previous work undertaken to verify the program and work calculations, this possibility is small.

Summary

An energy balance was obtained within acceptable limits between the work performed by the oil pressure film and the rotor energy. This verifies the role of the oil film in exciting or damping the rotor motion.

VI.3 PREDICTION OF ROTOR STABILITY

If the force exerted by a rotor on a bearing can be represented by a simple force locus, then the stability of the bearing-rotor system can be determined from the work performed by the oil film on the journal when the bearing is loaded with this locus. However, if this is not possible because the force locus changes with time, for example if it is composed of more than one frequency, the energy transfer calculated for any one part of the locus will be applicable only for a short time and thus have only a small effect on the system stability. If a number of loci are required to describe the system, this method of analysis loses its advantage and it would be preferable to march out the journal and rotor displacement locus for the complete system.

The problem resolves into two questions :

(a) Under what conditions does the rotor exert a constant simple force locus on the bearing?

(b) How dependent is the oil film work on the shape of this locus?

The dynamic bearing characteristics are complex. Both the displacement and velocity terms are non-linear, coupled and the principal values differ. An established vibration of a system in which the shaft deflection accounts for the majority of the rotor movement is therefore the most likely to provide a simple force locus. Consider such a situation and assume the bearing coefficients to be linear and uncoupled. If the bearing is rigid it will not affect the rotor locus and there is no energy transfer between the oil film and journal, thus this would be a trivial case. If the bearing stiffness is finite, however, the difference in the principal bearing stiffnesses will cause a difference in the total system principal stiffnesses and hence the frequency of the free vibration along these axes will also differ.

The effect of this can be seen by considering two orthogonal sinusoidal displacement vectors whose frequencies differ by a small quantity δ :

$$u = A \cos \omega t$$

$$v = A \sin (\omega + \delta) t$$

At $t = 0$ the locus is circular but in general, it is elliptical with the ratio of the major to minor axes a function of time. When $\delta.t = \pi/2$ the locus is a straight line at 45 degrees to the u axis and as $\delta.t$ increases further, the locus again tends towards a circle, but the direction of rotation is reversed.

For a flexible rotor the force on the bearing is almost completely defined by the displacement of the rotor mass. (The journal movement by comparison is small and does not significantly affect the deflection of the rotor shaft). The force locus exerted on the bearing is thus similar to the displacement locus described. Reducing the stiffness of the rotor shaft slows the change in the locus, but does not prevent it. This also lowers the ratio of oil film work to rotor energy; thus the rate of decay or growth of the rotor motion is also slowed and the problem of a changing force locus is not avoided.

The change in the rotor mass locus can be seen in Figure 6-2. The single mass rotor model program was run with an elliptical bearing and a ratio of rotor shaft to bearing stiffness of approximately .04. The critical speed of the rotor alone is .47ω and the system ran at .463ω and .455ω for the first and last cycles computed respectively. The system was started on a slightly elliptical orbit, to allow for the non-circularity of the journal centre locus when loaded with a circular force locus, and it can be seen that the rotor orbit becomes increasingly more elliptical. Because of the low ratio of rotor shaft to bearing stiffness, the change between consecutive rotor locus cycles is small and thus only the first, fifth and tenth cycles are shown. The oil film work also changes with the locus. For the first cycle of the rotor locus the non-dimensional work performed by the film on the journal is .149, but by the final cycle the film is damping the rotor motion, the film work being -.183.

Increasing the shaft stiffness accelerates the change in the rotor locus. The single mass program was re-run with the same conditions except the rotor stiffness was increased by a factor of ten and the mass altered to give the same rotor critical speed (Figure 6-3.) In

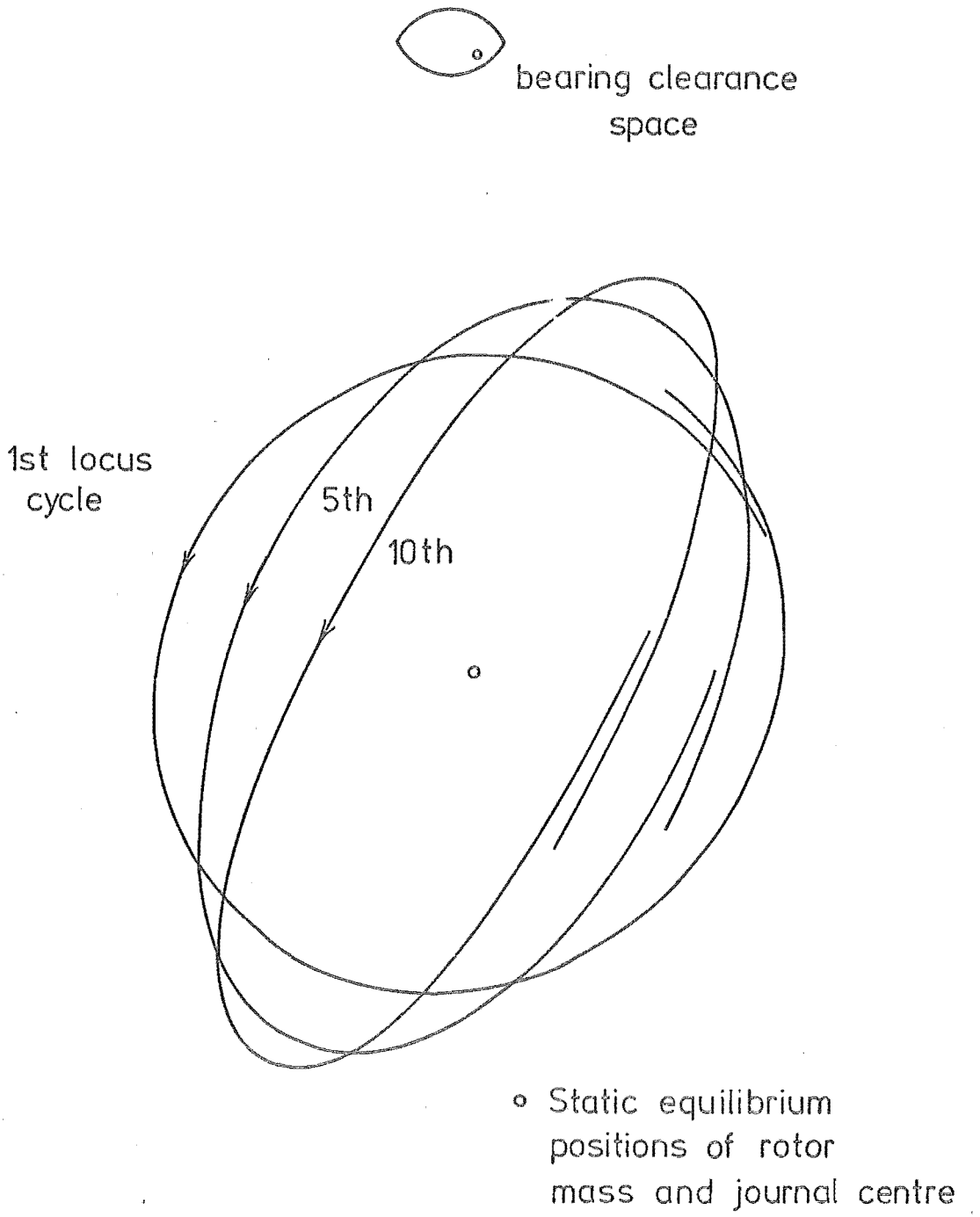

FIG. 6-2 ROTOR MASS LOCUS FOR FLEXIBLE ROTOR; FIRST, FIFTH AND TENTH CYCLES SHOWN. SINGLE MASS ROTOR MODEL, ELLIPTICAL BEARING.

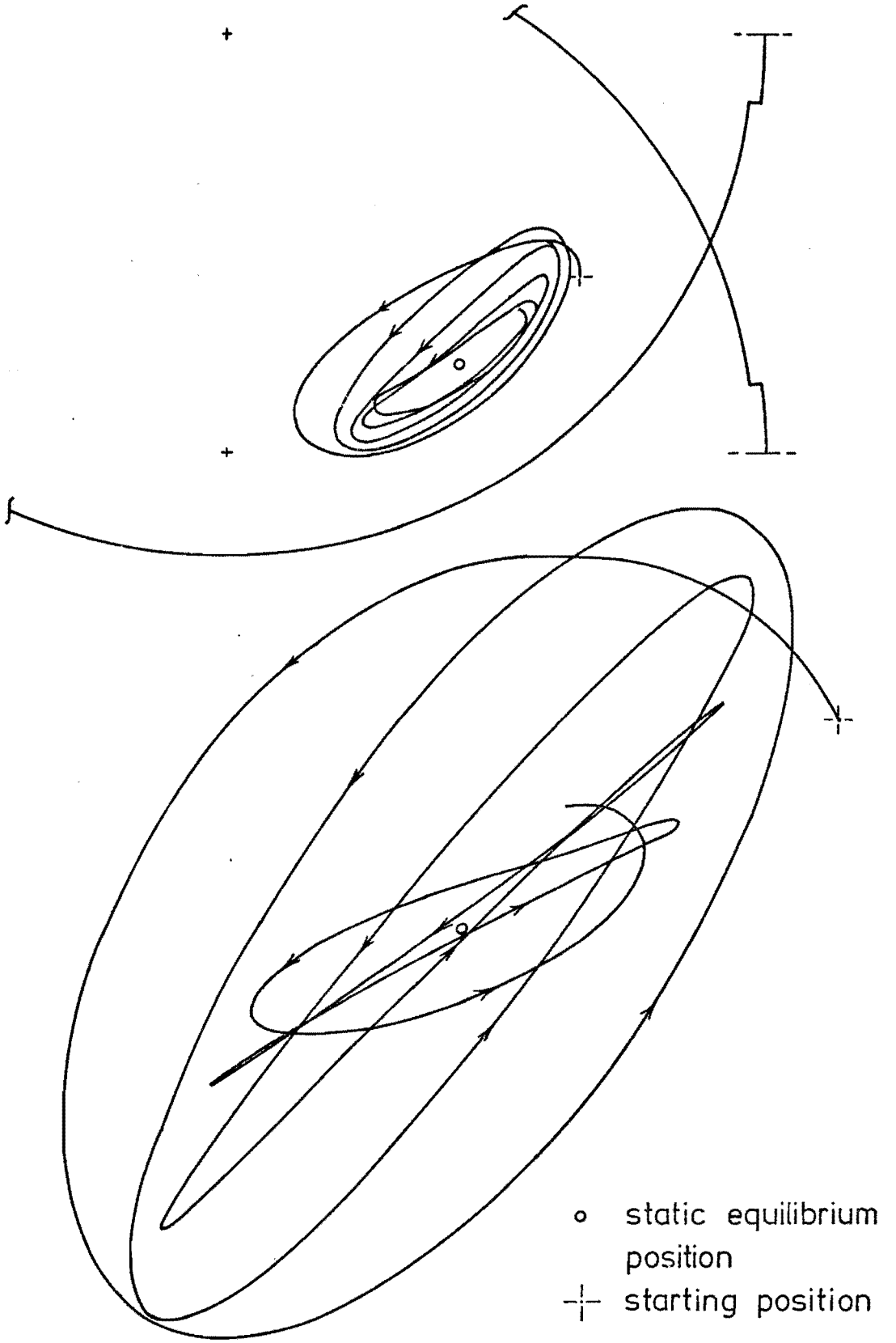

FIG. 6-3 JOURNAL CENTRE AND ROTOR MASS LOCI. SINGLE MASS ROTOR MODEL, ELLIPTICAL BEARING.

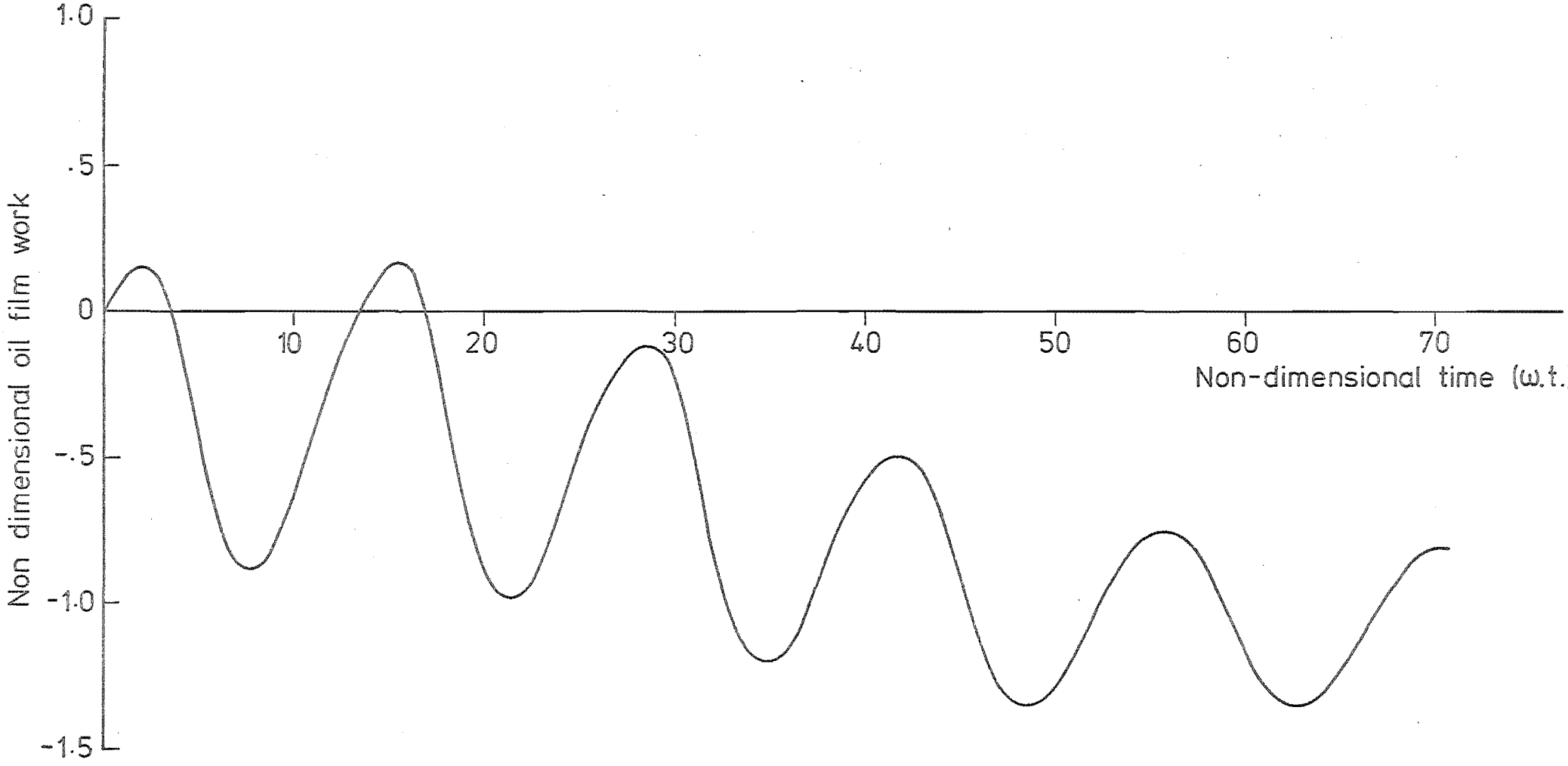

FIG. 6-4 WORK PERFORMED BY OIL FILM ON JOURNAL. SINGLE MASS ROTOR MODEL, ELLIPTICAL BEARING.

this case the program was run for sufficient time to allow the reverse rotation mode of the rotor locus to appear. The journal, under the force locus imposed by this motion, provides a high degree of damping, thus the mode exists for only one cycle and a forward rotor whirl reforms. Again, the oil film work was found to be very dependent on the form of the rotor locus, and hence the journal force locus, and this can be seen in the plot of oil film work against non-dimensional time (Figure 6-4).

There are particular situations in which the rotor can be represented by a single force locus. A circular force locus is adequate to describe a full whirl in a bearing with circumferential symmetry. If the bearing asymmetry is small, the same locus will suffice for a system with a flexible rotor shaft. Such situations are uncommon and, in general, it is the sub-orbital journal motions which are of interest when predicting the decay or growth of a vibration.

A preliminary investigation was conducted into modelling a bearing-rotor system subjected to an impulse. It was found that the system behaviour is not related to the oil film work calculated with a circular journal force locus. A sinusoidal force locus, aligned with the disturbance, is adequate to represent the initial motion of a flexible rotor, but the direction of the energy transfer does not necessarily indicate the stability of the system as here also the form of the rotor displacement locus varies with time.

A sinusoidal force locus was found to be inadequate to describe a system where the bearing stiffness is not significantly greater than the rotor shaft stiffness. Under these conditions, the bearing has a greater influence on the rotor and thus its displacement locus changes

rapidly. Also, because the journal displacement is a significant part of the system motion, the bearing response affects the force locus. Thus, because of the complexity of the dynamic bearing characteristics, the force locus cannot be described with a simple regular expression.

Summary

A direct assessment of a bearing-rotor system stability is not possible by representing the rotor with a single force locus and calculating the energy transfer between the oil film and the journal. For even the simplest conditions, an established motion of a flexible rotor, the rotor displacement locus and hence the journal force locus, vary with time. The work done by the oil film on the journal is very much dependent on the force locus, thus the energy transfer between the film and journal also changes between locus cycles. If the rotor motion becomes more complex, for example by increased rotor shaft stiffness, or by introducing transients such as a rotor disturbed from its static equilibrium position by an impulse, the difficulty in representing the rotor by a force locus is increased.

VI.4 SUMMARY

The importance of the work performed by the oil pressure film on the journal to the stability of a bearing-rotor system has been established. Thus, the possibility exists of predicting the stability of a system from a knowledge of the energy flow between the oil film and the journal when the bearing is loaded by a force locus representing the rotor. An investigation into the behaviour of a single mass bearing-rotor model was conducted and it was found that the rotor could not be represented by a single force locus and thus a simple direct assessment of a system stability is not possible.

A more complex approach is required and this must consider the interaction of the bearing and rotor. Although a useful method of system analysis was not evolved from this investigation, the idea of analysing the energy flow through the oil film has potential as it avoids the limitations of linearised analysis without introducing the expense of a full solution. In the opinion of the author further work in this direction is desirable.

In its present stage of development the directly loaded journal computer program permits a qualitative investigation into the behaviour of dynamically loaded bearings. The oil film work is a useful parameter on which to base comparisons and the versatility of the program, both in terms of bearing geometry and journal loading, allows a wide range of conditions to be considered. From such work an understanding of the behaviour of the oil pressure film can be obtained.

CHAPTER SEVEN

THE INFLUENCE OF BEARING PARAMETERS ON THE WORK DONE BY THE OIL PRESSURE FILM ON THE JOURNAL

In this chapter the effect on the oil film work of the bearing parameters - geometry, relative load velocity and load magnitude - is described. The results reported were obtained with the bearing journal directly loaded by a circular force locus comprised on a static and a constant magnitude, constant speed, dynamic component. Although, as previously discussed, this loading generally does not represent the forces generated by a rotor, the investigation does give an insight into the behaviour of the oil film.

VII.1 TEST DATA

The concept behind the choice of data was to approach the investigation from the point of view of bearing design. Many of the design parameters are determined by external factors; for example, shaft speed, journal diameter and static load, but there is usually sufficient freedom with the design specifications to choose others, such as bearing geometry, length to diameter ratio, clearance ratio and static journal eccentricity. For this investigation a basic design was assumed - a plain circular geometry of L/D ratio .75, clearance ratio .00125 and static eccentricity ratio .7 - and the parameters varied around these. The large number of variables involved in defining a bearing and its loading, even with the simple model assumed for this work, makes a complete analysis too long to undertake. The system of varying the bearing parameters about a basic design yields the greatest quantity of information useful for design for a given amount of computation.

The majority of the results are expressed in terms of non-dimensional variables. In some cases, however, a comparison of dimensional values is required, thus it is necessary to assign values to the shaft speed, journal diameter and lubricant viscosity. The values used were :

ω = 157.1 rad/sec (1,500 r.p.m.)

D = 4.0 in (102mm)

μ = 2.9×10^{-6} reyns (0.2 poises)

For the basic bearing design described above these give a non-dimensionalising factor for force of

DIML = 1750 lb (7780 N)

Throughout this investigation the value used for the load accuracy tolerance, LOADAC, was 5% for load ratios (ratio of dynamic to static bearing load) less than unity and 10% for those greater. The larger loads involved high journal eccentricities which make the locus computation difficult. The error in the oil film work for a 5% value of LOADAC was established in Chapter 6 to be 1%. To determine the effect of increasing the load tolerance to 10%, the basic circular bearing was run at a load ratio of two for both tolerances. The oil film work increased by 2.8%, but a 90% saving in computation time was obtained.

VII.2 EFFECT OF L/D ON FULL CIRCULAR JOURNAL WHIRL

The purpose of this section is to show the effect of the bearing length to diameter ratio and demonstrate the behaviour of the wedge oil film. This was achieved by considering a plain circular bearing loaded with a single rotating force of constant speed and magnitude. Under these conditions the oil pressure film is a wedge film and the oil film work can be calculated using :

$$\text{WORK}\,\frac{L}{D} = 2\pi\varepsilon.(\text{DEL}.\frac{L}{D}).\text{Sin}\,\psi \qquad \ldots 7.1$$

To take into consideration the rotation of the eccentricity vector, the shaft speed is replaced by the effective shaft speed, $1-2\dot{\gamma}/\omega$. Thus, for a relative load of 0.3, the value used for this investigation, the oil film force is determined by multiplying the static bearing film force by 1 - 2.3; that is, 0.4.

The non-dimensionalising factor chosen for the oil film force (see II.2) is directly proportional to the bearing length. Thus, if the non-dimensional force is maintained at a constant value, the dimensional value will increase in direct proportion to the bearing length. Work is the product of force and displacement; thus, the same proportionality applies to this parameter. For practical purposes it is more useful to consider constant dimensional load or oil film work. Using the parameters DEL.$\frac{L}{D}$ and WORK.$\frac{L}{D}$ achieves this, whilst retaining the independence of the results from the shaft speed, lubricant viscosity and bearing diameter and clearance.

Equation 7.1 was evaluated for bearing length to diameter ratios of 0.125 to 2.0 and the results are shown in Figure 7-1 as a plot of oil film work parameter against L/D. The lack of static load and the constant eccentricity whirl divorces the results from reality, but they do show the behaviour of the wedge film.

For a constant load magnitude the oil film work is a maximum for an eccentricity ratio of approximately 0.7. Decreasing the length to diameter ratio derates the bearing, thereby increasing the radius of journal whirl, but reducing the attitude angle. Above an eccentricity ratio 0.7 the effect of the change in attitude angle in Equation 7.1 predominates, thus the film work is reduced. Below 0.7 the reduction in the whirl radius is more important and again the work is reduced. The

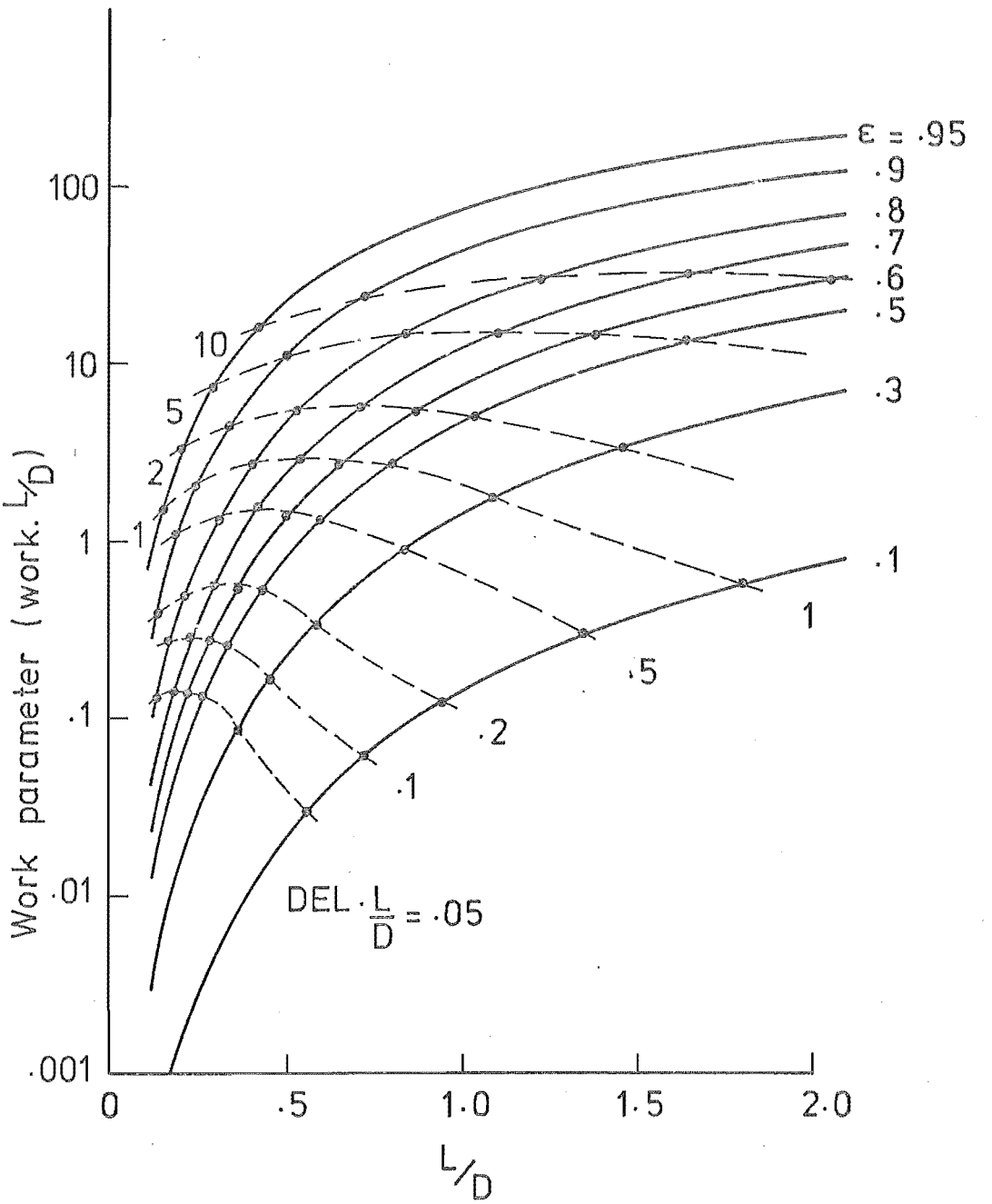

FIG. 7-1 EFFECT OF L/D RATIO ON WORK PERFORMED BY THE OIL FILM. FULL CIRCULAR WHIRL, PLAIN CIRCULAR BEARING.

STATIC LOAD = 0

WHIRL SPEED = $\cdot 3\omega$

(DEL. L/D) AND (WORK. L/D) ARE CONSTANT FOR CONSTANT DIMENSIONAL JOURNAL LOAD AND OIL FILM WORK.

product $\varepsilon \sin\psi$ can be considered as a measure of the asymmetry of the wedge film. It is the displacement of the journal perpendicular to the plane of the bearing load and it is this characteristic which allows the large energy transfer to occur between the rotational and vibrational modes of journal motion. The term $\varepsilon \sin\psi$ tends to zero at $\varepsilon = 0$ and 1 and has a maximum value at about 0.7 for all L/D in the range considered.

If the journal eccentricity ratio is held constant, the oil film work increases as the length to diameter ratio is raised. This is produced almost entirely by the uprating of the bearing. The remaining factor in Equation 7.1, the attitude angle, is almost independent of L/D and thus has only a minor influence.

The results presented here, although of little direct use for bearing design, show clearly that for a given load both the attitude angle and journal centre path length are important to the energy transfer between the journal and oil film.

VII.3 INFLUENCE OF BEARING GEOMETRY

Seven bearing geometries were analysed, including the basic circular design, all with length to diameter ratio 0.75. Except for the second three-lobe design, the minimum radial clearance ratio of the land supporting the static journal load is equal to the clearance ratio of the circular bearing, that is, 0.00125. The second three-lobe design has a segm radial clearance ratio of this value. In all cases the minimum oil film thickness with the bearings subjected to equal static loads is l than for the plain circular design. If a comparison of bearing ge etries for equal static minimum film thickness is required, the re presented in Section VII.5 can be used to modify the circular be results. One important implication of the choice of bearing

ratio is that the non-dimensionalising factors are the same for six of the bearing geometries permitting direct comparison of the non-dimensional results.

The bearing geometries are shown diagramatically in Figure 7-2 and are :

(1) Plain Circular - This is the basic circular design described previously. It was not intended as a practical design; thus there are no grooves for oil supply and drainage.

(2) Circular Three-Lobe - This design has a circular cross-section but the bearing surface is broken into three lands by pairs of axial grooves at 0, 90 and 180 degrees. (Angular displacement on the bearing surface is measured from the positive x axis). The grooves are in pairs to provide drainage and supply for each land. For the computer program each pair was taken as a single groove 15 degrees long and of full bearing width. To simulate the lower lubricant temperature in the top two lands achieved by the grooving, the viscosity was increased by 50%. For Shell HVI 65 mineral oil, this represents a 10°C temperature drop[28]. Experimental and theoretical work[28,30] suggests that temperature variations of this magnitude can be expected.

Bearings of this and the following type are used by A.E.I. and are described by Smith[36].

(3) A.E.I. Grooved Circular - Another bearing circular in cross-section. The bearing surface is broken with full width 30 degree axial grooves at 0 and 180 degrees and the top land contains a circumferential groove of 25% of the bearing width. These groove proportions are not necessarily those used by A.E.I. As with the previous design, the bearing was run with the top land viscosity increased by 50%.

FIG 7-2

BEARING GEOMETRY

Circular three lobe

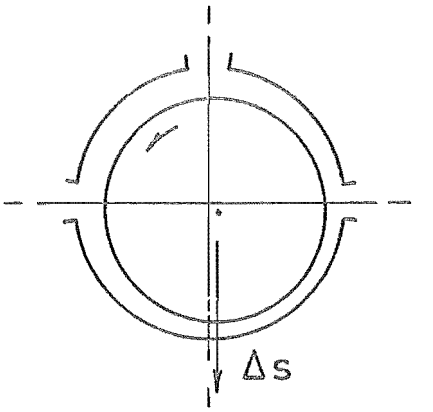

A.E.I. grooved circular

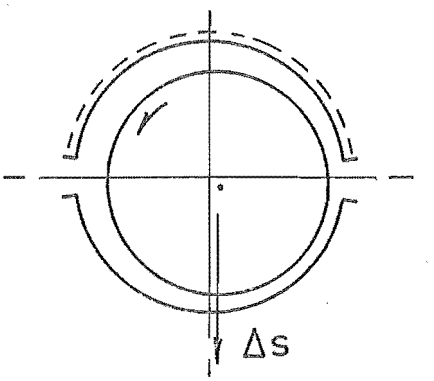

Elliptical

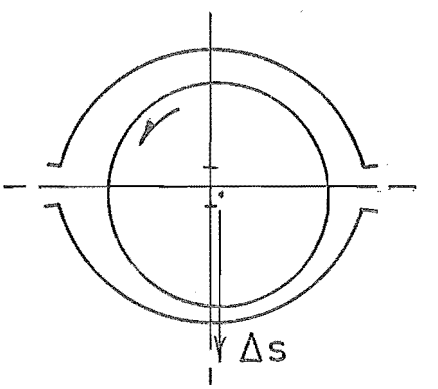

Spiral

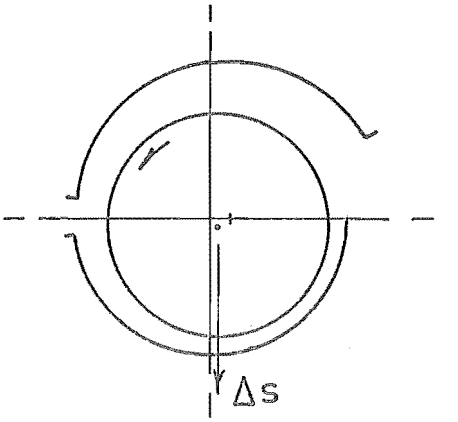

Three lobe

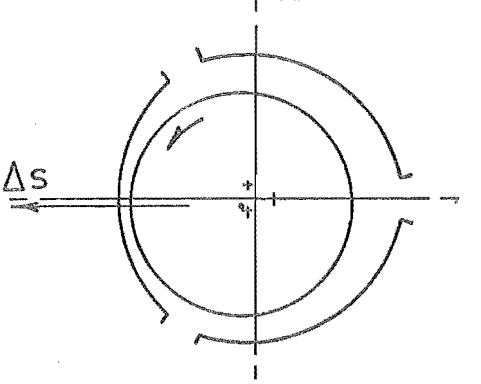

(4) Elliptical - The elliptical design is made up of two identical circular segments arranged such that the segment and bearing centres do not coincide and give a vertical bearing clearance less than the horizontal clearance. The ratio of minimum clearance to segment radial clearance is 0.67 and 30 degree axial grooves in the horizontal plane (i.e. 0 and 180 degrees) supply lubricant to the bearing.

(5) Spiral - This consists of two semi-circular segments, the upper one having a greater clearance and its centre displaced horizontally from the bearing centre by an amount equal to the difference in the radial clearances. Thus the bearing surface is continuous at 180 degrees, but contains a step at zero. The radial clearance of the top land is twice that of the bottom and axial supply grooves at 0 and 180 degrees are 30 and 15 degrees long respectively.

(6) Three-lobe - This is an extension of the elliptical design. The centre of each of the three identical segments is beyond the bearing centre on radial lines at 240, 0 and 120 degrees respectively. The ratio of minimum clearance to segment radial clearance is 0.67 and 15 degree axial grooves are incorporated at the junctions of the segments.

(7) Three-lobe, reduced clearance - This bearing is geometrically similar to the previous design. The bearing clearance is smaller making the radial segment clearance equal to that of the plain circular bearing. This reduces the minimum clearance ratio to .00085.

The bearings were subjected to the same dimensional loading. The static load chosen was that required for an eccentricity ratio of 0.7 on the basic circular bearing. Three ratios of dynamic to static load were used: 2.0 to give a full journal whirl, 0.5 for a suborbital whirl, that is, the journal locus not enclosing the bearing centre, and 0.1 for small journal motion. A relative load velocity of 0.3 was chosen as this involves a well established trailing film allowing the behaviour of each bearing in this unstable situation to be observed. In all cases the grooves were maintained at zero gauge pressure.

Results

The results are tabulated in Figure 7-3 showing the oil film work on the journal per load cycle and the percentage difference from the plain circular bearing. The minimum oil film thickness calculated is also given. The results for the three-lobe bearing with reduced clearance have been modified to allow a direct comparison with the other non-dimensional results. Thus the same non-dimensionalising factors apply to all the bearings. The journal centre loci are shown in Figures 7-4 to 7-10.

Results for the A.E.I. grooved circular design and spiral design with a load ratio of two are not included as difficulty was experienced in computing the journal loci. The upper lands of these bearings are severely derated and require a very low non-dimensional minimum film thickness (in the order of .01) to support the load. Besides being difficult to compute and involving high errors, the results have no practical relevance as oil films of this magnitude would be intolerable.

With the load ratio at 0.5 all bearings exhibit a suborbital journal

BEARING	$\Delta T/\Delta S = .1$ OIL FILM WORK	COMPARISON WITH CIRCULAR	MINIMUM FILM THICKNESS	$\Delta T/\Delta S = .5$ OIL FILM WORK	COMPARISON WITH CIRCULAR	MINIMUM FILM THICKNESS	$\Delta T/\Delta S = 2.0$ OIL FILM WORK	COMPARISON WITH CIRCULAR	MINIMUM FILM THICKNESS
Plain circular	·030		·27	·82		·198	12·5		·064
Circular, 3 lobe	·037	+23%	·27	·99	+21%	·193	10·9	-13%	·024
A.E.I. grooved circular	·041	+37%	·23	1·09	+33%	·188			
Elliptical	·043	+43%	·26	1·19	+45%	·160	9·6	-23%	·040
Spiral	·036	+20%	·26	·98	+20%	·188			
Three lobe	·046	+53%	·21	·95	+16%	·129	8·8	-30%	·052
* Three lobe Reduced clearance	·040	+33%	·24	·73	-11%	·148	7·0	-44%	·067

* Results corrected for difference in non-dimensionalising factors.

FIG 7-3 NON-DIMENSIONAL OIL FILM WORK PER LOAD CYCLE WITH VARIOUS BEARING GEOMETRIES. $L/D = .75$, RLV = .3

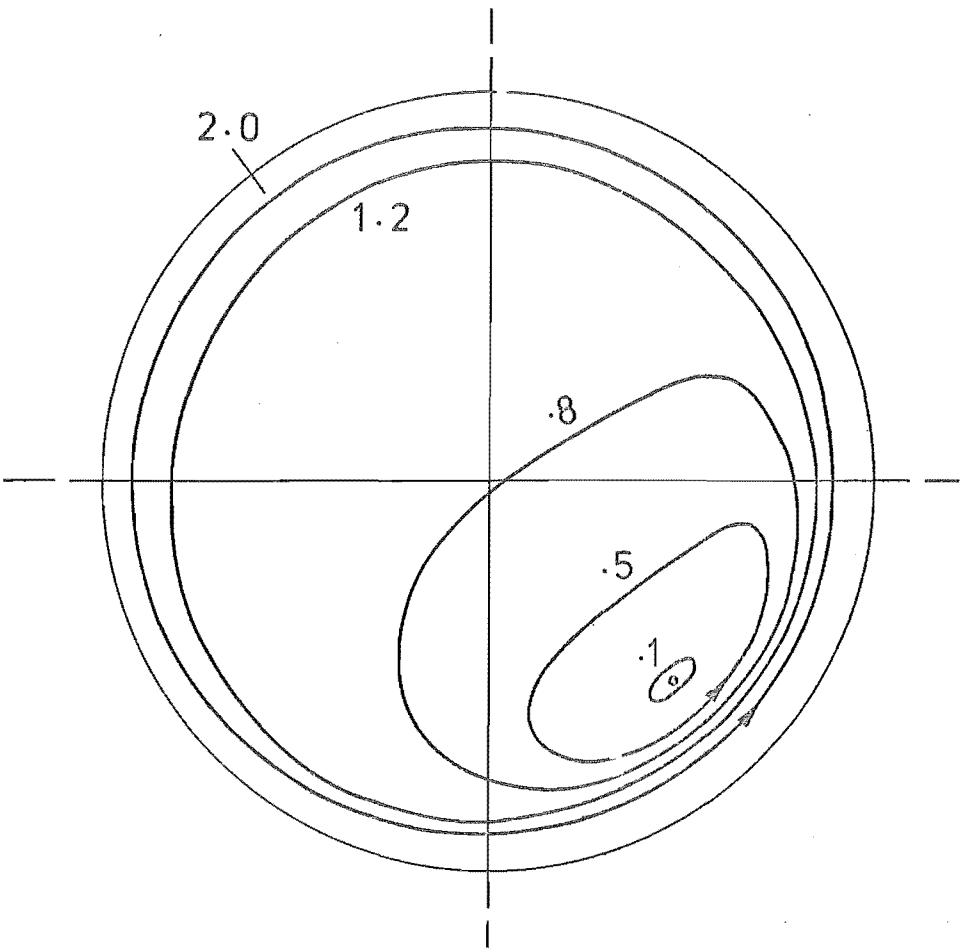

FIG. 7-4 JOURNAL CENTRE LOCUS, PLAIN CIRCULAR BEARING

L/D - ·75

RLV - ·3

LOAD RATIOS	·1	·5	·8	1·2	2·0
FILM WORK	·03	·82	2·27	5·79	12·5
MINIMUM OIL THICKNESS	·27	·198	·165	·115	·064
ANGULAR POSITION OF MINIMUM FILM	315°	315°	312°	253°	207°

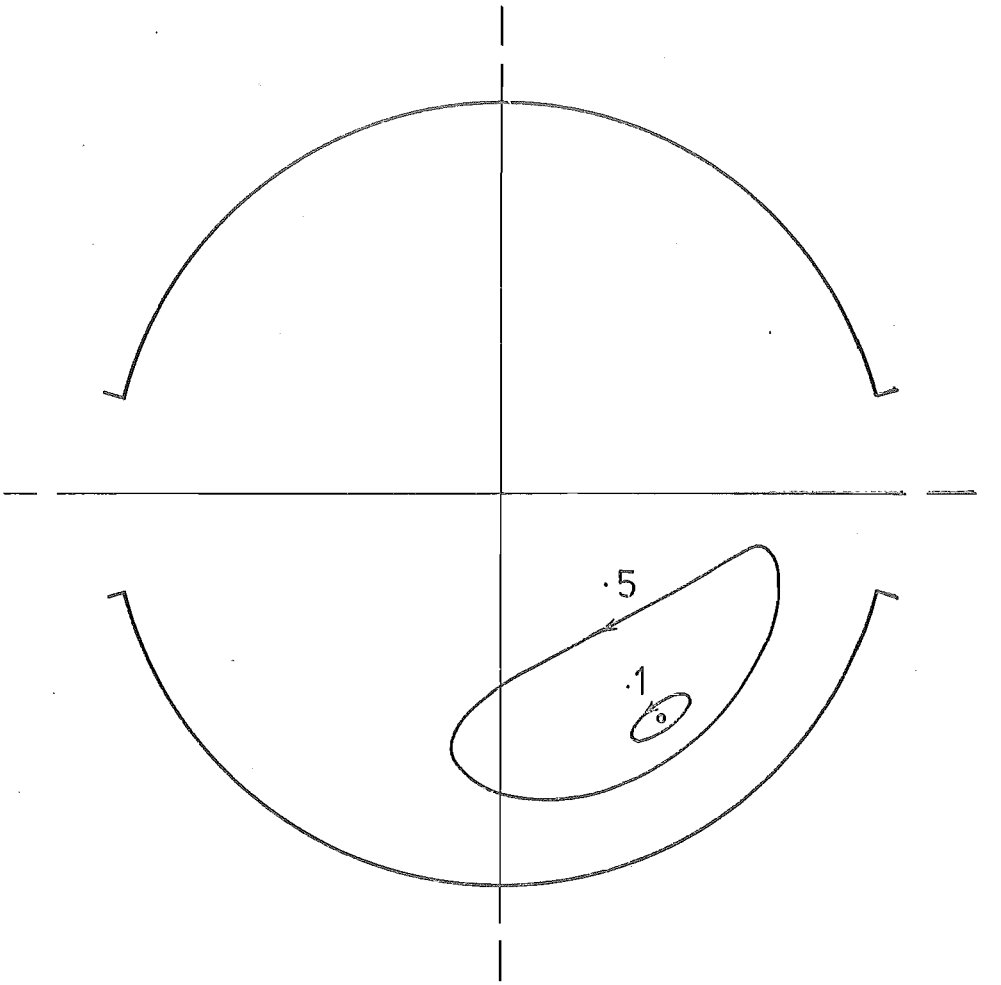

FIG 7·5 JOURNAL CENTRE LOCUS, A.E.I. GROOVED CIRCULAR

L/D - ·75

RLV - ·3

LOAD RATIOS	·1	·5
FILM WORK	·041	1·09
MINIMUM OIL FILM THICKNESS	·23	·188
ANGULAR POSITION OF MINIMUM FILM	305°	305°

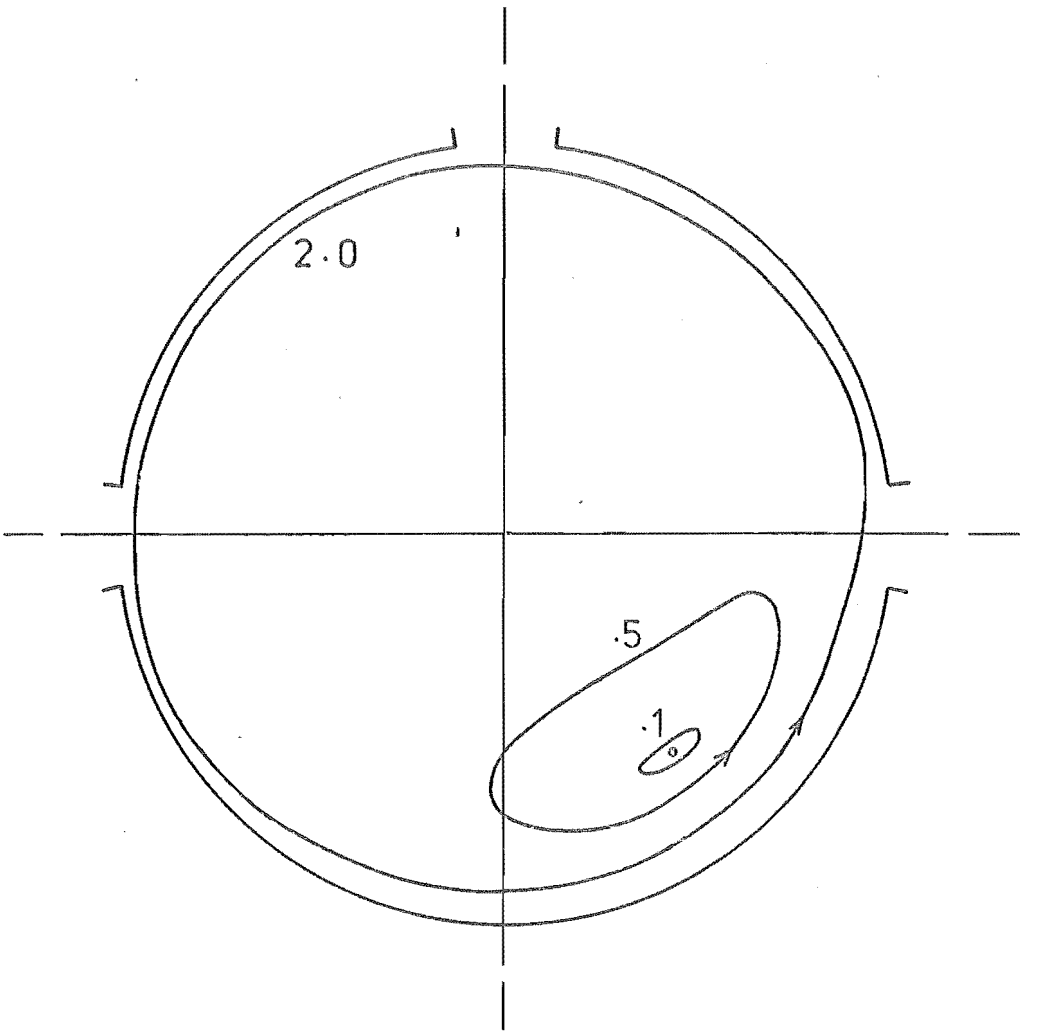

FIG. 7-6 JOURNAL CENTRE LOCUS, CIRCULAR THREE LOBE

L/D - ·75

RLV - ·3

LOAD RATIOS	·1	·5	2·0
FILM WORK	·037	·99	10·9
MINIMUM OIL FILM THICKNESS	·27	·193	·024
ANGULAR POSITION OF MINIMUM FILM	310°	310°	200°

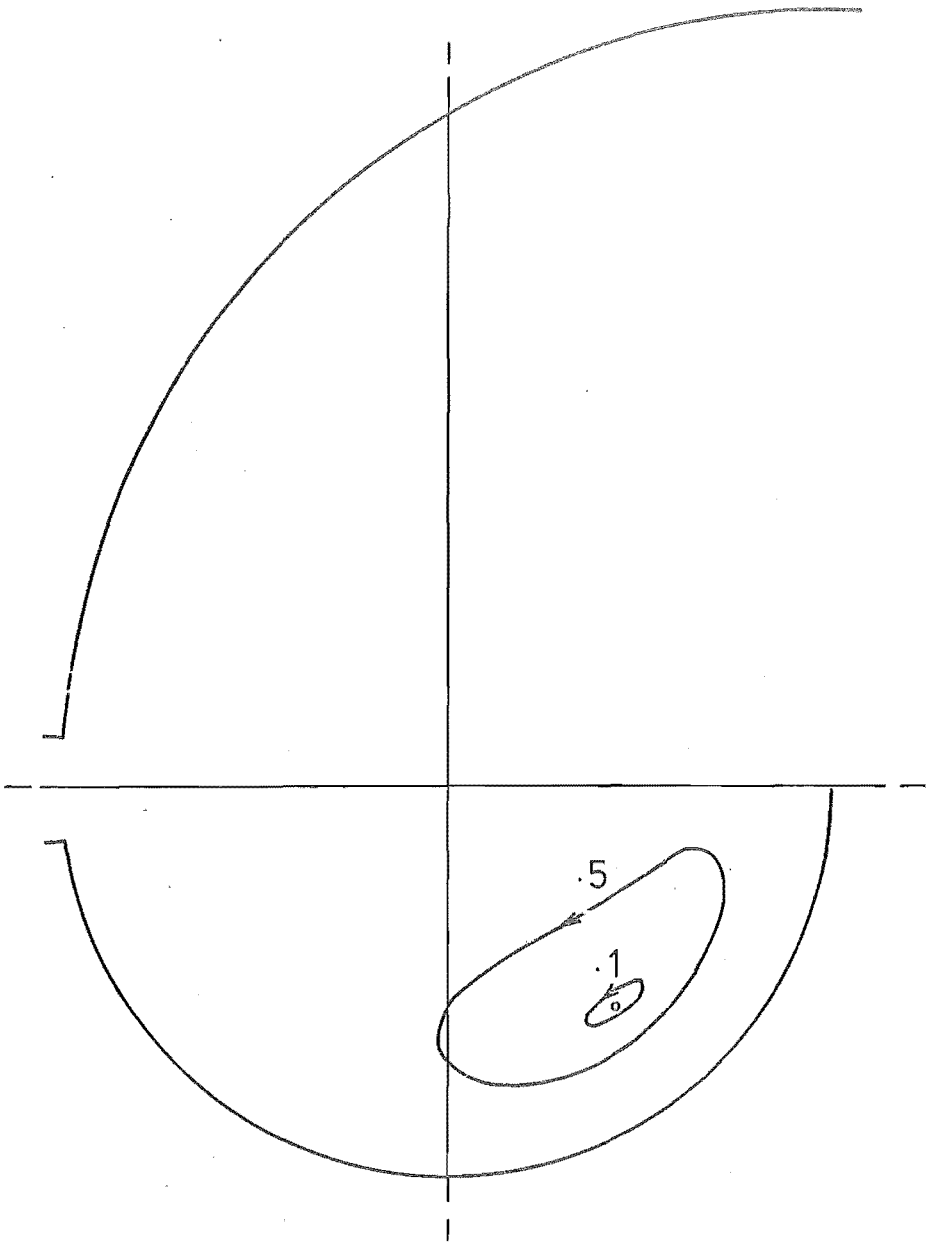

FIG 7-7 JOURNAL CENTRE LOCUS, SPIRAL BEARING.

$L/_D$ - ·75

RLV - ·3

LOAD RATIOS	·1	·5
FILM WORK	·036	·98
MINIMUM OIL FILM THICKNESS	·26	·188
ANGULAR POSITION OF MINIMUM FILM	308°	305°

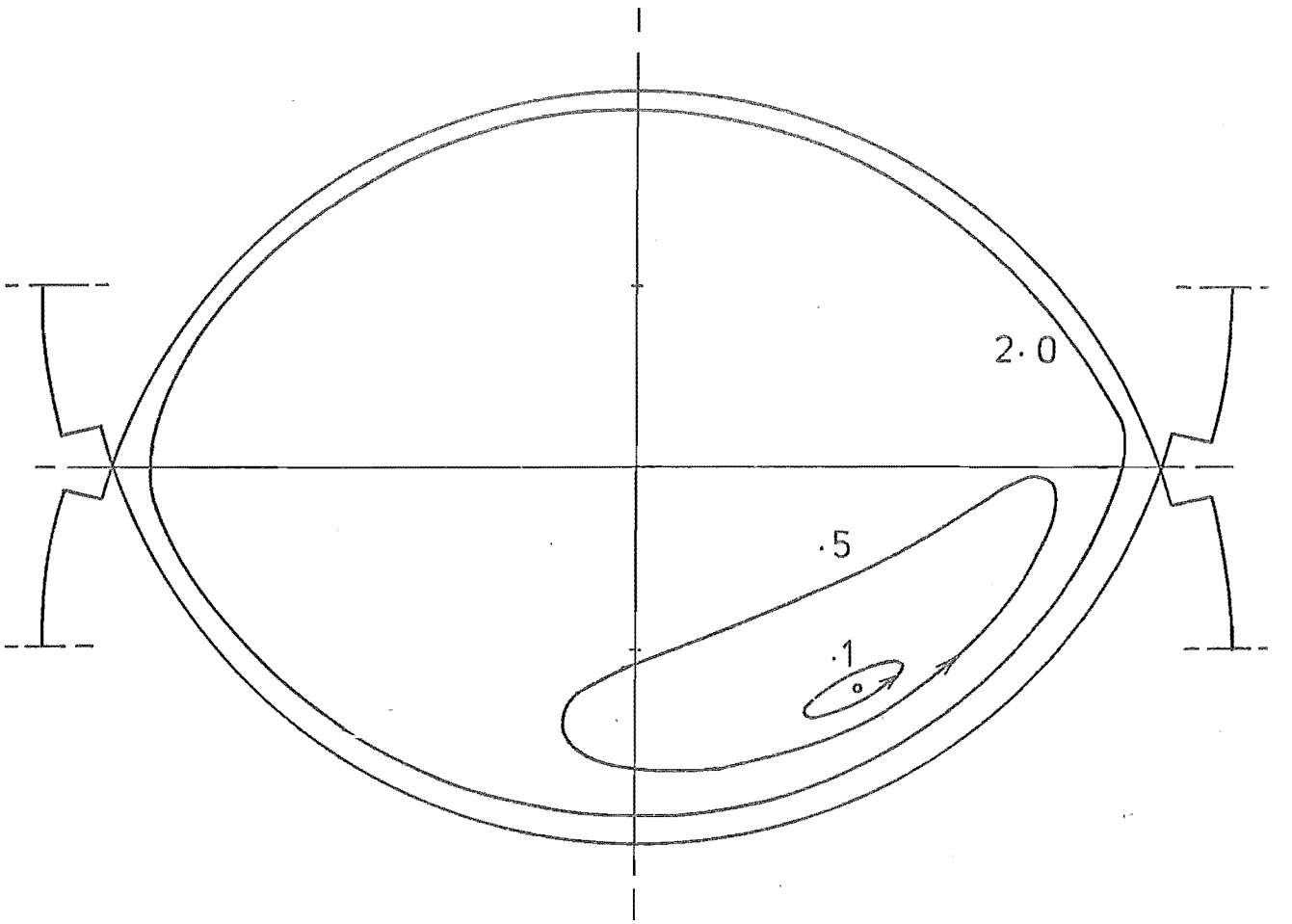

FIG 7–8 JOURNAL CENTRE LOCUS, ELLIPTICAL BEARING.

L/D - ·75

RLV - ·3

LOAD RATIOS	·1	·5	2·0
FILM WORK	·043	1·19	9·60
MINIMUM OIL FILM THICKNESS	·26	·16	·04
ANGULAR POSITION OF MINIMUM FILM	300°	300°	208°

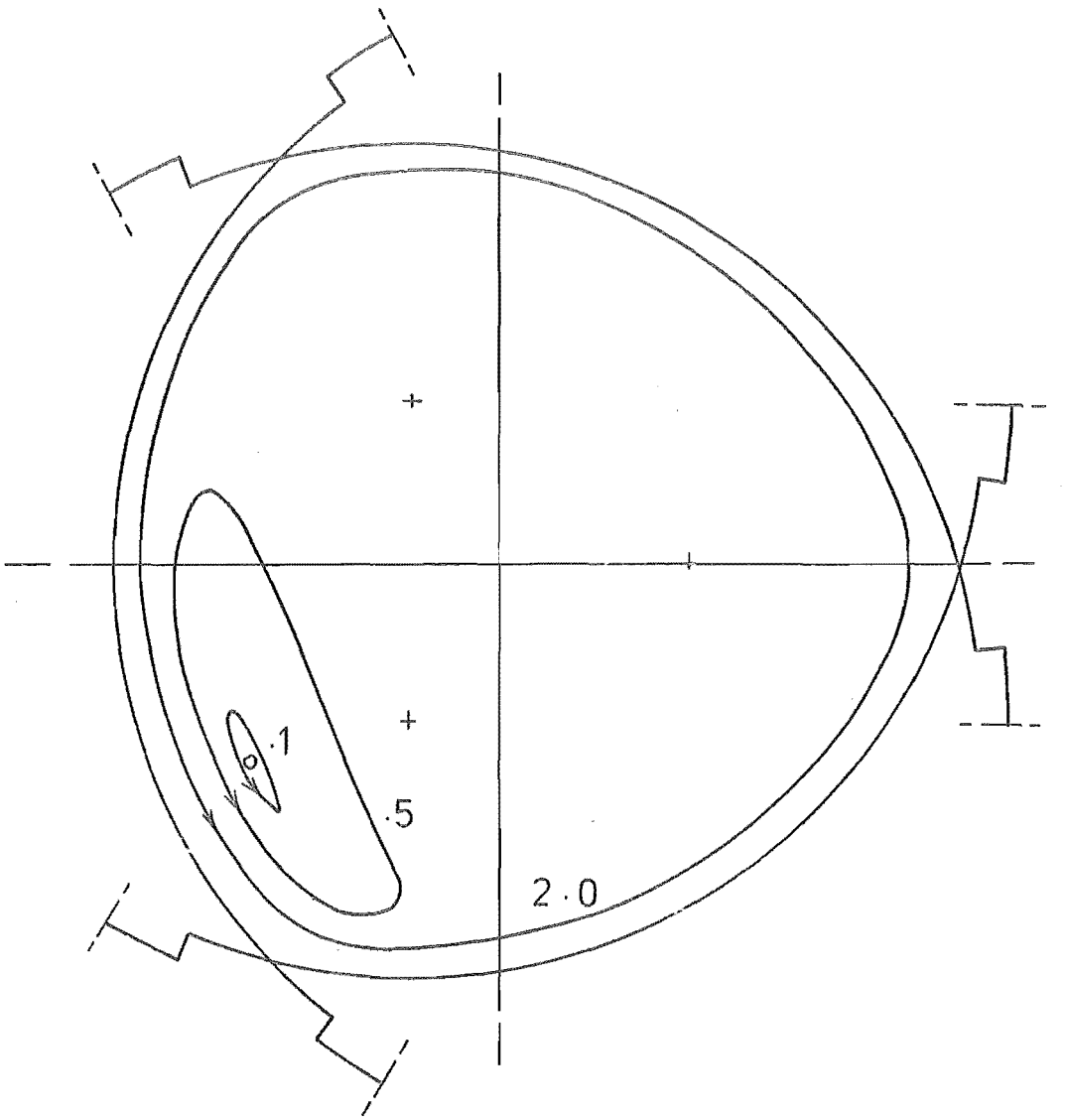

FIG. 7-9 JOURNAL CENTRE LOCUS, THREE LOBE BEARING

$C_m/_R$ - ·00125

$L/_D$ - ·75

RLV - ·3

STATIC LOAD ANGLE - 180°

LOAD RATIOS	·1	·5	2·0
FILM WORK	·046	·95	8·8
MINIMUM OIL FILM THICKNESS	·21	·129	·052
ANGULAR POSITION OF MINIMUM FILM	204°	264°	262°

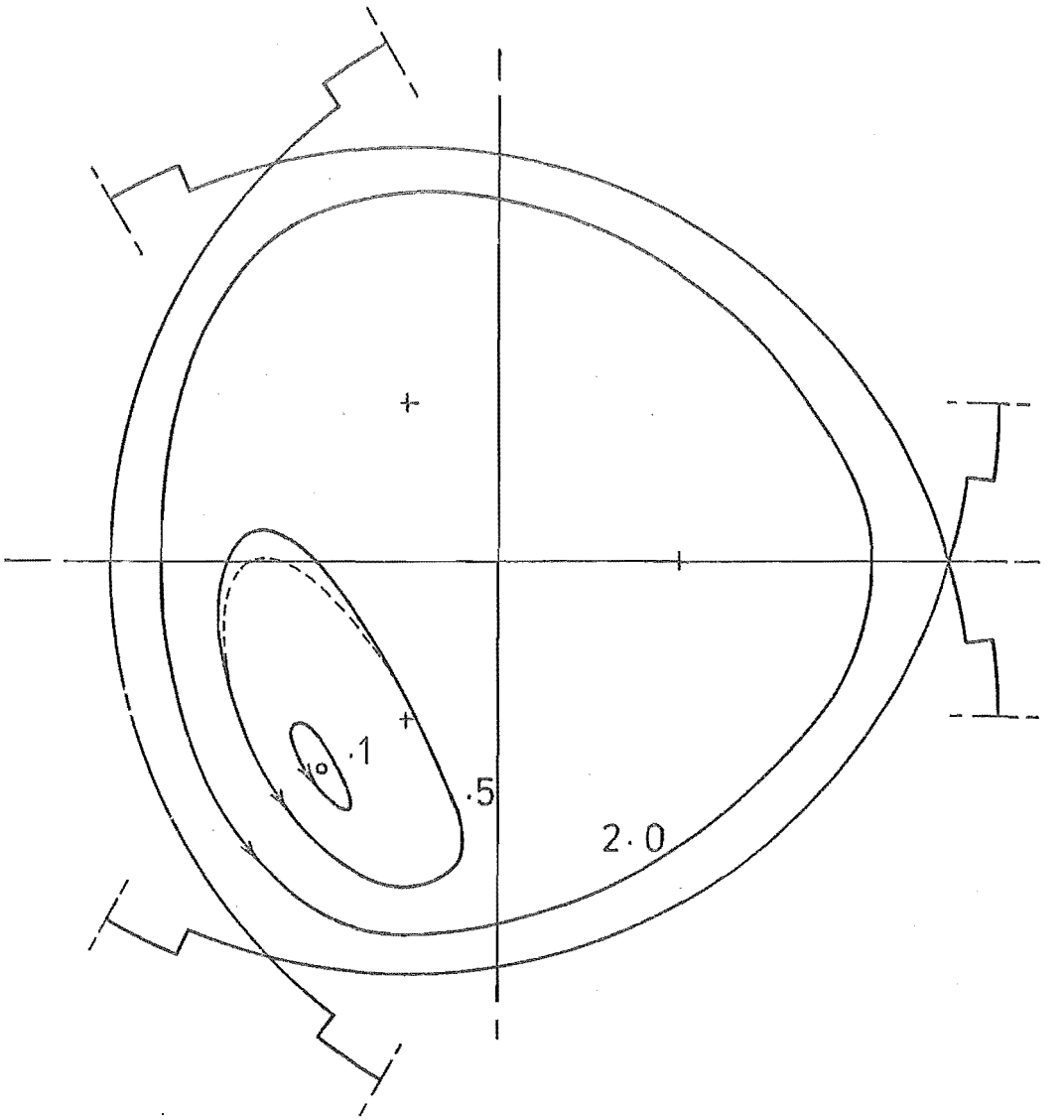

FIG 7-10 JOURNAL CENTRE LOCUS THREE LOBE BEARING

$Cm/_R$ - ·00085

$L/_D$ - ·75

RLV - ·3

STATIC LOAD ANGLE = 180°

LOAD RATIOS	·1	·5	2·0
FILM WORK	·040	·73	7·0
MINIMUM OIL FILM THICKNESS	·24	·148	·067
ANGULAR POSITION OF MINIMUM FILM	208°	270°	270°

---- LOCUS WITH OIL VISCOSITY IN THE FIRST SEGMENT INCREASED 50% ($\Delta T/\Delta S$ = ·5)

motion and the oil film transfers energy to the journal. Of the six bearing designs with a minimum clearance ratio of .00125, the plain circular bearing has the lowest oil film work. This bearing provides the greatest limitation on the journal motion, for this loading, and by this means suppresses the oil film work. The elliptical design offers the least resistance to the journal and the energy flow is correspondingly high. This effect is also shown with the three-lobe design. Reducing the radial segment clearance by 50% reduces the locus size and hence the film work. In the preceding section it was shown that uprating a circular bearing to operate closer to an eccentricity ratio of 0.7 increases the oil film work. A similar phenomenon can be seen here. If the reduction in the journal path length because of the reduced bearing clearance is compensated for by multiplying the work value by 1.5, the result is 16% greater than the film work of the larger clearance bearing. Although the journal locus is not a full circular whirl, the bearing load is still carried partially by wedge films and the larger attitude angles associated with the lower journal eccentricity influence the film work.

The effect of higher lubricant viscosity in the trailing land of the three-lobe bearing is shown in Figure 7-10. The computer program was run with the viscosity in this segment increased by 50% to simulate the influence of the cooler oil. The trailing end of the journal locus is reduced and the oil film work lowered by 4%. The effect is small because this bearing segment is only lightly loaded.

In Figure 7-11 the static load angle for the three-lobe bearing has been changed to 110, 130 and 210 degrees. In each case the journal locus has been reduced by the increased participation in the pressure film generation by the neighbouring segment and the reduction has been accompanied by a lower energy transfer. It should be noted, however, that the

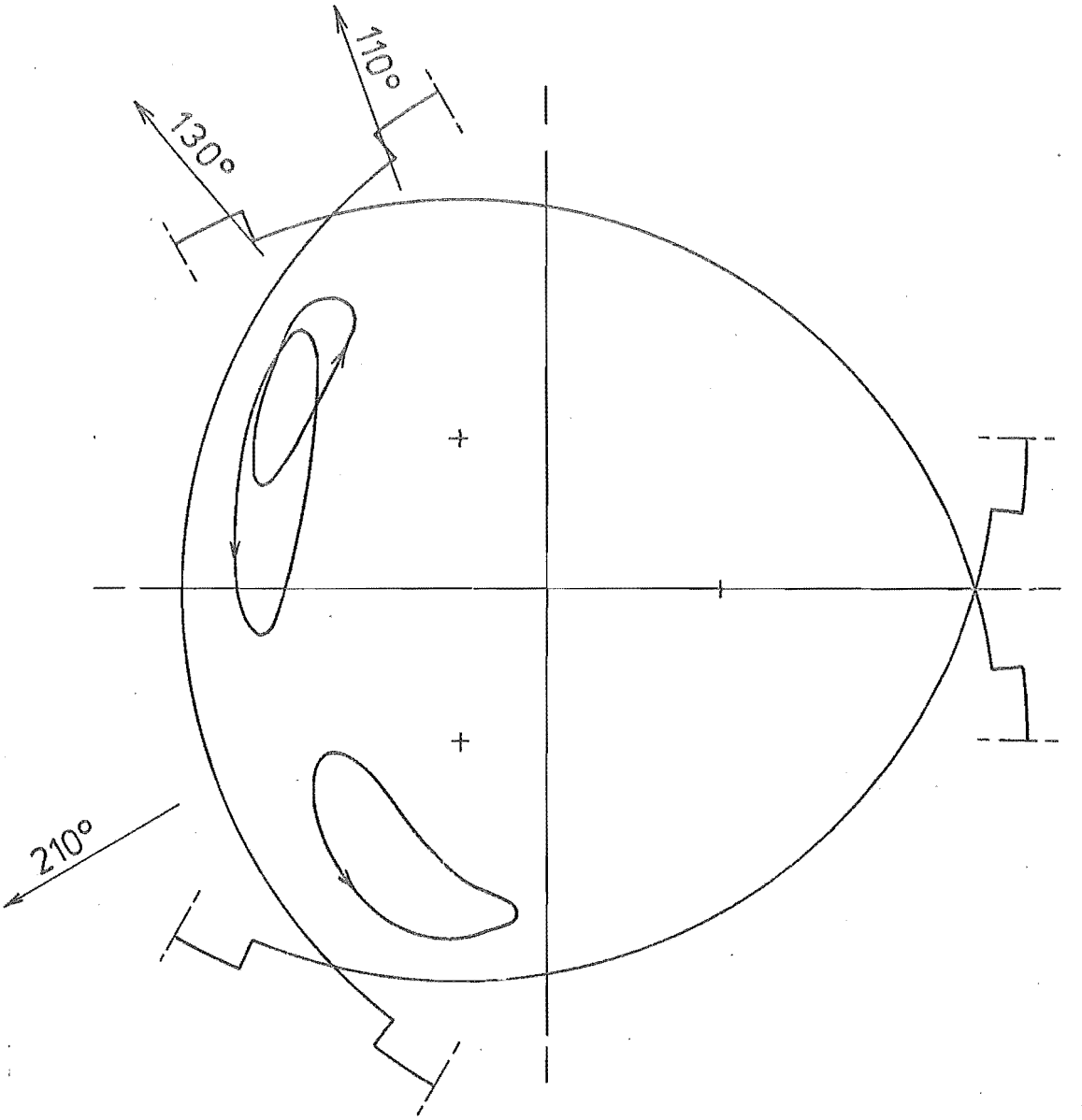

FIG. 7-11 JOURNAL CENTRE LOCUS, THREE LOBE BEARING

$C_m/_R$ .00125

$L/_D$ .75

RLV -.3

LOAD RATIO .5

STATIC LOAD ANGLES	110°	130°	210°
FILM WORK	.32	.49	.41
MINIMUM FILM THICKNESS	.088	.094	.092

saving is made at the expense of the minimum oil film thickness.

The bearings behave in a similar manner with the lower load ratio of 0.1; that is, the smaller the journal centre locus, the lower the oil film work. For the five bearing designs with a bottom land clearance ratio of .00125, the film work increases as the degree of grooving increases. The three-lobe bearing, minimum clearance ratio .00085, is slightly better than the A.E.I. grooved circular design, although it has a shorter arc of ungrooved bottom land (105 compared to 150 degrees). The saving is made by formation of stronger oil films in the leading and trailing segments.

The elliptical design has a lower energy transfer than the three-lobe bearing with the same minimum clearance ratio. The journal, in the latter, runs at a higher eccentricity ratio than the smaller clearance three-lobe design and this prevents the formation of a film in the leading segment. The length of the bottom land is, therefore, the important factor, hence the lower film work with the elliptical bearing.

The plain circular bearing has the highest oil film work of the bearing designs tested with a load ratio of two. In all cases the journal performs a full whirl and as with the lighter load ratio of 0.5, the lower clearance three-lobe design gives the smallest energy transfer. The oil film work is dependent on both the angle made by the oil film force and the locus, for this chapter loosely termed the 'phase angle', and the journal locus size . For non-circular motions the phase angle is not necessarily equal to the attitude angle. The reduction in energy transfer by the circular three-lobe design is almost entirely due to the lowering of the average phase angle as the locus paths are nearly equal in length. The oil film work for the elliptical bearing is less than

either circular design and the journal path length is about 20% greater (estimated from the journal centre locus, Figure 7-8). The mean phase angle is, therefore, considerably reduced. This is caused partially by the journal running at a higher segment eccentricity, hence a lower attitude angle, and partially by the interaction of the two bearing lands. The three-lobe design operates in a similar manner and the additional segment reduces the length of the journal locus. Reducing the radial clearance of this design up-rates the bearing, thus reducing the operating eccentricity and increasing the attitude angle. However, this is more than compensated for by the reduced overall size of the journal locus, hence the lower film work for the smaller clearance three-lobe bearing. The mechanism of the interaction of the segments is discussed later.

Grooves in the bearing surface are undesirable. For small journal motions they reduce the circumferential stiffness of the bearing and thereby increase the oil film work on the journal. The effect of grooves is illustrated well by the results for the plain circular, circular three-lobe and A.E.I. grooved circular designs. As the degree of grooving increases, the film work also increases for load ratios of both 0.1 and 0.5. The spiral bearing has grooving of the bottom land similar to the circular three-lobe design and the film work is also similar. This trend is also reflected in the size of the journal locus.

With the full whirl journal motion the grooves derate the bearing but do not provide additional energy absorption. The top land of the A.E.I. bearing is derated to such an extent that running the computer program on this design for a load ratio of two was not possible. The circular three-lobe design gives a considerable reduction in minimum film thickness, but only a 13% saving in film work. Derating a plain circular bearing by reducing either the oil viscosity or shaft speed would also reduce the film work. From Figure 7-20 a reduction of 33% in the

parameter $\mu\omega$ is required and this increases the non-dimensional bearing load to 4.43 and hence the static journal eccentricity to 0.77. Operating a plain bearing with a static eccentricity ratio of 0.8 and load ratio of 2 results in a minimum film thickness of .034, 40% greater than the circular three-lobe design. Thus, from the point of view of oil film work, derating by grooving the bearing surface is undesirable.

The abrupt change in the bearing surface curvature present in the elliptical and three-lobe designs permits these bearings to achieve a ratio of oil film work to minimum film thickness not obtainable by derating the plain circular geometry. To determine why, the three-lobe design was run with zero static load and a non-dimensional rotating load of 2.95. With this simplified loading each segment behaves in the same manner. In Figure 7-12 the journal centre locus is shown, together with the journal load vectors for the first segment. The variation of the phase angle is clearly shown. When the journal is in the centre of the segment, the phase angle is 16 degrees, but at the junction of the segments it increases to nearly twice this value. The reason for this is shown by the pressure distributions in Figure 7-13.

The solid line in Figure 7-13b is the bearing centreline pressure distribution for a journal angular position of 70 degrees with respect to the bearing centre. The load is supported almost entirely by the wedge film in segment 1, although there is a small squeeze film in segment 2 and an even smaller wedge film in the third segment. The journal eccentricity ratio for segment 1 is 0.935 which would imply an attitude angle of 21 degrees for a plain circular bearing. The orientation of segment 3 is such that the journal velocity produces a negative squeeze film destroying the wedge film that would have existed in the circular bearing. Thus the trailing portion of the film is removed and the

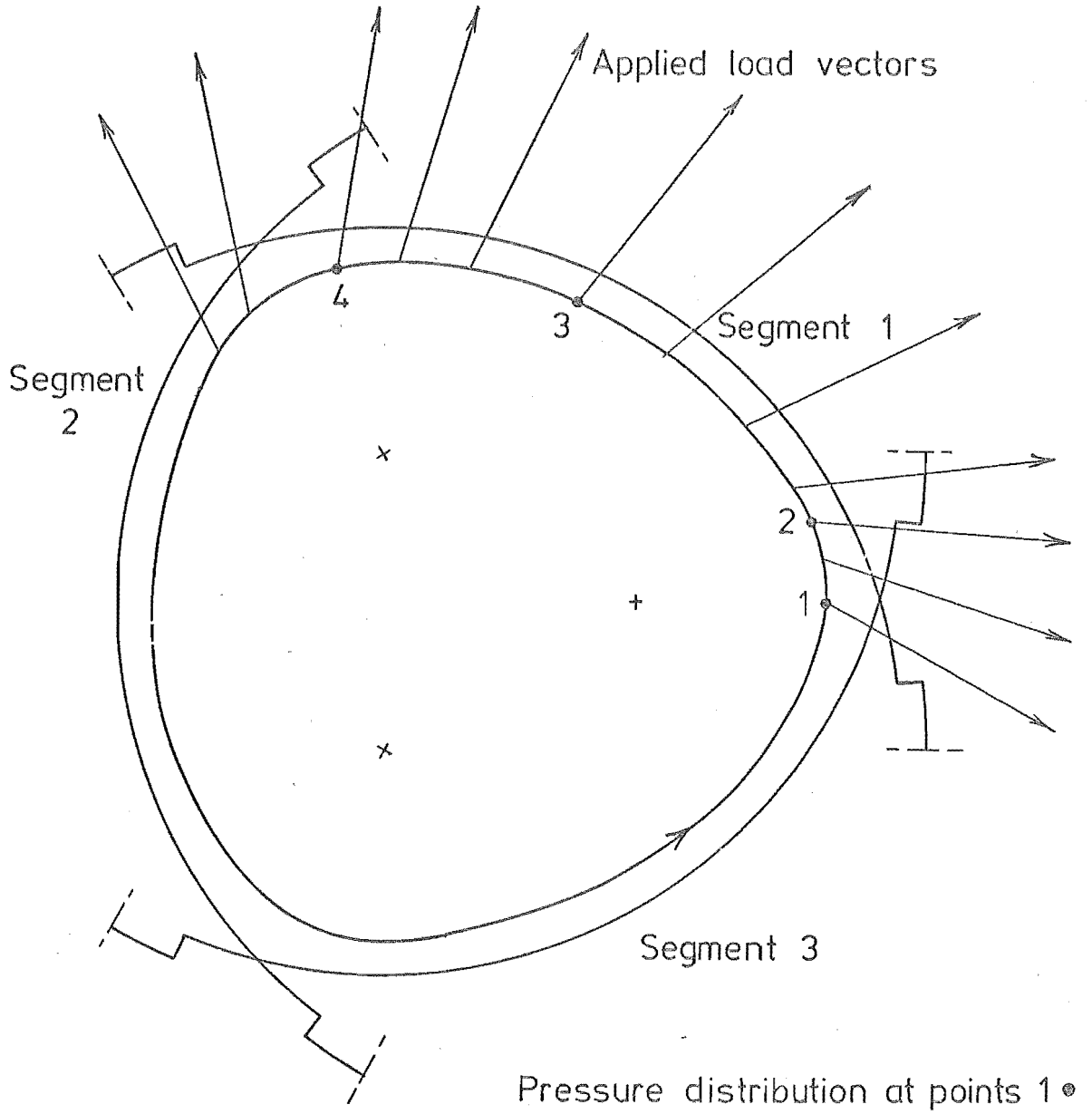

FIG 7-12. JOURNAL CENTRE LOCUS, THREE LOBE BEARING. OIL FILM BEHAVIOUR WITH SINGLE ROTATING LOAD.

$Cm/_R$	-.00125
STATIC LOAD	- 0
DYNAMIC LOAD	- 2.95
RLV	-.3
OIL FILM WORK	- +6.1

(a)

--- position 1; $\varepsilon = 1.03$, $\gamma = 0$

—— position 2; $\varepsilon = 1.01$ $\gamma = 14°$

V journal velocity

Δ resultant film force

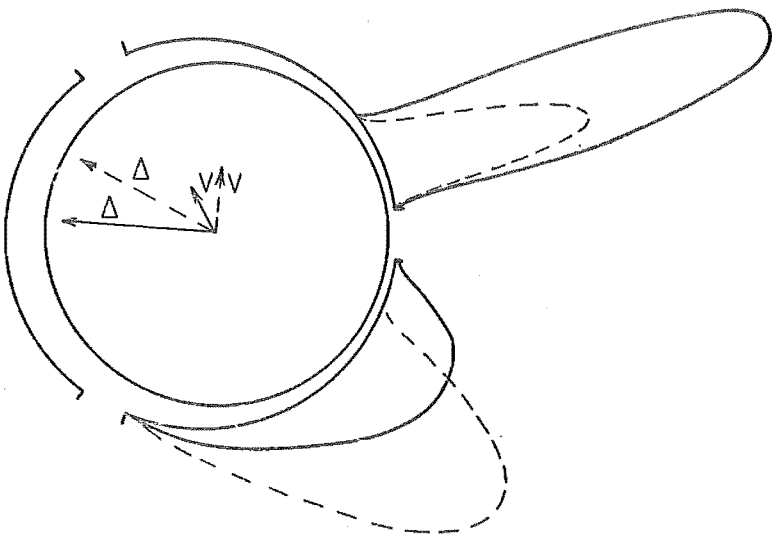

(b)

—— position 3; $\varepsilon = .91$, $\gamma = 70°$

--- position 4; $\varepsilon = 1.01$, $\gamma = 112°$

V journal velocity

Δ resultant film force

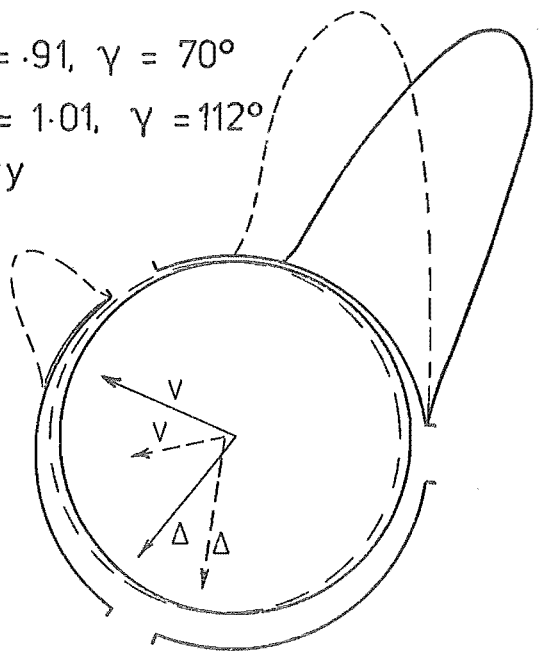

FIG. 7·13 OIL FILM PRESSURE DISTRIBUTION, THREE LOBE BEARING WITH SINGLE ROTATING LOAD. JOURNAL CENTRE LOCUS SHOWN IN FIG. 7-12

$Cm/_R$ – .00125

STATIC LOAD – 0

DYNAMIC LOAD – 2·95

RLV – .3

attitude angle reduced to 16 degrees. The reduction in the oil film work thus results from the journal operating at a higher eccentricity ratio and by the bearing cross-sectional shape modifying the wedge film.

The journal approaching the end of the segment increases the squeeze film on the leading land. This maintains the segment attitude angle at 16 degrees, balancing the increasing length of the wedge film, but the curvature of the journal locus increases, thereby increasing the phase angle. The broken line in Figure 7-13a is the pressure for a journal angular position of zero degrees. The leading squeeze film is now reinforced by a wedge action. The wedge film in the trailing segment is more aligned with the journal motion and thus an increase in film work occurs. The fourth pressure distribution (solid line, Figure 7-13a) is at the point of maximum phase angle and minimum journal centre velocity. The load is shared between the two wedge films but the trailing film is aligned with the journal velocity, thus a considerable transfer of energy occurs. However, this condition exists for only a small part of the locus length, thus the reduction in the oil film work achieved within the segment is not negated.

Conclusion

From the bearing designs and loadings tested the following conclusions may be drawn :

(i) For small bearing loads the prime consideration is to limit the journal motion. A plain circular design gives a good combination of oil film work and minimum film thickness.

(ii) The size of the journal locus is determined by the clearance space for large bearing loads and reduction of the oil film work is achieved by lowering the phase angle.

(iii) From the point of view of oil film work, grooves in the bearing surface are undesirable. However, they are necessary for oil supply and drainage.

(iv) Modification of the bearing cross-sectional shape can be beneficial.

VII.4 THE INFLUENCE OF LOAD ANGULAR VELOCITY

The angular velocity of the dynamic load has considerable effect on the oil film work. To determine the nature of this, the plain circular and three-lobe (C_m/R = .00125) bearing designs were run with load ratios of .1, .5 and 2.0 for a range of relative load velocities ($\dot{\phi}/\omega$). The results are shown in Figures 7-14 and 7-15 as plots of oil film work per load cycle against relative load velocity.

Under the high dynamic load the oil film performs work on the journal at low load speeds, but the energy flow is reversed at high speeds. The change in sign occurs slightly above a relative load velocity of 0.5 and is caused by the pressure film changing from trailing to leading wedge. For the circular bearing the relative load velocity for zero energy flow tends to .5 as the load ratio tends to infinity. The three-lobe bearing behaves in a similar manner. In the preceding section this design was found to act as three circular arcs under these conditions of high dynamic load. The bearing load is supported largely by wedge films, hence the similarity in the behaviour of these two designs.

The shape of the suborbital whirl produced by a load ratio of 0.5 is very much dependent on the relative load velocity. In Figure 7-16 the journal centre locus for $\dot{\phi}/\omega$ of .1 and 1.0 are shown for both bearing

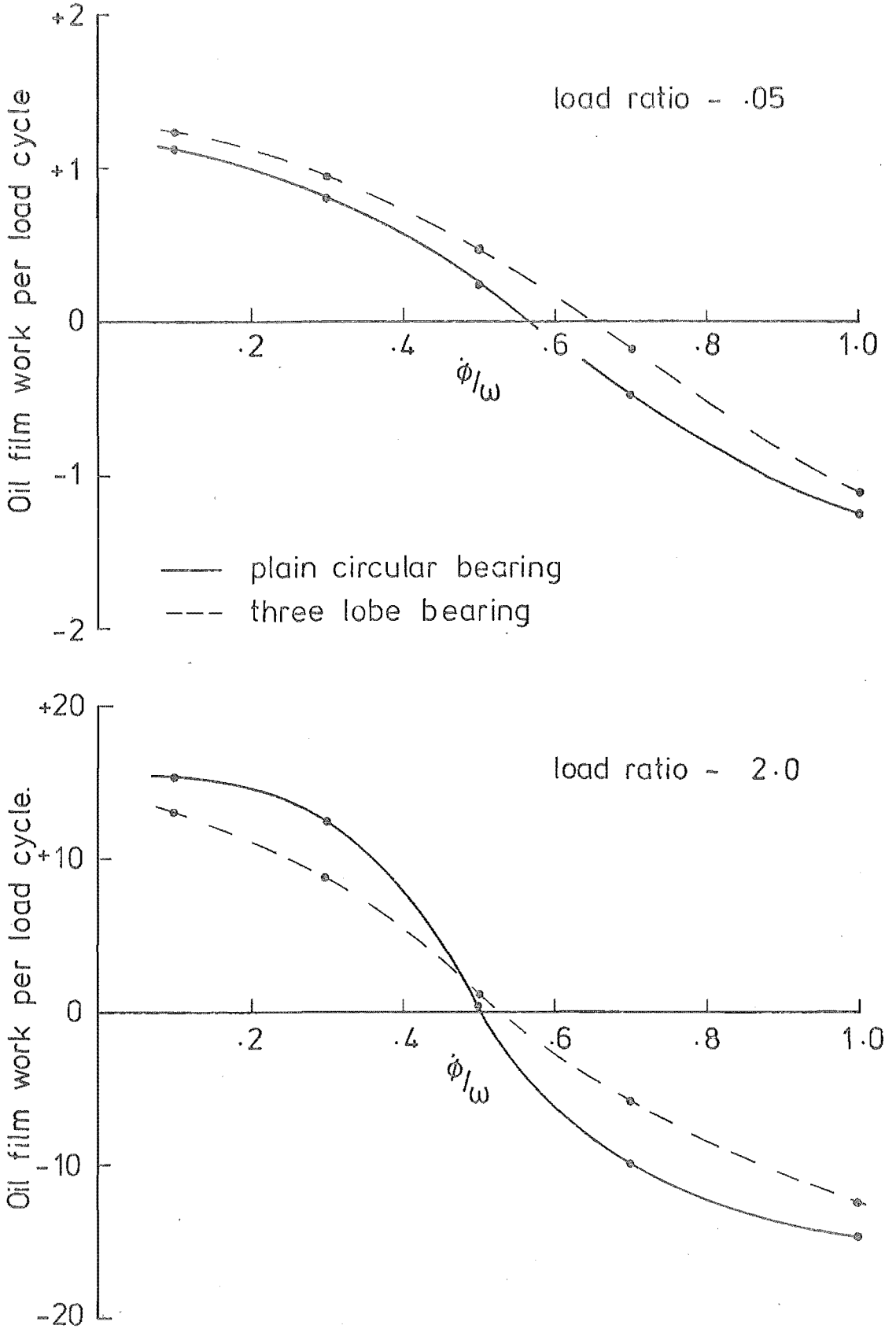

FIG 7-14 EFFECT OF RELATIVE LOAD VELOCITY ON OIL FILM WORK. PLAIN CIRCULAR AND THREE LOBE BEARINGS, STATIC LOAD 2·95.

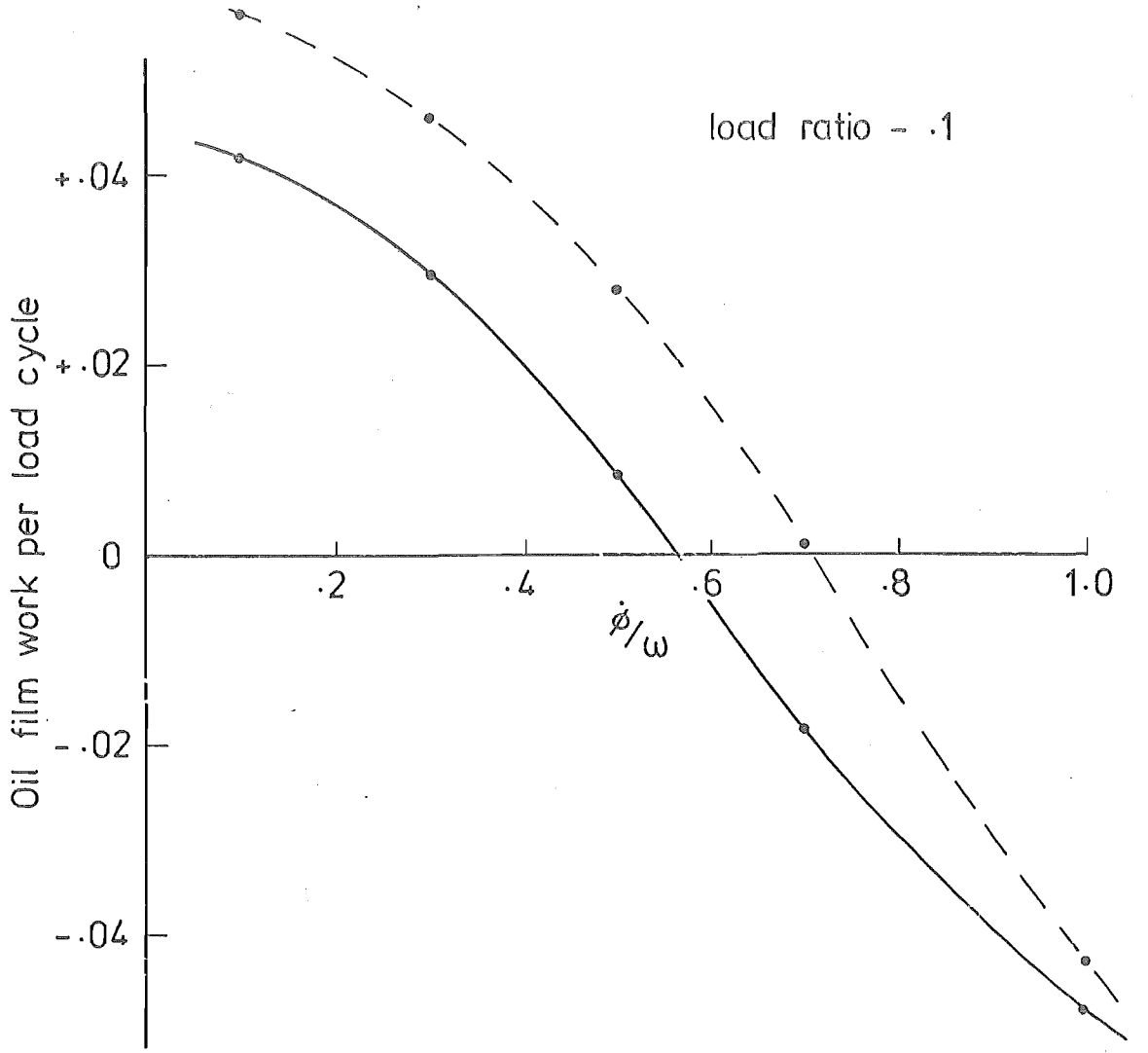

FIG. 7·15 EFFECT OF RELATIVE LOAD VELOCITY ON OIL FILM WORK. PLAIN CIRCULAR AND THREE LOBE BEARINGS. STATIC LOAD - 2·95.

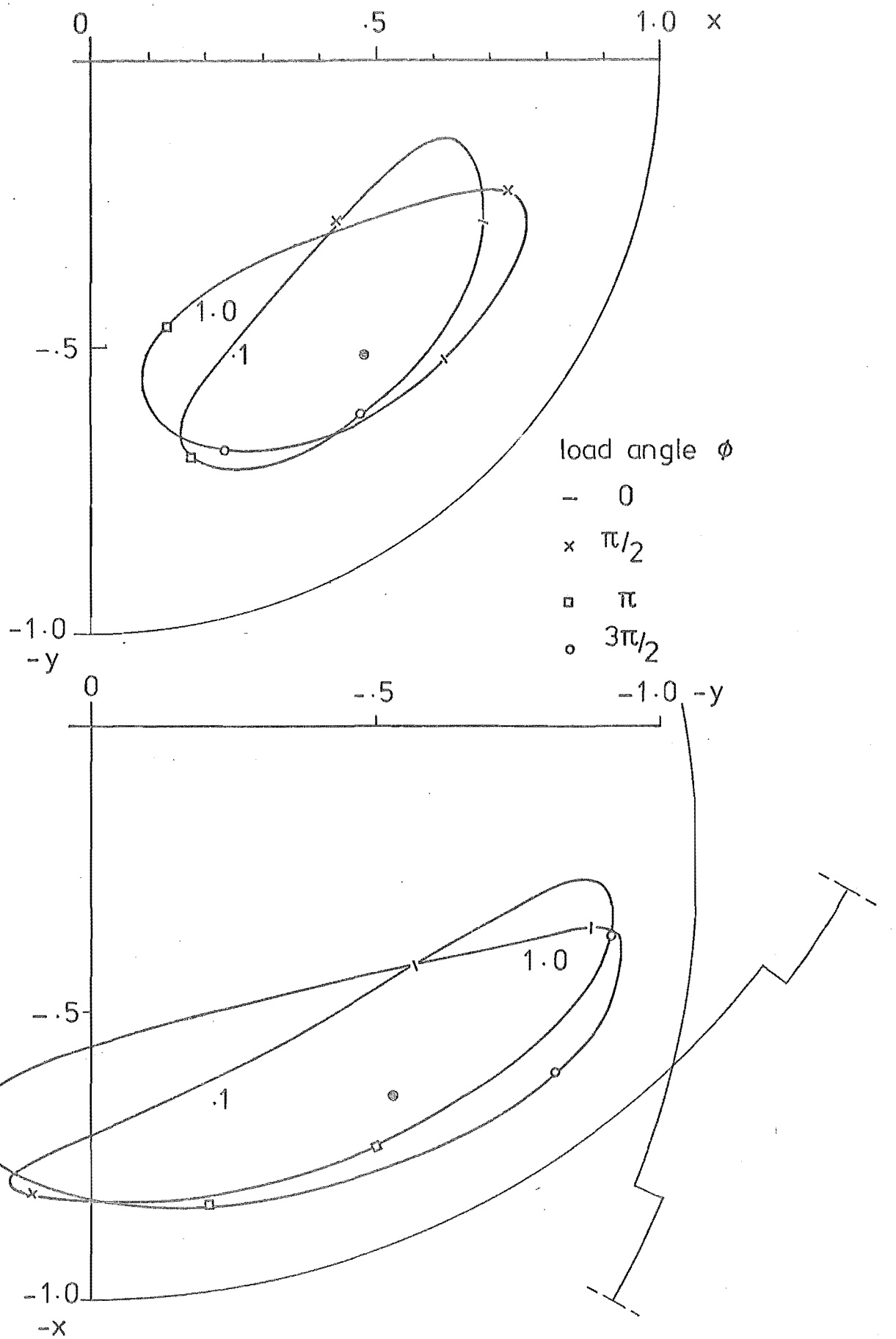

FIG. 7-16. JOURNAL CENTRE LOCUS, CIRCULAR AND THREE LOBE BEARINGS, RELATIVE LOAD VELOCITY 0·1 AND 1·0, LOAD RATIO 0·5.

designs. Increasing the load velocity increases the journal velocity and thus a larger proportion of the oil pressure film generation is due to the journal centre motion. Referring to Figure 7-16 the high journal velocity on the top section of the locus reinforces the wedge film causing the journal to rise and giving a strong leading film, thereby damping the motion. With forward journal motion the trailing wedge film is weakened and this, added to the higher initial eccentricity ratio, results in a squeeze film being required to support a portion of the load. The phase angle is thus reduced and the oil film work lowered. Both bearing designs behave in a similar manner again illustrating the basic circular nature of the three-lobe geometry.

The relative load velocity at which the energy flow between the film and journal changes sign is lower when the journal motion is a full whirl. This offers the possibility of a stable limited amplitude journal motion at frequencies slightly above half the shaft speed. The positive oil film work would supply energy to the journal vibration until the force magnitude reached the value for zero film work. Any increase or decrease in the journal motion would be resisted by the energy drain or supply through the oil film. Such a situation existing is, however, unlikely, as a single mode journal-rotor vibration is difficult to produce (see Chapter 6).

Conclusion

The oil film work is largely dependent on the form of the force locus with which the bearing is loaded. The results show that for a circular force locus the oil film performs work on the journal at low relative load speeds and the reverse occurs at high speeds. If the dynamic load is large the transition point is approximately 0.5ω, but for suborbital journal motion it is appreciably higher than this.

The basic behaviour of higher load velocities reducing the film work will occur with all force loci. Pressure films generated by the journal centre velocity are energy absorbing and as the relative load velocity increases, a higher proportion of the load is carried by these films.

VII.5 INFLUENCE OF LOAD MAGNITUDE

The investigation of the effect of the bearing load magnitude was conducted using the plain circular bearing geometry. The object was to determine how the oil film work changes when either the static or dynamic bearing load is altered. The results have also allowed an examination of the effect of derating the bearing by reducing the lubricant viscosity or shaft speed and by increasing the radial bearing clearance.

Results

The program was run for three static loads, corresponding to static eccentricity ratios of 0.6, 0.7 and 0.8, and for load ratios of .5, .8, 1.2 and 2.0. An additional run was made at a ratio of 1.6 and static eccentricity ratio of 0.7 to improve the accuracy of the curves plotted. The results are presented in graphical form in Figures 7-17 to 7-20. They are divided into three groups describing the effect of the dynamic load, static load and bearing derating.

(a) Dynamic Load - The information is presented in two forms, firstly as a function of the load ratio and secondly as a direct plot of oil film work against dynamic load (Figures 7-17 and 7-18).

As expected, the oil film work increases with dynamic load. Above a load ratio of one, the relationship is

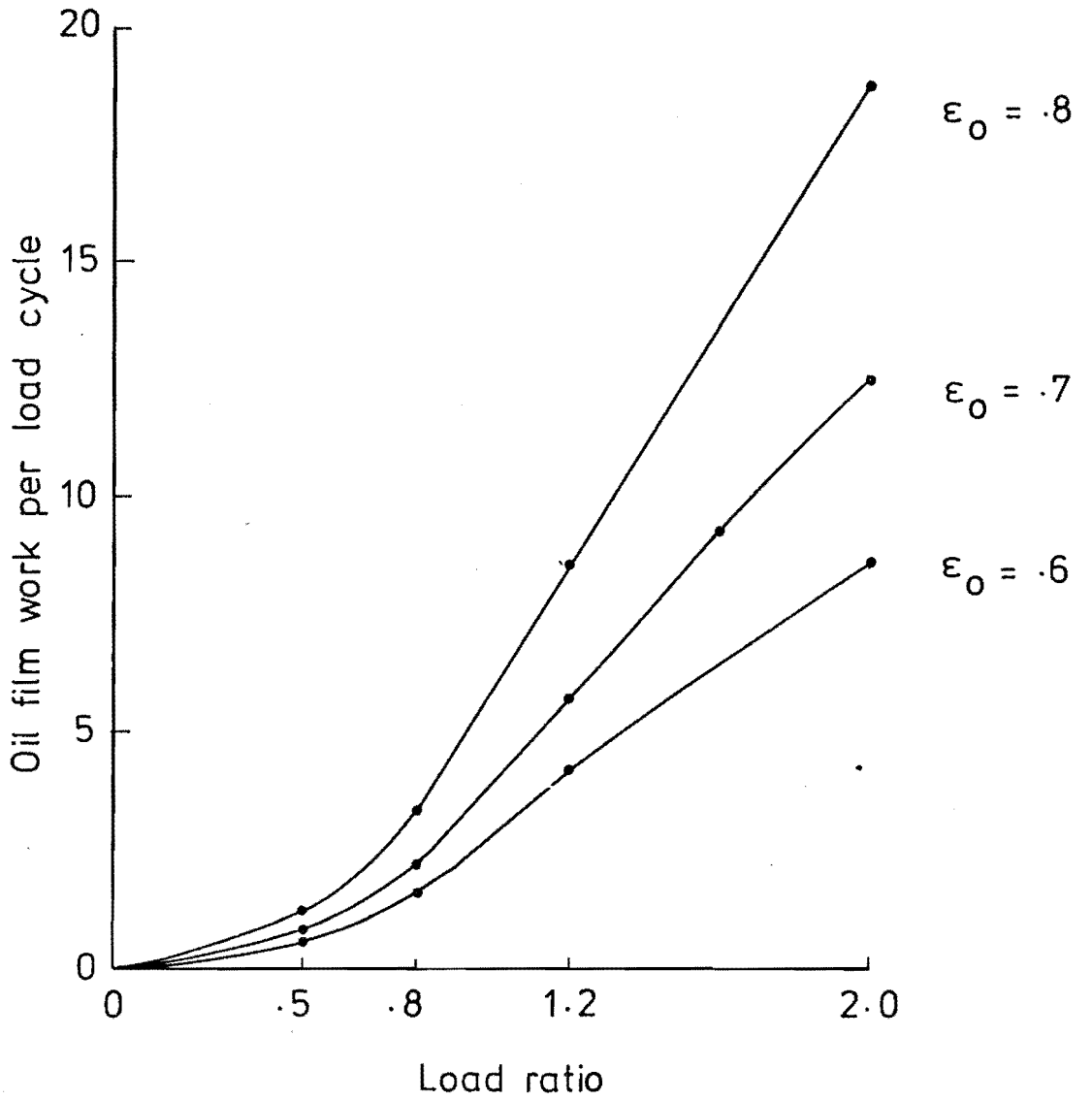

FIG 7-17 EFFECT OF LOAD RATIO ON OIL FILM WORK. PLAIN CIRCULAR BEARING, RLV ·3.

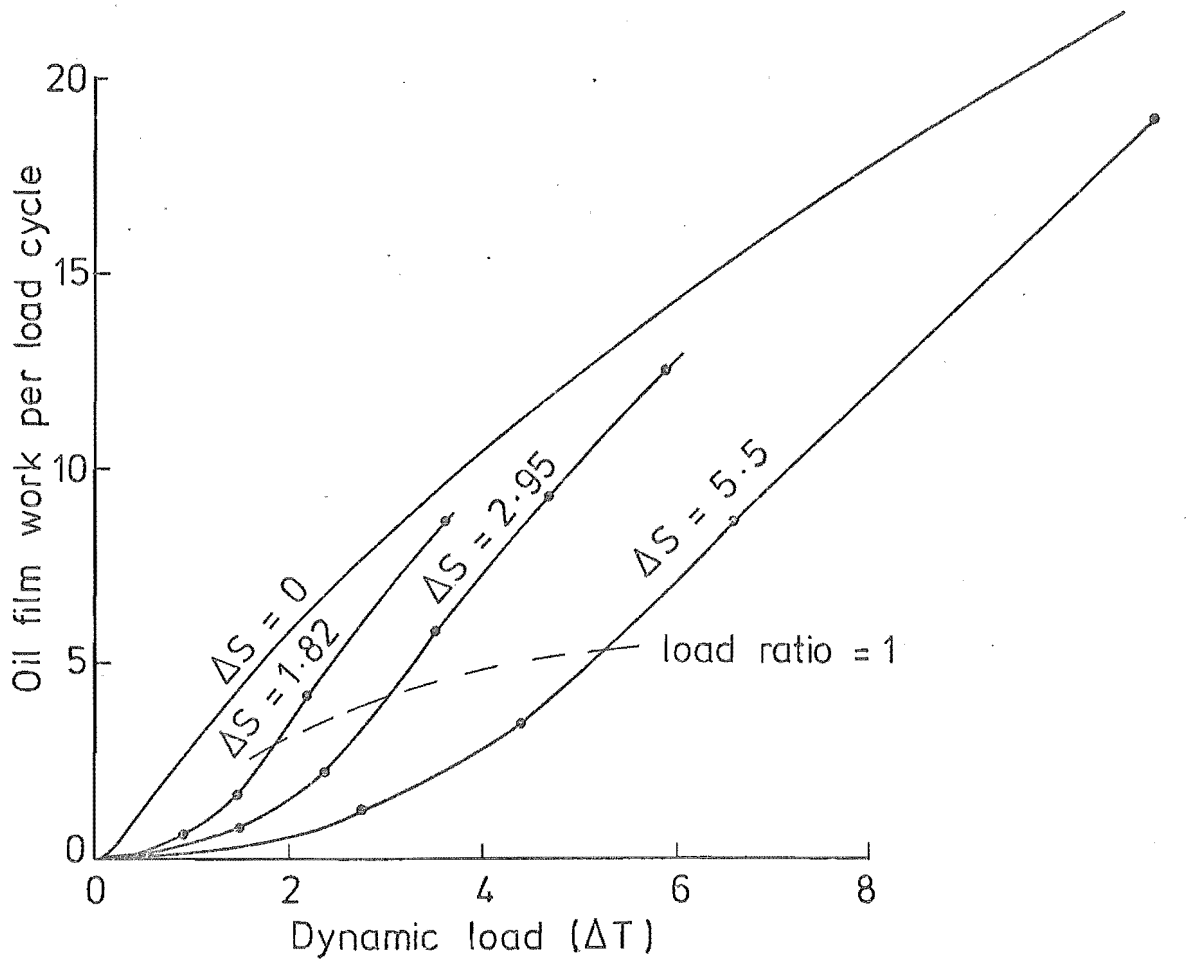

FIG. 7-18 EFFECT OF DYNAMIC LOAD ON OIL FILM WORK PLAIN CIRCULAR BEARING, RLV ·3.

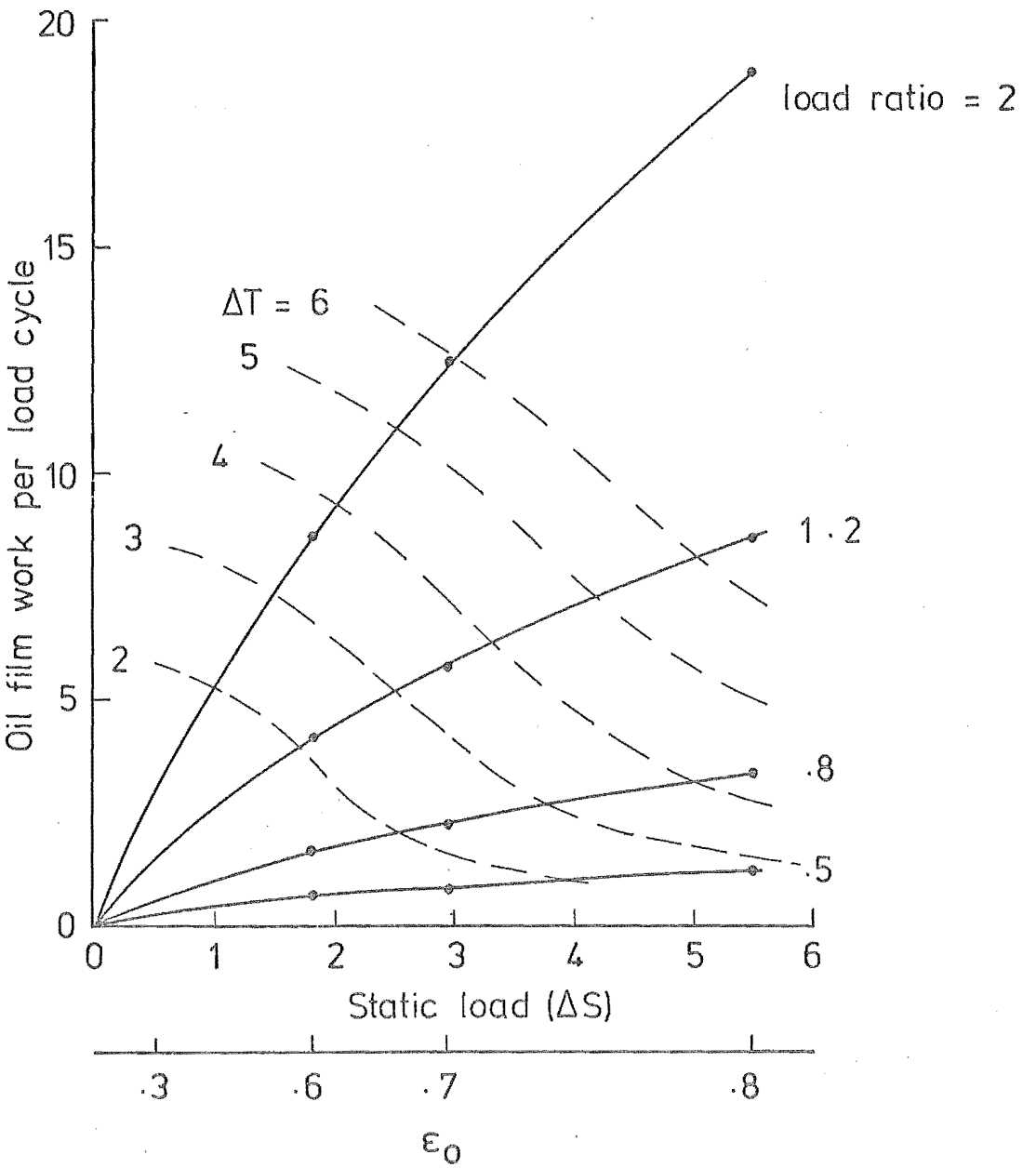

FIG. 7-19 EFFECT OF STATIC LOAD ON OIL FILM WORK. PLAIN CIRCULAR BEARING, RLV ·3

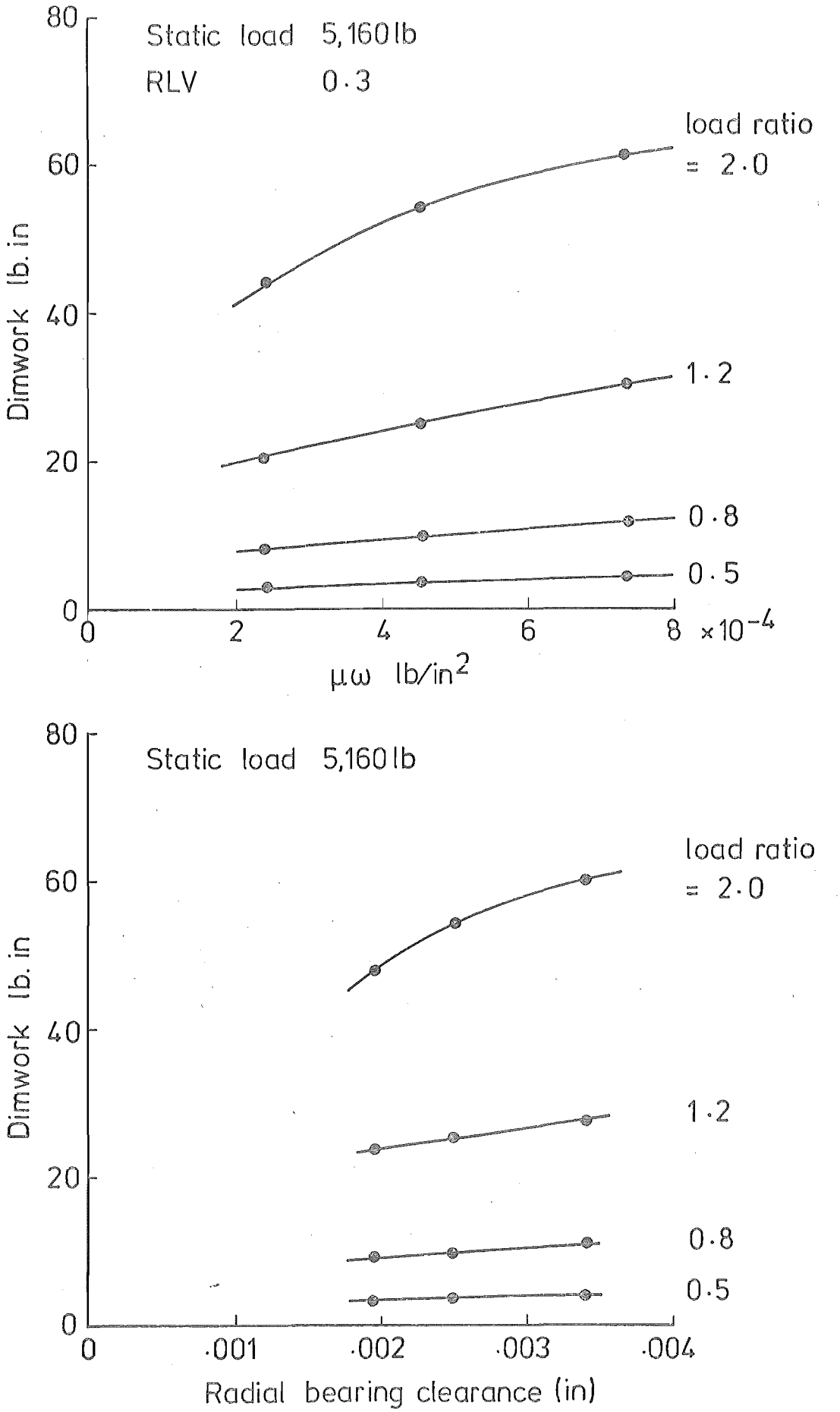

FIG 7-20 EFFECT OF DERATING BEARING ON OIL FILM WORK. PLAIN CIRCULAR BEARING, RLV ·3, STATIC LOAD 5,160 lb

almost linear. The journal centre locus under these conditions is a full whirl, thus further load increases enlarge the radius of the whirl slightly, but otherwise have little effect on its shape. At the high journal eccentricities involved (Figure 7-4), the change in the average attitude angle with load is small, and thus the oil film work is primarily a function of the dynamic load.

Below unity load ratio the journal centre path is very dependent on the magnitude of the dynamic load and thus the plot of oil film work against dynamic load is not linear. From Figure 7-4, the length of the journal centre path can be measured and thus the product of load and path length calculated and compared to the oil film work.

ΔT	Path Length S	$S.\Delta T$	WORK	$S.\Delta T$/WORK
1.48	1.83	2.71	.82	3.30
2.36	3.2	7.55	2.26	3.34
3.54	5.3	18.8	5.79	3.25
5.9	5.7	33.6	12.5	2.70

The ratio is nearly constant, thus the oil film work is approximately proportional to the product of the dynamic bearing load and the journal centre path length.

For suborbital journal motion the oil film work is approximately proportional to the square of the dynamic load. Estimating the work in this way is not as accurate, but it is more convenient as it does not require an exact knowledge of the journal centre locus.

ΔT	WORK	ΔT^2/WORK
.295	.030	2.90
1.48	.82	2.67
2.36	2.26	2.46

The generation of the oil film work can be viewed as having two components resulting from the two bearing loads. The dynamic load, besides exciting the journal motion, is responsible for the actual energy transfer. The static load does not take part in this, as the integral of a constant around a closed curve is zero. The role of the static load is to suppress the journal motion and by this means reduce the film work. Once the full whirl is developed the static load loses control of the motion as the dynamic load is increased, and its initial influence is slowly relinquished. This is shown in Figure 7-18 by the curves tending towards the line for zero static load as the load ratio increases.

(b) Static Load - The graph shown in Figure 7-19 shows the effect of varying the static bearing load. The lines of constant dynamic load have been plotted and these illustrate the stablizing effect of increasing static load. The maximum reduction in work occurs in the region of unity load ratio at which point the journal whirl is being compressed into a suborbital motion.

(c) Bearing Derating - A bearing can be derated, that is, its load carrying capacity reduced, by lowering the shaft speed or lubricant viscosity, or by increasing the clearance

ratio. These also change the non-dimensionalising factors; thus, to allow a direct comparison of the results, the oil film work is expressed in dimensional form.

In Figure 7-20 the film work is plotted against the product of the viscosity and shaft speed for a relative load velocity of .3 and constant static load of 5,150 lb (22,900 N). The energy input to the journal is lowered by the derating, but the change is smaller than the reduction in $\mu\omega$. The reduction in the film work is produced by the bearing operating at a higher eccentricity ratio.

The reverse occurs when the clearance ratio is increased to derate the bearing. Although the journal runs at a higher eccentricity ratio, the increase in the locus size outweighs this and the dimensional film work is increased. Again, the effect is small, a significant increase in the bearing clearance causing a minor change in the energy flow.

Conclusion

For the relative load velocity of 0.3 used in this investigation, the magnitude of the static or dynamic load does not affect the direction of the energy flow. From the graphs showing the influence of relative load velocity (Figures 7-14 and 7-15), it can be seen that this is true for plain circular bearings at all load speeds except those just above $.5\omega$.

The other results arising from this investigation are :

(i) Increasing dynamic load increases the energy flow;

(ii) the static load suppresses the journal motion and thereby limits the oil film work;

(iii) derating the bearing by reduction of the viscosity or shaft speed lowers the film work, but the reduction is small;

(iv) reducing the clearance ratio lowers the energy flow, but again the change is small.

VII.6 EFFECT OF SUPERIMPOSED SYNCHRONOUS FORCE

Small synchronous dynamic loads occur frequently in turbo-machinery due to out of balance of the rotor. To determine the effect of this, a force, rotating at shaft speed, of 5% of the static bearing load was added to the bearing loading. A range of dynamic load velocities were run with the plain circular bearing geometry and a load ratio of 0.5. The phase relationship of the two rotating loads, defined as the angle of the synchronous force when the dynamic load angle is zero, is important and two values were used: 0 and 180 degrees. The results are tabulated in Figure 7-21, showing the change in oil film work per cycle of the resultant load and per cycle of the synchronous force.

Results

For all cases tested, except for the synchronous dynamic load, the additional synchronous force reduced the work done by the oil film on the journal. The magnitude of the reduction is dependent on the rotational speed of the dynamic load and its phase relationship with the synchronous force. The results for unit relative load velocity have been included for comparison, although they do not have any physical significance. They were calculated by modifying the magnitude of the dynamic load and

RLV	FILM WORK WITHOUT SYN. FORCE	LOAD PHASE 0° FILM WORK	LOAD PHASE 0° FILM WORK PER LOAD CYCLE	LOAD PHASE 0° REDUCTION PER SYN. FORCE CYCLE	LOAD PHASE 180° FILM WORK	LOAD PHASE 180° FILM WORK PER LOAD CYCLE	LOAD PHASE 180° REDUCTION PER SYN. FORCE CYCLE
·125	1·1*	·98	·12	·015	·99	·11	·014
·2	1·0*	·93	·07	·014	·93	·07	·014
·333	·73*	·70	·03	·010	·70	·03	·010
·5	+ ·25	+ ·18	·07	·035	+ ·20	·05	·025
·667	− ·72*	− ·74	·02	·007	− ·74	·02	·007
1·0	−1·23	−1·49	·26	·26	−1·02	−·21	−·21

* Values estimated from Fig. 7-18

Oil film work per load cycle, synchronous load 5% of static load, = 0·011

FIG 7-21 EFFECT OF ADDITIONAL SYNCHRONOUS FORCE ON OIL FILM WORK.
LOAD RATIO - ·5, SYNCHRONOUS FORCE - 5% OF STATIC LOAD
PLAIN CIRCULAR BEARING.

it can be seen that they comply with the relationship that the film work is proportional to the square of the rotating load for suborbital journal motions. (See VII.5)

The errors incurred in the calculation of the reduction in the oil film work are high because it involves the subtraction of numbers of similar magnitude. The results should, therefore, be used with caution.

For the lower values of dynamic load velocity, below 0.5ω , the reduction in oil film work per cycle of synchronous force is approximately equal to the oil film work of the synchronous and static loads alone. In the extreme condition of an infinitely slow dynamic load velocity the synchronous force cycles at each point on the journal centre locus. The response of the bearing at each point is different, but by summing over the entire locus, an average of the bearing behaviour is obtained. The dynamic bearing coefficients are continuous functions over the range of journal positions encompassed by the locus; thus it is reasonable to expect the average bearing response to be similar to the response at the static equilibrium position. Under these conditions the angular relationship of the two rotating loads is unimportant and this can be seen in the similarity of the low frequency results.

The angular relationship does, however, become important as the dynamic load velocity increases. For relative load velocities of 0.5 and 1.0, the same load condition occurs at the same point on the journal locus each journal cycle; thus there is no opportunity for the response of the bearing to be averaged. In the extreme case of unit relative load velocity, the oil film work varies between -1.49 and -1.02. If the relative load velocity differs from 1 by an infinitely small amount, the angular relationship of the two rotating loads slowly changes and an

averaging of the journal response occurs.

The magnitude of the resultant synchronous dynamic load is :

$$DELR^2 = DELT^2 + DELOB^2 + 2.DELT.DELOB.\text{Cos } A \qquad ...7.2$$

Where

DELT = dynamic load magnitude

DELOB = synchronous force magnitude

A = phase relationship between the two loads.

Now, the oil film work is approximately proportional to the square of the rotating load, thus :

$$WORK_R = WORK_T . \left(\frac{DELR}{DELT}\right)^2$$

and the mean film work :

$$WORK_{Mean} = WORK_T \frac{(DELR^2)_{Mean}}{DELT^2}$$

From Equation 7.2 :

$$(DELR^2)_{Mean} = \frac{1}{2\pi} \int_0^{2\pi} DELT^2 + DELOB^2 + 2DELT.DELOB.\text{Cos } A \; dA$$

$$= DELT^2 + DELOB^2$$

Thus:

$$WORK_{Mean} = WORK_T \left[1 + \left(\frac{DELOB}{DELT}\right)^2\right]$$

$$= 1.01 \; WORK_T$$

$$= -1.01 \times 1.23$$

The reduction in the oil film work over a complete cycle of loading is thus 0.0123, again a value close to the oil film work for the synchronous force alone.

To determine if a similar phenomenon occurs at a relative load velocity of 0.5, two additional computer runs were made with the load phase at 45 and 90 degrees. The reduction in oil film work per cycle of synchronous force was -.0015 and -.0035 respectively; that is, the

synchronous force increased the film work. Thus, if the relative load velocity is not exactly 0.5 an averaging process will occur here also.

The two results for .667 relative load velocity are equal as the force locus is not changed by a 180 degree phase shift. A complete cycle of the resultant load locus involves two cycles of the dynamic load and these differ by a change in the load phase angle of 180 degrees. This results in alternate cycles of high and low resultant dynamic load and this tends to average the oil film work. Hence, the reduction in the film work for this relative load velocity is comparable to the other results.

Conclusion

A small synchronous force superimposed on the normal bearing loading of a static and dynamic load reduces the oil film work by an amount similar in magnitude to the film work with the bearing loaded by the static and synchronous forces alone. If the ratio of shaft speed to dynamic load velocity can be expressed exactly in terms of small integers, for example, 1, 2, 3/2, the phase relationship between the dynamic and synchronous loads is important and can greatly increase or decrease the oil film work. These specific conditions are, however, unlikely to occur.

VII.7 SUMMARY

The work performed by the oil pressure film on the journal is the major factor determining the stability of a bearing-rotor system. Thus, a knowledge of the effect of the bearing parameters on this energy transfer is beneficial for bearing design.

Although the results were obtained with a circular force locus in this investigation, the following general conclusions can be drawn :

(i) Both the length of the journal centre locus and the angle between the force and velocity vectors are important in determining the oil film work. The energy transfer can be reduced by modifying either term.

(ii) Changes in the bearing cross-sectional shape modify the oil pressure film and this can be used to reduce the oil film work.

(iii) For circular force loci at least, grooves which disrupt the oil pressure film are undesirable.

(iv) The oil film work increases with increasing dynamic load. Increasing the static bearing load suppresses the journal motion thereby reducing the film work.

(v) Higher load frequencies are more stabilizing as the load carrying capacity of the bearing is less reliant on the de-stabilizing trailing wedge film.

(vi) The addition of a small synchronous component to a basic circular force locus is stabilizing.

The work reported in this chapter demonstrates the possible usefulness of this approach in the design of bearings. Although a direct assessment of the stability of a bearing-rotor system is not possible at this stage, this technique permits an understanding of the oil film behaviour to be obtained. This approach offers the following features :

(a) A comprehensive range of bearing designs and loadings are possible and the journal motion is not restricted to small amplitudes.

(b) The oil film work summarises in a single scalar quantity the bearing's ability to excite or dampen the rotor motion. This facilitates comparisons between different bearing

(c) The bearing load is easily defined. This also is important if comparisons are to be made.

(d) The choice of a rotor model and starting conditions is unnecessary and the transients associated with a rotor mass avoided.

(e) The computer program is easy to operate and is less expensive to run than a full solution.

CHAPTER EIGHT

CONCLUSION

The aim of the work reported in this thesis was to develop a versatile method of assessing the stability of a bearing-rotor system that would not be prohibitively expensive to compute. Such a method would be of value in bearing design as existing techniques are either limited in their applications or expensive to run.

This goal was not achieved. Two approaches to the problem were tried. The first attempted to reduce the computation necessary for a full solution, that is, a solution obtained by marching out the bearing and rotor loci, by improved utilisation of the data calculated with the oil film equations. Although significant reductions were achieved these were insufficient to justify the additional program complexity and the limitations placed on the system to be analysed.

The second approach was to determine the energy flow between the oil pressure film and the journal and, with a knowledge of the work performed by the external forces on the rotor, determine whether the vibration would grow or decay. If the influence of the rotor on the bearing could be represented by a simple force locus the oil film work could be calculated without the expense of a full system solution. However, analysis of a single bearing-rotor system showed that this is not possible and thus a direct assessment of the system stability cannot be made with this technique.

Replacing the rotor with a force locus is, however, useful for comparisons of bearing design features and load conditions. The transients associated with the rotor mass are avoided and the bearing

loading is easier to control. The work performed by the oil pressure film is a useful parameter on which to base a comparison as it summarises the ability of a bearing to excite or damp the rotor motion in a single scalar quantity. An investigation was undertaken into the effect of bearing design, load magnitude and load frequency for a circular force locus.

VIII.1 FUTURE WORK

The computation required for a full solution of a bearing-rotor system is largely determined by the non-linearity of the dynamic bearing coefficients. It was found that their variation around a journal centre locus is too large and too complex to enable them to be estimated for any large change in the journal displacement and velocity. In view of this, further work in this area is not recommended. If the full solution computation is to be reduced, a radically new approach will be necessary.

Of the three methods of analysis discussed in this thesis, assessment of the system energy balance has the greatest potential for development. Research is required into :

(a) The relationship between the work performed by the oil film and the form of the journal force locus. The force locus exerted by a simple flexible rotor on a bearing is a series of ellipses. A suitable place to start this research would be to investigate a range of elliptical force loci of varying ratio of major to minor axes.

(b) The response of a system to a disturbance to determine why a forward whirl develops in some cases and how this can be predicted. It may be possible to measure the

response by calculating the oil film work perpendicular to the disturbing impulse, but this would require a more sophisticated method of representing the rotor than a sinusoidal force locus directly applied to the journal. This could be achieved with a light rotor and spring and confining the rotor to a sinusoidal displacement locus.

These two areas of research cover the likelihood of a whirl developing from a disturbance and its behaviour once the motion is established. From these a technique of assessing the stability of a bearing-rotor system may emerge, for a flexible rotor at least. Even if this is not achieved, a better understanding of the behaviour of the oil film will certainly be obtained.

Before a further program of research is instigated it would be desirable to communicate with the industries involved in bearing design to obtain a better understanding of their problems and requirements. A simple direct solution is, at this stage, unobtainable and it would be desirable for any development of approximate methods to be made with full consideration for their eventual industrial applications.

ACKNOWLEDGEMENTS

I would like to thank Professor H. McCallion for his supervision of this work. His advice and encouragement were very much appreciated.

I am grateful to Professor D.C. Stevenson for the use of the facilities of the Department of Mechanical Engineering. Also, I would like to thank Mrs J. Ritchie for assisting with the preparation of the drawings, diagrams and graphs, and Mrs B. Stout for typing this thesis.

A special thank you to Jill and Ross for their patience and assistance over the last three years.

REFERENCES

1. Tower, B. "First Report on Friction Experiments", Proc. I.Mech.E., Vol. 34, 1883.

2. Reynolds, O. "On the Theory of Lubrication and its Application to Mr Beauchamp Tower's Experiments ....", Phil. Trans.Roy.Soc. London, A177, 1886.

3. Sommerfeld, A. "Zur Hydrodynamischen Theorie der Schmiermittel-reibung", Z. Angew.Math.u. Phys., Vol. 50, 1904.

4. Swift, H.W. "The Stability of Lubricating Films in Journal Bearings", Proc.Inst.Civil Eng., Vol. 233, 1931.

5. Ocvirk, F.W. "Short-bearing Approximation for Full Journal Bearings", N.A.C.A. Tech.Note 2808, 1952.

6. Christopherson, D.G. "A New Mathematical Method for the Solution of Film Lubrication Problems", Proc.I.Mech.E., Vol. 146, 1941.

7. Southwell, R.V. "Relaxation Methods in Engineering Science", Clarendon Press, Oxford, 1940.

8. Newkirk, B.L. & Taylor, H.D. "Shaft Whipping due to Oil Action in Journal Bearings", Gen.Elec.Rev., Vol. 28, 1925.

9. Stodola, A. "Kritische Wellenstörung Infolge der Nachgiebigkeit des Oelpolsters im Lager", Schweizerische Bauzeitung, Vol. 85, 1925.

10. McCallion, H. "Vibration of Linear Mechanical Systems", Longman, 1973.

11. Warner, P.C. "Static and Dynamic Properties of Partial Journal Bearings", J.Basic Eng., Trans. A.S.M.E., Series D, Vol. 85, 1963.

12. Shelly, P. & Ettles, C. "A Tractable Solution for Medium Length Journal Bearings", Wear, Vol. 16 (No.3), 1970.

13. Someya, T. "Stability of a Balanced Shaft Running in Cylindrical Journal Bearings", Lub. and Wear 2nd Conv., I.Mech.E., 1964, Paper 21.

14. Lloyd, T. "Dynamically Loaded Journal Bearings", Ph.D. Thesis, University of Nottingham, 1966.

15. Ware, P.M. Unpublished Ph.D. Thesis, University of Canterbury.

16. Pinkus, O. & Sternlicht, B. "Theory of Hydrodynamic Lubrication", McGraw-Hill, 1961.

17. Jakobsson, B. & Floberg, L. "The Finite Journal Bearing Considering Vaporization", Report No. 3, Chalmers University of Technology, 1957.

18. McCallion, H., Lloyd, T. & Yousif, F. "The Influence of Oil Supply Conditions on the Film Extent and Oil Flow in Journal Bearings", Trib.Conv., I.Mech.E., 1971, Paper C55/71.

19. Smalley, A.J. "Steadily Loaded Journal Bearings", Ph.D. Thesis, University of Nottingham, 1966.

20. Smalley, A.J., Lloyd, T., Horsnell, R., & McCallion, H. "A Comparison of Performance Predictions for Steadily Loaded Journal Bearings", Lub. and Wear 4th Conv., I.Mech.E., 1966, Paper 12.

21. Lloyd, T. & McCallion, H. "Recent Developments in Fluid Film Lubrication Theory", Lub. and Wear: Fundamentals and Application to Design, I.Mech.E., 1967, Paper 3.

22. Carre, B.A. "The Determination of the Optimum Accelerating Factor for Successive Over-relaxation", Comp.J., Vol. 4 (No.1), 1961.

23. Cameron, A., Akers, A. & Michaelson, S. "Stability Contours for a Whirling Finite Journal Bearing", Journal of Lub.Tech., Trans. A.S.M.E., Vol. 93, 1971, Paper 70-LubS-3.

24. Cameron, A. "Basic Lubrication Theory", Longman, 1971.

25. Huggins, N.J. "Tests on a 24-in diameter Journal Bearing: Transition from Laminar to Turbulent Flow". Journal Bearings for Reciprocating and Turbo Machinery, I.Mech.E., 1966, Paper 1.

26. Duffin, S. & Johnson, B.T. "Some Experimental and Theoretical Studies of Journal Bearings for Large Turbine-Generator Sets", Journal Bearings for Reciprocating and Turbo Machinery, I.Mech.E., 1966, Paper 4.

27. McCallion, H. & Smalley, A.J. "The Influence of Viscosity Variation with Temperature on Journal Bearing Performance", Journal Bearings for Reciprocating and Turbo Machinery, I.Mech.E., 1966, Paper 2.

28. Dowson, D., Hudson, J.D., Hunter, B. & March, C.N. "An Experimental Investigation of the Thermal Equilibrium of Steadily Loaded Journal Bearings", Journal Bearings for Reciprocating and Turbo Machinery, I.Mech.E., 1966, Paper 3.

29. Middleton, V. "An Experimental Investigation into Journal Bearing Performance", Ph.D. Thesis, University of Nottingham, 1966.

30. McCallion, H., Yousif, F. & Lloyd, T. "The Analysis of the Thermal Effects in a Full Journal Bearing", Journal of Lub.Tech., Trans. A.S.M.E., Vol. 93, 1971, Paper 70-LubS-23.

31. McCallion, H. & Smalley, A.J. "The Effect of Journal Misalignment on the Performance of a Journal Bearing under Steady Running Conditons", Journal Bearings for Reciprocating and Turbo Machinery, I.Mech.E., 1966, Paper 5.

32. Hooke, C.J., Brighton, D.K. & O'Donoghue, J.P. "The Effect of Elastic Distortions on the Performance of Thin Shell Bearings", Journal Bearings for Reciprocating and Turbo Machinery, I.Mech.E., 1966, Paper 10.

33. Glienicke, J. "Experimental Investigation of the Stiffness and Damping Coefficients of Turbine Bearings and their Application to Instability Prediction", Journal Bearings for Reciprocating and Turbo Machinery, I.Mech.E., 1966, Paper 13.

34. Shawki, G.S.A. & Freeman, P. "Journal Bearing Performance under Sinusoidally Alternating and Fluctuating Loads", Proc. I.Mech.E., Vol. 169, 1955.

35. Brown, R.D. & France, D. "Non-linear Vibtation of a Shaft in Plain Hydrodynamic Journal Bearings", Trib.Conv., I.Mech.E., 1971, Paper C57/71.

36. Smith, D.M. "Journal Bearings in Turbomachinery", Chapman and Hall, 1969.

APPENDIX

COMPUTER PROGRAM - DESCRIPTION AND SOURCE LISTING

In this appendix the computer program source listing for a bearing directly loaded with a circular force locus is shown and a brief description of the function of each subroutine is given. The single and twin mass rotor model programs are similar in structure and employ the same subroutines to solve the oil film equations. The language used is FORTRAN IV and the program was run on IBM 360/44 and Burroughs B6700 computers.

Main Routine : This controls the program and the majority of the subroutine calls are made from here. Apart from the bearing geometry data, all normal input and output is done in this routine. It also contains the locus stepping routine.

Subroutine GEOM : This subroutine reads in the data describing the bearing geometry, calculates the radius and clearance of each segment, and the position of its centre in relation to the bearing centre, and determines which grid points lie within grooves.

Subroutine MINH : For a given journal centre position this subroutine calculates the minimum oil film thickness and its angular position on the bearing surface. A warning is printed out if a negative film thickness is encountered, but it is left to the main routine to rectify the situation or halt the program.

Subroutine COFUV : In this the coefficients required by the three relaxation subroutines for the solution of the oil film equations are calculated.

Subroutine RELAXP : This subroutine contains the finite difference over-relaxation scheme for the solution of Reynolds equation. The pressure distribution is calculated from the pressure-height parameter used in this solution before control is returned to the main routine.

Subroutine GROOP : Called from RELAXP, this subroutine calculates the pressure-height parameter for each grid point within the bearing grooves. The grooves are divided into two categories, grooves and slots, and the program permits their oil pressure to be set at different values, PG and PC respectively.

Subroutine BOUNDS : This subroutine determines the extent of the oil pressure films. This information is used in the summation subroutine and the two subroutines calculating the dynamic bearing coefficients.

Subroutine SUM : This performs the integration over the finite difference grid to obtain the x and y components of the oil film force and the dynamic bearing coefficients.

Subroutine RELAXS : The finite difference over-relaxation scheme to solve the partial differential equation for the bearing displacement coefficients is contained in this subroutine. It is similar in structure to RELAXP.

Subroutine RELAXD : This is similar to RELAXS, but calculates the bearing velocity coefficients.

Subroutine PANIC : This subroutine is called when the program develops an error condition or when the program run has been completed. It prints out the important variables contained in the common storage blocks.

```
      B6700/B7700   F O R T R A N   C O M P I L A T I O N   M A R K   2.0.000


      INTEGER    BUF,BU,BUF,COUNT,CTRL,MP,PLUS,REV,STEPOP,ZERO
      REAL       LAM,LG,LOADAC,MAXOT,MINOT
      COMMON/C1/BUF(6),BU(5)),BUF(5),CTRL(50,5),MP(9,3)
      COMMON/C2/COUNT,I,III,IOUT,J,JIN,JOUT,K,KOUT,M,N,NOP,NOS,PLUS,
     1          REV,STEPOP,ZERO,ACC,AN,CC,CMS,CSQ,DEL,DELS,DLLT,OT,
     2          DX,DY,E,ED,F,FV,FX,FXS,FXT,FY,FYS,FYT,GAM,GM,HM,LG,
     3          LOADAC,MAXOT,MINOT,ORF,PC,PG,PHIS,PHIT,PHITI,PY,PY2,
     4          R,RLV,SNG,SPEED,WORK,X,XI,YJ,YI
      COMMON/C3/CA(50),CH(50),CO(50),CEU(50),CEV(50),CFU(50),CFV(50),
     1          CS(50),H(50),HM(50),HMU(50),HMV(50),HXH(50),
     1          CGU(50),CGV(50),CL(3),CLO(4),CM(3),LAM(3)
      COMMON/C4/P(51,6),PI(51,6),RMSO(50),RMSU(50,6)
      COMMON/C5/RMSV(50,6),RMUV(50),RMVV(50),RO(3),ROD(3),RS(3),SN(50)
C
      REAL KXX,KYX,KXY,KYY,LOAD,LSTEP
C
C     ***DAISY***
C
C      PROGRAM CALCULATES THE JOURNAL LOCUS FOR A MASS-LESS
C     HYDRODYNAMIC BEARING UNDER A STATIC AND ROTATING LOAD. ALSO
C     CALCULATES THE WORK DONE BY THE OIL FILM ON THE JOURNAL.
C
C     TIMING ROUTINE TO TERMINATE RUN AFTER JOBTYM MINUTES
      READ(5,116)JOBTYM,LOADAC

      JOBTYM=JOBTYM*3600
  116 FORMAT(I3,F5.2)
C
      LOGICAL ALA(80)
      J=2
      DO 43 I=1,J
      READ(5,118)ALA
   43 WRITE(6,118)ALA

  118 FORMAT(80A1)
C
C     SEMI-PERMANT VARIABLES
      M=48
      N=8
      PY=3.141593
      MINOT=0.001
      MAXOT=0.3
      ACC=1.0E-03
      LSTEP=(0.4/LOADAC)**0.33333
      PLUS=100
      ZERO=11
      PY2=2*PY
C
C     OUTER PROGRAM LOOP
   42 CONTINUE
      LOADAC=0.4
C
C     DATA INPUT
      READ(5,100,END=38)PHIS,PC,PG,SPEED,VISC,NOS
      CALL GEOM
      READ(5,100)DELS,DELT,PHITI
      READ(5,100)E,GAM
  100 FORMAT(5E10.3,2I5)
C
      ANG=180./PY
      SPEED=SPEED*PY/30
      DIMP=VISC*SPEED*(R/CMS)**2
      DIML=DIMP*LG*R
      RLV=ABS(PHITI)/SPEED
C
C     OVER RELAXATION FACTOR
      A=(PY*R/LG)**2
      A=(1-2*(PY**2)*(1+A)/(M**2+4*(N**2)*A))**2
      ORF=2*(1-SQRT(1-A))/A
C
      IOUT=M*2
```

```
      DO 1 I=2,IOUT
      R=PY2*(I-2)/M
      SN(I)=SIN(R)
    1 CS(I)=COS(R)
C
C     DATA OUTPUT
      WRITE(6,102)DELS,PHIS,DELT,PHIT1,SPEED,RLV,PG,PC
  102 FORMAT(1H0,'STATIC LOAD MAGNITUDE',11X,F10.4,'  LB'
     1       /14X,'ANGLE',10X,F10.4,'  DEG'
     2       /' ROTATING LOAD MAGNITUDE',9X,F10.4,'  LB'
     3       /16X,'ANGULAR VELOCITY ',F10.4,'  RAD/S'
     4       /' SHAFT RAD/S ',20X,F10.4,'  RAD/S'
     5       /' RELATIVE LOAD VELOCITY',10X,F10.4
     6       /' GROOVE PRESSURE',17X,F10.4,'  PSI'
     7       /' JACKING PRESSURE',16X,F10.4,'  PSI')
      WRITE(6,105)E,GAM,ORF
  105 FORMAT('0STARTING ECCENTRICITY',11X,F10.4
     1       /10X,'ATTITUDE',15X,F10.4,'  DEG'
     2       /' OVER RELAXATION FACTOR',10X,F10.4)
      WRITE(6,110)DIML,DIMP,CMS,ANG
  110 FORMAT('0NON DIMENSIONALIZING FACTORS'
     1       /'      LOAD  (DIML)',19X,E11.4
     2       /'      PRESSURE  (DIMP)',15X,E11.4
     3       /'      LENGTH  (CMS)',16X,E11.4
     4       /'      ANGLE  (ANG)',19X,E11.4)
C
      PC=PC/DIMP
      PG=PG/DIMP
      PHIS=PHIS/ANG
      GAM=GAM/ANG
      DELS=DELS/DIML
      DELT=DELT/DIML
      PHIT1=PHIT1/ABS(PHIT1)
      EXS=DELS*COS(PHIS)
      EYS=DELS*SIN(PHIS)
C
C     STARTING VALUES AND SETTING COUNTERS
      ED=E*CMS
      XJ=E*COS(GAM)
      YJ=E*SIN(GAM)
      X1=0.
      Y1=0.
      WORK=0.
      DT=MINDT
      PHIT=0.0
      EXT=EXS+DELT*COS(PHIT)
      EYT=EYS+DELT*SIN(PHIT)
      BPHIT=90.0
      REV=1.0
      NSTEP=-20
      STEPOP=5
C
C     OUTPUT HEADINGS.
      WRITE(6,106)
  106 FORMAT('0   LOAD',6X,'STEP',7X,'E',8X,'ATTITUDE    LOAD',
     1       6X,'WORK',7X,'MINIMUM FILM',4X,'ANGLE    LENGTH',15X,
     2       'ANGLE   PARAMETER     ON',2X,'XJ',7X,'YJ',6X,
     3       'OIL FILM EXTENT=BOF,BOF',53X,'JOURNAL',4X,'DEG',7X,
     4       'DEG',17X,'DEG',27X,'INCH',6X,'DEG')
C
C
C     MAIN LOOP BEGINS
    2 IF(E-0.0001)3,4,4
    3 GAM=0.0
      SNG=0.
      CSG=1.
      GO TO 5
    4 GAM=ATAN2(YJ,XJ)
      SNG=SIN(GAM)
      CSG=COS(GAM)
    5 CONTINUE
      CALL MINH
      IF(HM)31,31,33
   31 IF(DT-MINDT)32,32,13
   32 DX=DX/2.
      DY=DY/2.
      NSTEP=NSTEP+1
```

```
      WRITE(6,111)
  111 FORMAT(' NEGATIVE FILM  DT AT MINIMUM VALUE')
      IF(NSTEP.LT.5)GO TO 23
      I=5
      CALL PANIC
      STOP 30
C
C     CALCULATION OF OIL FILM FORCE.
   33 CONTINUE
      CALL COFUV
      CALL RELAXP
      CALL BOUNDS
      CALL SUM
      FX=FU
      FY=FV
      DEL=SQRT(FX*FX+FY*FY)
C
C     LOAD ACCURACY
      ADT=DT*ANG
      XDTI=1.0/DT
      A=FXT*FXT+FYT*FYT
      IF(A.LT.DELS*0.2)A=DELS*0.2
      WACC=SQRT(((FX-FXT)**2+(FY-FYT)**2)/A)
      IF(WACC-0.1-LOADAC)8,9,9
    8 IF(DT.LT.MA*DT)DT=1.4142*DT
      GO TO 12
    9 IF(WACC-0.5*LOADAC)12,10,10
   10 IF(WACC-LOADAC)11,13,13
   11 IF(DT.GT.MINDT)DT=DT/1.4142
   12 STEPOP=STEPOP+1
      NSTEP=0
      IF(PHIT-PY2)20,20,19
   19 PHIT=PHIT-PY2
      REV=REV+1
      XDT=1.0/XDTI
      A=(PHIT-XOT)*ANG
      AB=XDT*ANG
      B=SQRT(XXJ*XXJ+XYJ*XYJ)
      BB=ATAN2(XYJ,XXJ)*ANG
      AA=SQRT(XFX*XFX+XFY*XFY)*DIML
      WRITE(6,107)A,AB ,B,BB,AA,WORK
   20 CONTINUE
      APHIT=PHIT*ANG
      PHIT=PHIT+DT*PHIT1
      GO TO 18
C
   13 NSTEP=NSTEP+1
      IF(DT-MINDT)14,14,15
   14 XDTI=0.0
      IF(NSTEP.LT.25)GO TO 20
      WRITE(6,103)
  103 FORMAT(1H1,'LOAD NOT CONVERGING')
      I=1
      CALL PANIC
      STOP 10
C
   15 CONTINUE
      KXX=S1
      KYX=S2
      KXY=S3
      KYY=S4
      BXX=D1
      BYX=D2
      BXY=D3
      BYY=D4
      IF(NSTEP-10)16,16,17
   16 DT=DT/1.4142
      PHIT=PHIT-DT*0.4142*PHIT1
      GO TO 39
   17 PHIT=PHIT-(DT-MINDT)*PHIT1
      DT=MINDT
      GO TO 39
C
   18 CONTINUE
      XXJ=XJ
      XYJ=YJ
      XXI=XI
```

```
      XY1=Y1
      XFX=FX
      XFY=FY
      A=(APHIT-ADT*0.5)/ANG
      WORK=WORK-(FXS*DELT*COS(A))*DX-(FYS*DELT*SIN(A))*DY
   35 CONTINUE
      XKXX=S1
      XKYX=S2
      XKXY=S3
      XKYY=S4
      XBXX=D1
      XBYX=D2
      XBXY=D3
      XBYY=D4
C
C     STIFFNESS AND DAMPING COEFFICIENTS
      IOUT=M+2
      JOUT=N/2+1
      DO 21 I=2,IOUT
      EU=CEU(I)
      FU=CFU(I)
      EV=CEV(I)
      GU=CGU(I)
      FV=CFV(I)
      GV=CGV(I)
      DO 21 J=2,JOUT
      DP=M*(PI(I+1,J)-PI(I-1,J))/2
      PT=PI(I,J)
      RHSU(I,J)=(EU+2*PT*FU+DP*GU)
   21 RHSV(I,J)=(EV+2*PT*FV+DP*GV)
      CALL RELAXS(RHSU,HHU)
      CALL RELAXS(RHSU,HHU)
      CALL SUM
      S1=FU
      S2=FV
      CALL RELAXS(RHSV,HHV)
      CALL SUM
      S3=FU
      S4=FV
      CALL RELAXD(RHUV)
      CALL SUM
      D1=FU
      D2=FV
      CALL RELAXD(RHVV)
      CALL SUM
      D3=FU
      D4=FV
      B=DT*XDTI/2.0
      A=1+B
      KXX=S1*A-XKXX*B
      KYX=S2*A-XKYX*B
      KXY=S3*A-XKXY*B
      KYY=S4*A-XKYY*B
      BXX=D1*A-XBXX*B
      BYX=D2*A-XBYX*B
      BXY=D3*A-XBXY*B
      BYY=D4*A-XBYY*B
C
C     OUTPUT
      IF(RSV-2)40,34,22
   40 IF(APHIT-BPHIT)34,34,41
   41 LOADAC=LOADAC/LSTEP
      BPHIT=BPHIT+90.0
      GO TO 34
   22 CONTINUE
      DELS=DELS*DIML
      DELT=DELT*DIML
      AGAM=GAM*ANG
      IF(AGAM.LT.0.0)AGAM=AGAM+360.0
      AGM=GM*ANG
      DEL=DEL*DIML
      WRITE(6,107)APHIT,ADT,E,AGAM,DEL,WORK,HM,AGM
      WRITE(6,114)XJ,YJ,(BUF(I),BUF(I),I=1,NOP)
      A=(JOBTYM-TIME(2))/3600.0
      WRITE(6,104)TIME(2)/3600.0
  104 FORMAT('OLDCUS COMPLETED - ELAPSED JOB TIME ',F4.1,' MINUTES')
      IF(A-4.0)28,42,42
```

```
C
   28 I=11
   38 CONTINUE
      CALL PANIC
      STOP
C     **********************************
C
C
   34 IF(STEPOP.LT.3)GO TO 39
      STEPOP=3
      AGAM=GAM*ANG
      IF(AGAM)36,37,37
   36 AGAM=AGAM+360.0
   37 AGM=GM*ANG
      DEL=DEL*DIML
      WRITE(6,107)APHIT,ADT,E,AGAM,DEL,WORK,MM,AGM
      WRITE(6,114)XJ,YJ,(BUF(1),BUF(I),I=1,NOP)
  107 FORMAT(F7.1,F12.3,F11.5,F6.1,F12.2,F10.4,F10.6,F8.2)
  114 FORMAT(1H+,50X,2F9.4,2X,6(2I2,2X))
C
      IF(TIME(2)-JOBTYM)30,29,29
   29 WRITE(6,117)JOBTYM/360
  117 FORMAT('0TIME LIMIT',I3,'MINUTES EXCEEDED.')
      GO TO 28
   30 CONTINUE
C
   24 CONTINUE
   39 CONTINUE
C
C     LOCUS STEP
      FXT=FXS+DELT*COS(PHIT)
      FYT=FYS+DELT*SIN(PHIT)
      AA=2*BXX+KXX*DT
      AB=2*BXY+KXY*DT
      AC=2*(FXT-FX)-XX1*(KXX*DT-2*BXX)-XY1*(KXY*DT-2*BXY)
      BA=2*BYX+KYX*DT
      BB=2*BYY+KYY*DT
      BC=2*(FYT-FY)-XY1*(KYY*DT-2*BYY)-XX1*(KYX*DT-2*BYX)
      DEN=1.0/(AA*BB-BA*AB)
      X1=(AC*BB-BC*AB)*DEN
      Y1=(BC*AA-AC*BA)*DEN
      DX=0.5*DT*(X1+XX1)
      DY=0.5*DT*(Y1+XY1)
   23 CONTINUE
      XJ=XXJ+DX
      YJ=XYJ+DY
      E=SQRT(XJ*XJ+YJ*YJ)
      ED=E*CMS
      GO TO 2
      END
```

```
      SUBROUTINE GEOM
      INTEGER    BDF,BU,BUF,COUNT,CTRL,IP,PLUS,REV,STEPOP,ZERO
      REAL       LAM,LG,LOAD,MAXDT,MINDT
      COMMON/C1/BDF(6),BU(50),BUF(6),CTRL(50,5),MP(9,3)
      COMMON/C2/COUNT,I,IIN,IOUT,J,JIN,JOUT,K,KOUT,M,N,NOP,NOS,PLUS,
     1          REV,STEPOP,ZERO,ALC,ANG,CC,CMS,CSG,DEL,DELS,DELT,DT,
     2          DX,DY,E,ED,EU,EV,EX,EXS,EXT,EY,EYS,EYT,GAM,GM,HM,LG,
     3          LOADAC,MAXDT,MINDT,ORF,PC,PG,PHIS,PHIT,PHITI,PY,PY2,
     4          R,RLV,SNG,SPEED,WORK,XJ,X1,YJ,Y1
      COMMON/C3/CA(50),CB(50),CD(50),CEU(50),CEV(50),CFU(50),CFV(50),
     1          CS(50),H(50),HH(50),HHU(50),HHV(50),HXH(50),
     1          CGU(50),CGV(50),CL(3),CL1(3),CM(3),LAM(3)
      COMMON/C4/P(51,6),PI(51,6),RHSU(50),RHSV(50,6)
      COMMON/C5/RHSV(50,6),RHOV(50),RHVV(50),RO(3),ROD(3),RS(3),SN(50)
      INTEGER T
      REAL TI,TC,TO,ORD,ANG,LOR,HO,X,Y
      READ(5,101)R,LG,HO
      LOR=LG/R
      WRITE(6,102)R,LG,LOR,HO
      WRITE(6,103)
      R=R/2
      IOUT=M*2
      JOUT=N/2+1
      DO 8 I=2,IOUT
      DO 8 J=1,JOUT
      CTRL(I,J)=PLUS
    8 CONTINUE
      DO 26 K=1,NOS
      MP(1,K)=M*(K-1)/NOS+2
      MP(2,K)=M*K/NOS+2
      READ(5,101)TI,TC,TO,ORDI,ORDO,ORD,T
      X=(TO-TI)/2
      Y=(TI+TO)/2-TC
      ROD(K)=SQRT(X**2+Y**2)
      LAM(K)=PY2*(K-1)/NOS
      IF(ROD(K))9,10,9
    9 LAM(K)=ATAN2(Y,X)+LAM(K)
   10 RS(K)=(HO-TI-TO)/2
      CLD(K)=RS(K)-R
      CM(K)=CLD(K)-ROD(K)
      ANG=LAM(K)*180/PY
      WRITE(6,104)TI,TC,TO,X,Y,ROD(K),RS(K),ANG,CLD(K),CM(K)
      ORDI=ORDI/R
      ORDO=ORDO/R
      ANG=ATAN2(ORDI,SQRT(1-ORDI**2))
      IGROV=M*ANG/(2*PY)+0.5
      MP(3,K)=MP(1,K)+IGROV
      ANG=ATAN2(ORDO,SQRT(1-ORDO**2))
      IGROV=M*ANG/(2*PY)+0.5
      MP(4,K)=MP(2,K)-IGROV
      MP(5,K)=(N*ORD/LG+0.5)+1
      IF(N/2+1-MP(5,K))13,14,13
   13 JIN=MP(5,K)
      JOUT=N/2+1
      DO 15 J=JIN,JOUT
      IF(MP(3,K)-MP(1,K))16,17,16
   16 IIN=MP(1,K)
      IOUT=MP(3,K)
      DO 18 I=IIN,IOUT
      CTRL(I,J)=ZERO
   18 CONTINUE
   17 IF(MP(2,K)-MP(4,K))19,15,19
   19 IIN=MP(4,K)
      IOUT=(MP(2,K))
      DO 20 I=IIN,IOUT
      CTRL(I,J)=ZERO
   20 CONTINUE
   15 CONTINUE
   14 CONTINUE
      IF(T)21,22,21
   21 CONTINUE
      READ(5,101)ANGI,ANGO,ORDO,ORDI
      MP(6,K)=MP(1,K)+     (M*ANGI/360.0)
      MP(7,K)=MP(1,K)+     (M*ANGO/360.0)
```

```
      MP(8,K)=  (N*ORDO/LG+0.5)+1
      MP(9,K)=MP(8,K)+     (N*(ORDI-ORDO)/LG+0.5)
      IIN=MP(6,K)
      IOUT=MP(7,K)
      JIN=MP(4,K)
      JOUT=MP(9,K)
      DO 25 I=IIN,IOUT
      DO 25 J=JIN,JOUT
      CTRL(I,J)=ZERO
   25 CONTINUE
      GO TO 26
   22 DO 27 T=6,9,1
   27 MP(T,K)=999
   26 CONTINUE
      CMS=CM(NOS)
      JOUT=N/2+1
      T=M+2
      I=0
      DO 44 J=1,JOUT
      IF(CTRL(T,J)-ZERO)41,45,44
   45 I=I+1
   44 CONTINUE
      IF(I)46,47,46
   46 DO 48 J=1,JOUT
   48 CTRL(2,J)=CTRL(T,J)
      GO TO 49
   47 DO 28 J=1,JOUT
   28 CTRL(T,J)=CTRL(2,J)
   49 WRITE(6,106)
      DO 33 K=1,NOS
      RO(K)=ROO(K)/CMS
      CL(K)=CLO(K)/CMS
      WRITE(6,107)K,(MP(J,K),J=1,9)
   33 CONTINUE
      WRITE(6,108)
      IOUT=M+2
      JOUT=N/2+1
      DO 35 J=1,JOUT
      WRITE(6,112)J,(CTRL(I,J),I=2,IOUT)
   35 CONTINUE
      DO 50 J=2,JOUT
      K=JOUT-J+1
      KOUT=J+4
   50 WRITE(6,112)KOUT,(CTRL(I,K),I=2,IOUT)
      RETURN
   41 WRITE(6,111)
      STOP
  101 FORMAT(6F10.4,I5)
  102 FORMAT(15HOSHAFT DIAMETER,F12.4,
     1/15H BEARING LENGTH,F12.4,
     2/17H LENGTH/DIA RATIO,F10.4,
     3/17H HOUSING DIAMETER,F10.4)
  103 FORMAT(22HOCIRCULAR ARC GEOMETRY,//
     1       'N       TI          TC          TO          X           Y',
     2       9X,'RO          RS          LAM         CL          CM')
  104 FORMAT(10F10.4)
  105 FORMAT(I4)
  106 FORMAT(49HOMESH POINTS DEFINING SEGMENT AND GROOVE GEOMETRY,
     1       /'    SEGMENT SEGMENT  SEGMENT   INLET     OUTLET    ',
     2       'GROOVE  CONTROL CONTROL   SLOT       SLOT'
     3       /'    NUMBER  INLET    OUTLET    GROOVE    GROOVE    ',
     4       'WIDTH   SLOT    SLOT     OUTER     INNER'
     5       /30X,'END       START',12X,'START   END',7X,
     6       'EDGE      EDGE')
  107 FORMAT(1H ,I5,9I9)
  108 FORMAT(1H )
  109 FORMAT(3H+ 0)
  110 FORMAT(3H+ +)
  111 FORMAT(23HOCONTROL ARRAY IN ERROR)
  112 FORMAT(1H ,I4,2X,49I2)
      END
```

```
      SUBROUTINE MINM
      INTEGER    BDF,HU,BUF,COUNT,CTRL,MP,PLUS,REV,STEPOP,ZERO
      REAL       LAM,LG,LOADAC,MAXDT,MINDT
      COMMON/C1/BDF(6),HJ(50),BUF(6),CTRL(50,5),MP(9,3)
      COMMON/C2/COUNT,I,IIA,IOUT,JJ,JIN,JOUT,K,KOUT,M,N,NOP,NOS,PLUS,
     1          REV,STEPOP,ZERO,ACC,AI,CC,CMS,CSG,DEL,DELS,DELT,DT,
     2          DX,DY,E,ED,FO,FV,F(,FXS,FXT,FY,FYS,FYT,GAM,GM,HM,LG,
     3          LOADAC,MAXDT,MINDT,ORF,PC,PU,PHIS,PHIT,PHITI,PY,PY2,
     4          R,RLV,SNG,SPEED,WORK,XJ,XI,YJ,YI
      COMMON/C3/CA(50),CR(50),CU(50),CEU(50),CEV(50),CFU(50),CFV(50),
     1          CS(50),H(50),HH(50),HMU(50),HMV(50),HXH(50),
     1          CGU(50),CGV(50),CL(3),CLD(3),CM(3),LAM(3)
      COMMON/C4/P(51,6),PI(51,6),RHSO(50),RMSO(50,6)
      COMMON/C5/RHSV(50,6),RHJV(50),RHVV(50),ROD(3),ROD(3),RS(3),SN(50)
C     CHECK TO ENSURE JOURNAL WITHIN BEARING
      HM=1.0
      DO 10 K=1,NOS
      X=XJ+CMS*ROD(K)*COS(LAM(K))
      Y=YJ+CMS*ROD(K)*SIN(LAM(K))
      ES=SQRT(X*X+Y*Y)
      HS=CLD(K)-ES
      ES=ES/CLD(K)
      GS=0.
      IF(ES-0.0001)5,6,6
    6 GS=ATAN2(Y,X)
      IF(GS-0.0)7,7,8
    7 GS=GS+PY2
    8 FI=PY2*(K-1)/NOS
      FO=PY2*K/NOS
      IF(GS-FI)4,9,9
    9 IF(GS-FO)5,4,4
    4 X=CLD(K)*ROD(K)*COS(LAM(K)-FI)-ED*COS(GAM-FI)
      Y=CLD(K)*ROD(K)*COS(LAM(K)-FO)-ED*COS(GAM-FO)
      IF(X-Y)11,11,12
   11 HS=X
      GS=FI
      GO TO 5
   12 HS=Y
      GS=FO
    5 IF(HM-HS)10,10,14
   14 HM=HS
      GM=GS
   10 CONTINUE
      IF(HM)15,16,16
   15 GM=GM+ANG
      WRITE(6,100)XJ,YJ,HM,GM
  100 FORMAT(' NEGATIVE FILM'/4X,'XJ       YJ       HM       GM'
     1       /1X,3F8.5,F6.1)
   16 CONTINUE
      RETURN
      END
```

```
      SUBROUTINE COFUV
      INTEGER    BUF,BU,BUF,COUNT,CTRL,MP,PLUS,REV,STEPOP,ZERO
      REAL       LAM,LG,LOADAC,MAXOT,MINOT
      COMMON/C1/BUF(6),BU(50),BUF(6),CTRL(50,5),MP(9,3)
      COMMON/C2/COUNT,I,IIN,IOUT,J,JIN,JOUT,K,KOUT,M,N,NOP,NOS,PLUS,
     1          REV,STEPOP,ZERO,ACC,AN,CC,CMS,CSQ,DEL,DELS,DLLT,DT,
     2          DX,DY,E,EJ,EU,EV,FX,FXC,FXT,FY,FYS,FYT,GAM,GM,HM,LG,
     3          LOADAC,MAXOT,MINOT,OPF,PC,PG,PHIS,PHIT,PHITI,PY,PY2,
     4          R,RL,SNG,SPEED,UOPC,XJ,Y1,YJ,Y1
      COMMON/C3/CA(50),CB(50),CD(50),CEU(50),CEV(50),CFU(50),CFV(50),
     1          CS(50),H(50),HH(50),HHU(50),HHV(50),HXH(50),
     1          CGU(50),CGV(50),CL(3),CLD(3),CM(3),LAM(3)
      COMMON/C4/P(51,6),PI(51,6),RHSO(50),RHSU(50,6)
      COMMON/C5/RHSV(50,6),RHUV(50),RHVV(50),RO(3),ROD(3),RS(3),SN(50)
C
      A=2*PY
      B=A**2
      CC=(A*R*N/LG)**2
      C=M**2+CC
      AB=2*RLV*Y1
      BA=2*RLV*X1
      G=6.0*R
      AC=-2.0*RLV*G
      DO 6 K=1,NOS
      CT=XJ-RO(K)*COS(LAM(K))
      ST=YJ-RO(K)*SIN(LAM(K))
      AA=CT-AB
      BB=ST+BA
      CLR=CL(K)
      IIN=MP(1,K)
      IOUT=MP(2,K)
C
      DO 1 I=IIN,IOUT
      CO=CS(I)
      SI=SN(I)
      HXX=CO*CT+SI*ST
      D=CLR-HXX
      HXX=B*HXX/D
      CO=CO/D
      SI=SI/D
      HX=A*(SI*CT-CO*ST)
      RHS=G*(SI*AA-CO*BB)
      H(I)=D
      HH(I)=D*D
      HXH(I)=HX
      CA(I)=M*(M-HX/2)
      CB(I)=M*(N+HX/2)
      CD(I)=2*(C+HXX)
      RHSO(I)=RHS
      CEU(I)=G*SI+RHS*CO
      CEV(I)=-G*CO+RHS*SI
      CFU(I)=CO*(B+HXX)
      CFV(I)=SI*(B+HXX)
      CGU(I)=A*SI+HX*CO
      CGV(I)=-A*CO+HX*SI
      RHUV(I)=AC*CO
      RHVV(I)=AC*SI
      HHU(I)=-2.0*CO
      HHV(I)=-2.0*SI
    1 CONTINUE
    6 CONTINUE
C
      RETURN
      END
```

```
      SUBROUTINE RELAXP
      INTEGER    BUF,BU,BUF,COUNT,CTRL,MP,PLUS,REV,STEPOP,ZERO
      REAL       LAM,LG,LOADAC,MAXJT,MINOT
      COMMON/C1/BUF(6),BU(50),BUF(6),CTRL(50,5),MP(9,3)
      COMMON/C2/COUNT,I,IIN,IOUT,J,JIN,JJUT,K,KOUT,M,N,NOP,NOS,PLUS,
     1          REV,STEPOP,ZERO,ACC,AN,CC,CMS,CSU,DEL,DELS,DELT,DT,
     2          DX,DY,E,ED,FU,FV,FX,FXS,FXT,FY,FYS,FYT,GAM,GM,MM,LG,
     3          LOADAC,MAXJT,MINOT,ORF,PC,PG,PHIS,PHIT,PHITI,PY,PY2,
     4          R,RLV,SNG,STEED,VORK,XJ,Y1,YJ,Y1
      COMMON/C3/CA(50),CB(50),CD(50),CEU(50),CEV(50),CFU(50),CFV(50),
     1          CS(50),H(50),HH(50),HHU(50),HHV(50),HXH(50),
     1          CGU(50),CGV(50),CL(3),CLD(3),CM(3),LAM(3)
      COMMON/C4/P(51,6),PI(51,6),RHSD(50),RHSU(50,6)
      COMMON/C5/RHSV(50,6),RHUV(50),RHVV(50),RU(3),ROD(3),RS(3),SN(50)
      REAL A,B,D,NP,OP,RHS,PMAX,OPMAX
      IOUT=M+3
      JOUT=N/2+2
      DO 1 I=1,IOUT
      DO 1 J=1,JOUT
    1 PI(I,J)=0
      CALL GROUP
      COUNT=0
      IOUT=M+2
      JOUT=N/2+1
    2 NRC=0
      DO 3 I=2,IOUT
      A=CA(I)
      B=CB(I)
      D=CD(I)
      RHS=RHSD(I)
      IF(I-IOUT)15,16,15
   16 DO 17 J=2,JOUT
   17 PI(M+3,J)=PI(3,J)
   15 CONTINUE
      DO 4 J=2,JOUT
      IF(CTRL(I,J)-ZERO)4,4,5
    5 OP=PI(I,J)
      IF(J-JOUT)10,20,10
   20 PI(I,JOUT+1)=PI(I,JOUT-1)
   10 CONTINUE
      NP=(A*PI(I+1,J)+B*PI(I-1,J)+CC*(PI(I,J+1)+PI(I,J-1))-RHS)/D
      NP=UP+ORF*(NP-OP)
      IF(NP)6,7,7
C     FITS DP/DX=0
    6 NP=0
    7 IF(ABS(NP-OP),GT,ACC*NP)NRC=1
    8 PI(I,J)=NP
    4 CONTINUE
    3 CONTINUE
      COUNT=COUNT+1
      IF(COUNT-200)11,11,21
   21 I=2
      CALL PANIC
      GO TO 12
   11 DO 13 J=1,JOUT
      PI(1,J)=PI(M+1,J)
   13 CONTINUE
      IF(NRC)12,12,2
   12 JOUT=N/2+2
      DO 14 I=2,IOUT
      A=HH(I)
      DO 14 J=1,JOUT
   14 P(I,J)=PI(I,J)/A
      DO 22J=1,JOUT
      P(1,J)=P(M+1,J)
   22 P(M+3,J)=P(3,J)
      RETURN
      END
```

```
      SUBROUTINE GROOP
      INTEGER    BDF,BU,BUF,COUNT,CTRL,MP,PLUS,REV,STEPOP,ZERO
      REAL       LAM,LG,LOADAC,MAXDT,MINDT
      COMMON/C1/BDF(6),BU(50),BUF(6),CTRL(50,5),MP(9,3)
      COMMON/C2/COUNT,I,IIN,IOUT,J,JIN,JOUT,K,KOUT,M,N,NOP,NOS,PLUS,
     1          REV,STEPOP,ZERO,ACC,ANG,CC,CMS,CSG,DEL,DELS,DELT,DT,
     2          DX,DY,E,ED,FD,FV,FX,FXS,FXT,FY,FYS,FYT,GAM,GM,HM,LG,
     3          LOADAC,MAXDT,MINDT,ORF,PC,PG,PHIS,PHIT,PHITT,PY,PY2,
     4          R,RLV,SNG,SPEED,WORK,XJ,XI,YJ,YI
      COMMON/C3/CA(50),CR(50),CU(50),CEU(50),CEV(50),CFU(50),CFV(50),
     1          CS(50),H(50),HH(50),HHU(50),HHV(50),HXH(50),
     1          CUJ(50),CGV(50),CL(3),CLO(3),CM(3),LAM(3)
      COMMON/C4/P(51,6),PI(51,6),RHSO(50),RHSU(50,6)
      COMMON/C5/RHSV(50,6),RHOV(50),RHVV(50),ROO(3),ROD(3),RS(3),SN(50)
      DO 1 K=1,NOS
      IF(PG)2,3,2
    2 IIN=MP(1,K)
      IOUT=MP(3,K)
      JIN=MP(5,K)
      JOUT=N/2+1
      DO 4 I=IIN,IOUT
      A=PG*HH(I)
      DO 4 J=JIN,JOUT
    4 PI(I,J)=A
      IIN=MP(4,K)
      IOUT=MP(2,K)
      DO 5 I=IIN,IOUT
      A=PG*HH(I)
      DO 5 J=JIN,JOUT
    5 PI(I,J)=A
    3 IF(MP(6,K)-999)6,1,200
    6 IF(PC)7,1,7
    7 IIN=MP(6,K)
      IOUT=MP(7,K)
      JIN=MP(8,K)
      JOUT=MP(9,K)
      DO 8 I=IIN,IOUT
      A=PC*HH(I)
      DO 8 J=JIN,JOUT
    8 PI(I,J)=A
    1 CONTINUE
      RETURN
  200 STOP 30
      END
```

```
      SUBROUTINE BOUNDS
      INTEGER    BUF,BU,BUF,COUNT,CTRL,MP,PLUS,REV,STEPOP,ZERO
      REAL       LAM,LG,LOADAC,MAXDT,MINDT
      COMMON/C1/BUF(5),BU(5),BUF(6),CTRL(50,5),MP(9,3)
      COMMON/C2/COUNT,I,IIN,IOUT,J,JIN,JOUT,K,KOUT,M,N,NOP,NOS,PLUS,
     1          REV,STEPOP,ZERO,ACC,ANG,CC,CMS,CSG,DEL,DELS,DELT,DT,
     2          DX,DY,E,ED,FI,FV,FX,FXS,FXT,FY,FYS,FYT,GAM,GM,HM,LG,
     3          LOADAC,MAXDT,MINDT,ORF,PC,PG,PHIS,PHIT,PHITI,PY,PY2,
     4          R,RLV,SNG,SPEED,WORK,X1,XI,YI
      COMMON/C3/CA(50),CB(50),CD(50),CCU(50),CEV(50),CFU(50),CFV(50),
     1          CS(50),H(50),HH(50),HHU(50),HHV(50),HXH(50),
     1          CGU(50),CGV(50),CL(3),CLD(3),CM(3),LAM(3)
      COMMON/C4/P(51,6),PI(51,6),RHS(50),RHSU(50,6)
      COMMON/C5/RHSV(50,6),RHUV(50),RHVV(50),RO(3),ROD(3),RS(3),SN(50)
      DO 1 K=1,6
      BUF(K)=-1
      BDF(K)=-1
    1 CONTINUE
      K=1
      IOUT=M+2
      JOUT=N/2+1
      DO 2 I=2,IOUT
      BU(I)=-1
      DO 3 J=2,JOUT
      IF(P(I,J))3,3,4
    4 BU(I)=J
      GO TO 5
    3 CONTINUE
      GO TO 7
    5 IF(BUF(K))8,2,2
    8 BUF(K)=I
      GO TO 2
    7 IF(BUF(K))2,10,10
   10 BDF(K)=I-1
      K=K+1
    2 CONTINUE
      IF(BUF(K))12,11,11
   11 NOP=K
      IF(BDF(K))13,14,14
   13 BDF(K)=M+2
      GO TO 14
   12 NOP=K-1
   14 CONTINUE
      IF(BUF(1).LT.2)BUF(1)=2
      RETURN
      END
```

```
      SUBROUTINE SUM
      INTEGER    BOF,BU,BUF,COUNT,CTRL,MP,PLUS,REV,STEPOP,ZERO
      REAL       LAM,LG,LOADAC,MAXOT,MINOT
      COMMON/C1/BOF(6),BU(50),BUF(6),CTRL(50,5),MP(9,3)
      COMMON/C2/COUNT,I,III,IOUT,J,JIN,JOUT,K,KOUT,M,N,NOP,NOS,PLUS,
     1          REV,STEPOP,ZERO,ACC,ANG,CC,CKS,CSU,DEL,DELS,DELT,DT,
     2          DX,DY,E,EU,EV,FV,FX,FXS,FXT,FY,FYS,FYT,GAM,GM,HM,LG,
     3          LOADAC,MAXOT,MINOT,ORF,PC,PG,PHIS,PHIT,PHITT,PY,PY2,
     4          R,RLV,SNG,SPEED,XD,XJ,X1,YJ,Y1
      COMMON/C3/CA(50),CB(50),CD(50),CEU(50),CEV(50),CFU(50),CFV(50),
     1          CS(50),H(50),HH(50),HHJ(50),HHV(50),HXH(50),
     1          CGU(50),CGV(50),CL(3),CLQ(3),CM(3),LAM(3)
      COMMON/C4/P(51,6),PI(51,6),RHS(50),RHSU(50,6)
      COMMON/C5/RHSV(50,6),RHOV(50),RHVV(50),RO(3),ROD(3),RS(3),SN(50)
      REAL A,B,U,V,PU,PV,PUS,PVS
      FU=0
      FV=0
      DO 1 K=1,NOP
      PU=0
      PV=0
      IIN=BUF(K)
      IOUT=BOF(K)
      IF(IIN-2)200,8,7
    7 IIN=IIN-1
    8 IF(IOUT-(M+2))9,10,200
    9 IOUT=IOUT+1
   10 CONTINUE
      DO 2 I=IIN,IOUT
      A=0
      B=0
      JOUT=N/2
      DO 3 J=2,JOUT,2
    3 A=A+P(I,J)
      JOUT=N/2-1
      DO 4 J=3,JOUT,2
    4 B=B+P(I,J)
      JOUT=N/2+1
      A=4*A+2*B+P(I,JOUT)
      U=A*CS(I)
      V=A*SN(I)
      IF(I-IIN)200,5,6
    5 PUS=U
      PVS=V
    6 PU=PU+U
    2 PV=PV+V
      PU=2*PY*(2*PU-PUS-U)/(3*M*N)
      PV=2*PY*(2*PV-PVS-V)/(3*M*N)
      FU=FU+PU
    1 FV=FV+PV
      RETURN
  200 I=0
      CALL PANIC
      STOP 20
      END
```

```
      SUBROUTINE RELAXS(RHS,HHH)
      INTEGER    BUF,BU,BUF,COUNT,CTRL,MP,PLUS,REV,STEPOP,ZERO
      REAL       LAM,LG,LOADAC,MAXDT,MINDT
      COMMON/C1/BUF(6),BU(50),BUF(6),CTRL(50,5),MP(9,3)
      COMMON/C2/COUNT,I,IIN,IOUT,J,JIN,JOUT,K,KOUT,M,N,NOP,NOS,PLUS,
     1          REV,STEPOP,ZERO,ACC,ANG,CC,CMS,CSG,DEL,DELS,DELT,DT,
     2          DX,DY,E,EU,EV,FX,FXS,FXT,FY,FYS,FYT,GAM,GM,HM,LG,
     3          LOADAC,MAXDT,MINDT,ORF,PC,PG,PHIS,PHIT,PHITI,PY,PY2,
     4          R,RLV,SNG,SPEED,WORK,XJ,X1,YJ,Y1
      COMMON/C3/CA(50),CH(50),CD(50),CEU(50),CEV(50),CFU(50),CFV(50),
     1          CS(50),H(50),HH(50),HHU(50),HHV(50),HXH(50),
     1          CGU(50),CGV(50),CL(3),CLD(3),CM(3),LAM(3)
      COMMON/C4/P(51,6),PI(51,6),RHSU(50),RHSU(50,6)
      COMMON/C5/RHSV(50,6),RHUV(50),RHVV(50),RU(3),ROD(3),RS(3),SN(50)
      DIMENSION RHS(50,6),HHH(50)
      REAL  A,B,D,NP,OP,PMAX,OPMAX
      IOUT=M+J
      JOUT=N/2+2
      DO 1 I=1,IOUT
      DO 1 J=1,JOUT
      P(I,J)=0
    1 CONTINUE
      COUNT=0
      PMAX=0.
    6 OPMAX=PMAX*ACC*10
      PMAX=0.
      NRC=0
      JOUT=N/2+1
      DO 2 K=1,NOP
      IIN=BUF(K)
      IOUT=BUF(K)
      DO 2 I=IIN,IOUT
      A=CA(I)
      B=CH(I)
      D=CD(I)
      JIN=BU(I)
      IF(JIN)2,2,26
   26 IF(I-IOUT)24,23,24
   23 DO 25 J=2,JOUT
   25 P(M+3,J)=P(3,J)
   24 CONTINUE
      DO 3 J=JIN,JOUT,1
      IF(CTRL(I,J)-ZERO)3,3,4
    4 OP=P(I,J)
      IF(J-JOUT)21,22,21
   22 P(I,JOUT+1)=P(I,JOUT-1)
   21 CONTINUE
      NP=(A*P(I+1,J)+B*P(I-1,J)+CC*(P(I,J+1)+P(I,J-1))-RHS(I,J))/D
      NP=OP+ORF*(NP-OP)
      IF(ABS(NP).GT.PMAX)PMAX=ABS(NP)
      IF(ABS(NP-OP).GT.OPMAX)NRC=1
      P(I,J)=NP
    3 CONTINUE
    2 CONTINUE
   10 COUNT=COUNT+1
      IF(COUNT-200)15,15,30
   30 I=3
      CALL PANIC
      GO TO 17
   15 DO 16 J=2,JOUT,1
      P(1,J)=P(M+1,J)
      P(2,J)=P(M+2,J)
   16 CONTINUE
      IF(NRC)17,17,6
   17 IIN=2
      IOUT=M+2
      DO 20 I=IIN,IOUT,1
      IF(BU(I))20,20,19
   19 A=HH(I)
      B=HHH(I)
      DO 18 J=2,JOUT,1
      P(I,J)=(P(I,J)-B*PI(I,J))/A
   18 CONTINUE
   20 CONTINUE
      RETURN
      END
```

```
      SUBROUTINE RELAXD(RHS)
      INTEGER    BUF,BU,BUP,COUNT,CTRL,MP,PLUS,REV,STEPOP,ZERO
      REAL       LAM,LG,LOADAC,MAXDT,MINDT
      COMMON/C1/BUF(6),BU(50),BUF(6),CTRL(50,5),MP(9,3)
      COMMON/C2/COUNT,I,IIN,IOUT,J,JIN,JOUT,K,KOUT,M,N,NOP,NOS,PLUS,
     1          REV,STEPOP,ZERO,ACC,ASQ,CC,CMS,CSQ,DEL,DELS,DELT,DT,
     2          DX,DY,L,EU,FU,FV,FX,FXS,FXT,FY,FYS,FYT,GAM,GM,HM,LG,
     3          LOADAC,MAXDT,MINDT,ORF,PC,PG,PHIS,PHIT,PHIT1,PY,PY2,
     4          R,RLY,SNG,SPEED,WORK,XJ,X1,YJ,Y1
      COMMON/C3/CA(50),CB(50),CD(50),CEU(50),CEV(50),CFU(50),CFV(50),
     1          CS(50),HH(50),HHH(50),HHV(50),HXH(50),
     1          CGU(50),CGV(50),CL(3),CLD(3),CM(3),LAM(3)
      COMMON/C4/P(51,6),PI(51,6),RHS0(50),RHSU(50,6)
      COMMON/C5/RHSV(50,6),RHOV(50),RHVV(50),RO(3),ROO(3),RS(3),SN(50)
      DIMENSION RHS(50)
      REAL A,B,D,NP,OP,OPMAX,PMAX
      IOUT=M+3
      JOUT=N/2+2
      DO 1 I=1,IOUT
      DO 1 J=1,JOUT
      P(I,J)=0
    1 CONTINUE
      COUNT=0
      PMAX=0.
    6 OPMAX=PMAX*ACC*10
      PMAX=0.
      NRC=0
      JOUT=N/2+1
      DO 2 K=1,NOP
      IIN=BUF(K)
      IOUT=BUF(K)
      DO 2 I=IIN,IOUT
      A=CA(I)
      B=CB(I)
      D=CD(I)
      JIN=BU(I)
      IF(JIN)2,2,26
   26 IF(I-IOUT)24,23,24
   23 DO 25 J=2,JOUT
   25 P(M+3,J)=P(3,J)
   24 CONTINUE
      DO 3 J=JIN,JOUT,1
      IF(CTRL(I,J)-ZERO)3,3,4
    4 OP=P(I,J)
      IF(J-JOUT)21,22,21
   22 P(I,JOUT+1)=P(I,JOUT-1)
   21 CONTINUE
      NP=(A*P(I+1,J)+B*P(I-1,J)+CC*(P(I,J+1)+P(I,J-1))-RHS(I))/D
      NP=OP+ORF*(NP-OP)
      IF(ABS(NP).GT.PMAX)PMAX=ABS(NP)
      IF(ABS(NP-OP).GT.OPMAX)NRC=1
      P(I,J)=NP
    3 CONTINUE
    2 CONTINUE
      COUNT=COUNT+1
      IF(COUNT-200)15,15,30
   30 I=4
      CALL PANIC
      GO TO 17
   15 DO 16 J=2,JOUT,1
      P(1,J)=P(M+1,J)
      P(2,J)=P(M+2,J)
   16 P(M+3,J)=P(3,J)
      IF(NRC)17,17,6
   17 IIN=2
      IOUT=M+2
      DO 20 I=IIN,IOUT,1
      IF(BU(I))20,20,19
   19 A=HH(I)
      DO 18 J=2,JOUT,1
      P(I,J)=P(I,J)/A
   18 CONTINUE
   20 CONTINUE
      RETURN
      END
```

```
      SUBROUTINE PANIC
      INTEGER    BUF,BU,BUF,COUNT,CTRL,MP,PLUS,REV,STEPOP,ZERO
      REAL       LAM,LG,LOADAC,MAXDT,MINDT
      COMMON/C1/BUF(6),BU(50),BUF(6),CTRL(50,5),MP(9,3)
      COMMON/C2/COUNT,I,IIN,IOUT,J,JIN,JOUT,K,KOUT,M,N,NOP,NOS,PLUS,
     1          REV,STEPOP,ZERO,ACC,ANG,CC,CMS,CSG,DEL,DELS,DELT,DT,
     2          DX,DY,E,ED,FU,FV,FX,FXS,FXT,FY,FYS,FYT,GAM,GM,HM,LG,
     3          LOADAC,MAXDT,MINDT,ORF,PC,PG,PHIS,PHIT,PHIT1,PY,PY2,
     4          R,RLV,SNG,SPEED,WORK,XJ,X1,YJ,Y1
      COMMON/C3/CA(50),CH(50),CU(50),CEU(50),CEV(50),CFU(50),CFV(50),
     1          CS(50),H(50),HM(50),HMU(50),HMV(50),HXH(50),
     1          CGU(50),CG(50),CL(3),CLD(3),CM(3),LAM(3)
      COMMON/C4/P(51,6),PI(51,6),RHSD(50),RHSU(50,6)
      COMMON/C5/RHSV(50,6),RHUV(50),RHVV(50),RU(3),RUD(3),RS(3),SN(50)
      WRITE(6,100)I
  100 FORMAT(' PANIC CALL ',I3)
      WRITE(6,101)COUNT,I,IIN,IOUT,J,JIN,JOUT,K,KOUT,M,N,NOP,NOS,
     1PLUS,REV,STEPOP,ZERO
  101 FORMAT(1HO,'INTEGER VARIABLES'/1X,17I5)
      WRITE(6,102)ACC,ANG,CC,CMS,CSG,DEL,DELS,DELT,DT,DX,DY,E,ED,FU,
     1      FV,FX,FXS,FYT,FY,FYS,FYT,GAM,GM,HM,LG,LOADAC,MAXDT,MINDT,
     2      ORF,PC,PG,PHIS,PHIT,PHIT1,PY,PY2,R,RLV,SNG,SPEED,WORK,
     3      XJ,X1,YJ,Y1
  102 FORMAT(1HO,'REAL VARIABLES',5(/1X,1P10E13.5))
      RETURN
      END
```